ERDC TR-14-8

US Army Corps
of Engineers®
Engineer Research and
Development Center

ERDC
INNOVATIVE SOLUTIONS
for a safer, better world

Coastal Inlets Research Program

Dredging Operations and Environmental Research Program

Water Operations Technical Support Program

Modeling of Waves, Hydrodynamics and Sediment Transport for Protection of Wetlands at Braddock Bay, New York

Zeki Demirbilek, Lihwa Lin, Earl Hayter, Colleen O'Connell,
Michael Mohr, Shanon Chader, and Craig Forgette

March 2015

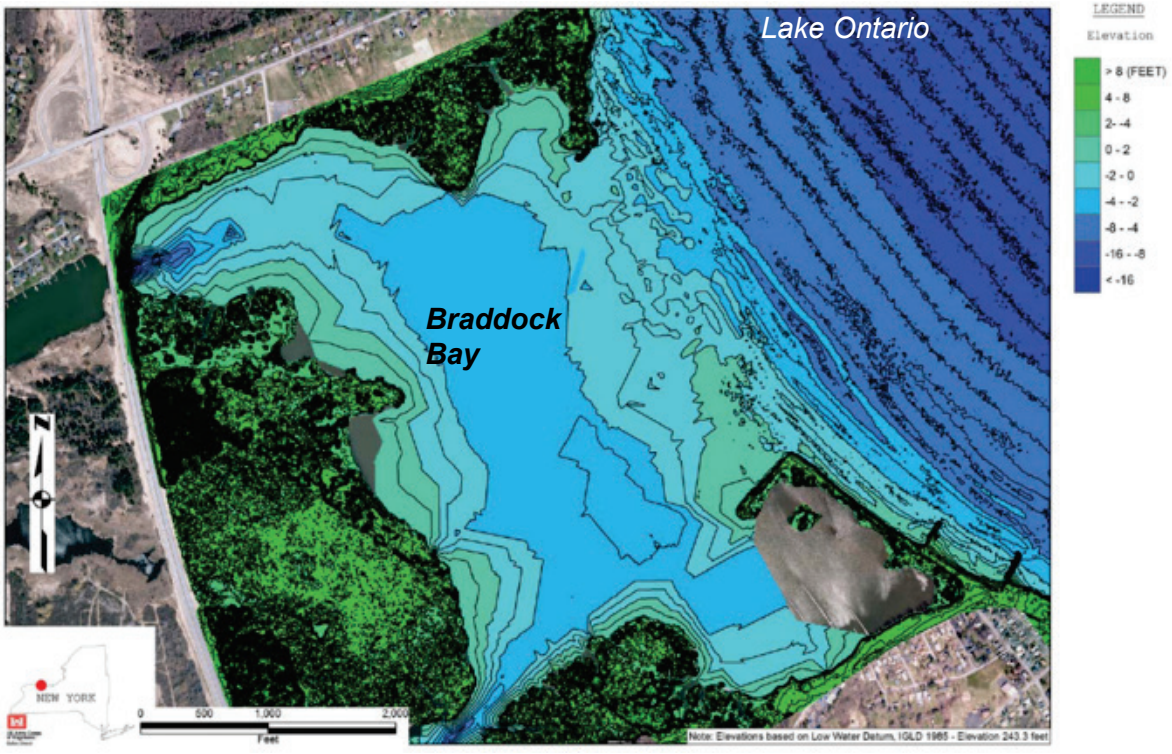

Approved for public release; distribution is unlimited.

Engineer Research and
Development Center

The U.S. Army Engineer Research and Development Center (ERDC) solves the nation's toughest engineering and environmental challenges. ERDC develops innovative solutions in civil and military engineering, geospatial sciences, water resources, and environmental sciences for the Army, the Department of Defense, civilian agencies, and our nation's public good. Find out more at www.erdc.usace.army.mil.

To search for other technical reports published by ERDC, visit the ERDC online library at http://acwc.sdp.sirsi.net/client/default.

Coastal Inlets Research Program
Dredging Operations and Environmental Research Program
Water Operations Technical Support Program

ERDC TR-14-8
March 2015

Modeling of Waves, Hydrodynamics and Sediment Transport for Protection of Wetlands at Braddock Bay, New York

Zeki Demirbilek and Lihwa Lin

Coastal and Hydraulics Laboratory
U.S. Army Engineer Research and Development Center
3909 Halls Ferry Road
Vicksburg, MS 39180-6199

Earl Hayter

Environmental Laboratory
U.S. Army Engineer Research and Development Center
3909 Halls Ferry Road
Vicksburg, MS 39180-6199

Colleen O'Connell, Michael Mohr, Shanon Chader, and Craig Forgette

U.S. Army Corps of Engineers, Buffalo District
1776 Niagara Street
Buffalo, NY 14207

Final report

Prepared for U.S. Army Corps of Engineers, Buffalo District
1776 Niagara Street, Buffalo, NY 14207

Under CIRP, DOER, WOTS Programs

Abstract

This report describes a numerical modeling study of waves, currents, and sediment transport at Braddock Bay, New York, that are affecting the wetlands in this estuary. The wetlands have had damage by waves that penetrate deep into the bay from the Lake Ontario side. The purpose of this study was to investigate three proposed alternatives using different structural systems at the entrance of Braddock Bay to minimize the impacts of environmental forces on wetlands. Braddock Bay has had steady erosion and retreat of the shorelines outside and within the bay system in the last century. The bay complex in the present state has become fully exposed directly to the winds and waves from the lake side.

The proposed structural alternatives at the bay entrance were evaluated on their ability to reduce potential impacts of waves and currents on wetlands. Study results indicated all three proposed alternatives were able to reduce waves, currents, and sediment transport substantially in the bay. The primary goal of the study was to develop a quantitative estimate of waves and flow in the bay for a relative comparison of the alternatives investigated.

Contents

Figures and Tables

Figures

Tables

Preface

This study was performed at the request of the U.S. Army Engineer District, Buffalo (LRB) by the Coastal and Hydraulics Laboratory (CHL) and Environmental Laboratory (EL) of the U. S. Army Corps Engineer Research and Development Center (ERDC).

ERDC researchers from the Coastal Inlets Research Program (CIRP), Water Operations Technical Support Program (WOTS), and Dredging Operations and Environmental Research (DOER) program participated in phases of this project. During the period of this modeling study, Program Managers for CIRP, DOER, and WOTS respectively were Drs. Julie Rosati, Todd Bridges, and Patrick Deliman. The CIRP provided partial support for the numerical modeling study. CIRP and DOER are two research and development programs in the Navigation Business Line administered by the USACE-Headquarters under the direction of W. Jeff Lillycrop, Technical Director, and Charles E. Wiggins, Associate Technical Director.

The numerical modeling study was conducted by Drs. Zeki Demirbilek, Lihwa Lin, and Earl Hayter, who also wrote this report. Colleen O'Connell and Michael Mohr, Shanon Chader and Craig Forgette, all of LRB, provided oversight of the study and reviewed the report. The report was reviewed internally by Dr. Sung-Chan Kim and Alison Sleath Grzegorzewski of ERDC. Technical work was conducted under the general administrative supervision of Dr. Jackie Pettway, the Acting Chief of the Navigation Division of CHL; Dr. Richard Styles and Jose Sanchez were the Acting Deputy Director and Director of CHL, respectively, during this study period.

COL Jeffrey R. Eckstein was the Commander of ERDC, and Dr. Jeffery P. Holland was the Director.

Unit Conversion Factors

Multiply	By	To Obtain
degree (angle)	0.01745329	radian
feet	0.3048	meter
inch	0.0254	meter
gallon (U.S. liquid)	0.003785412	cubic meter
gallon (U.S. liquid) per minute per foot	0.00020699	cubic meter per second per meter
pound (mass)	453.59237	gram
pound (force)	4.448222	Newton
cubic yard	0.7645549	cubic meter
feet	0.3048	meter
cubic yard	0.7645549	cubic meter
yard	0.9144	meter

1 Introduction

1.1 Background

Braddock Bay is located approximately ten miles northwest of Rochester, NY, and it is a relatively shallow estuary with an open entrance that connects the bay to Lake Ontario. The wetlands located in the back side of bay are unprotected from the storms in the lake. Storm waves and currents through the open entrance of the bay into the unsheltered shallow backbay of this estuary can damage the wetlands. Historical morphology changes at Braddock Bay have been attributed to sedimentation caused by waves, currents, and river inflows. Effects of these forces on wetlands and navigability are examined using the Coastal Modeling System (CMS), an integrated numerical tool which includes a spectral wave model and a two-dimensional depth-averaged hydrodynamic model with sediment transport calculations.

The calibration and validation of CMS has been described in detail in a series of four reports (see Demirbilek and Rosati 2011 for a summary), which included approximately 30 test cases. For field testing at bays and estuaries, the Grays Harbor, WA, and Matagorda Bay, TX, were amongst the calibration and validation cases. An application of CMS for mixed sediment transport in a bay and estuary setting similar to Braddock Bay has been described in the Matagorda Bay study report (Lambert et al. 2013). The development of fine-grained and mixed sediment capabilities in CMS is continuing. The goal of this numerical modeling study was to develop estimate of waves, currents, and sediment transport in the bay for a relative comparison of alternatives. Because there was no field data at Braddock Bay, the qualitative estimates of waves, flow, and sediment transport developed were used in the evaluation of proposed solutions. The preliminary modeling results helped to assess general sediment pattern changes in Braddock Bay caused by introduction of the proposed structural alternatives.

Braddock Bay is located about 10 miles northwest of Rochester, NY. As shown in Figures 1-1 and 1-2, the bay on Lake Ontario is the westernmost of a series of bays and ponds along this section of lakeshore. Figure 1-3 shows the shoreline change that has occurred at Braddock Bay from 1902 to 2009. The Salmon Creek and Buttonwood Creek (Figure 1-3) connect to

Lake Ontario through the bay. Figures 1-4 through 1-6 show the historical shoreline changes for 1961-1979, 1979-1994, and 1994-2009, respectively.

Figure 1-1. Location map for Braddock Bay, NY.

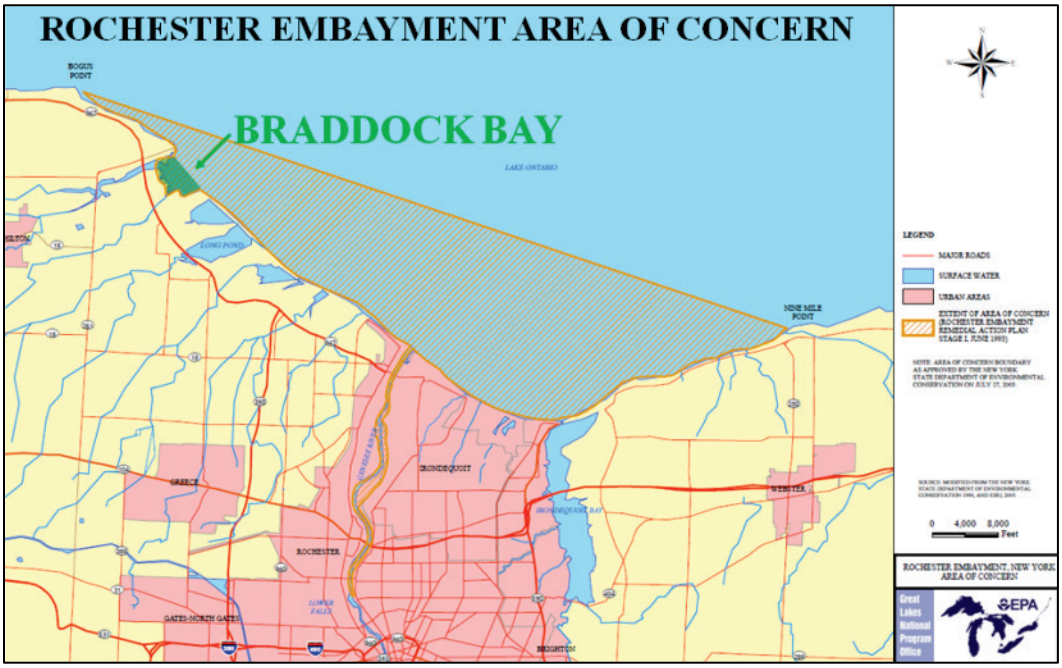

Figure 1-2. Ponds along the south shore of Lake Ontario.

Figure 1-3. Shoreline change in Braddock Bay from 1902-2009.

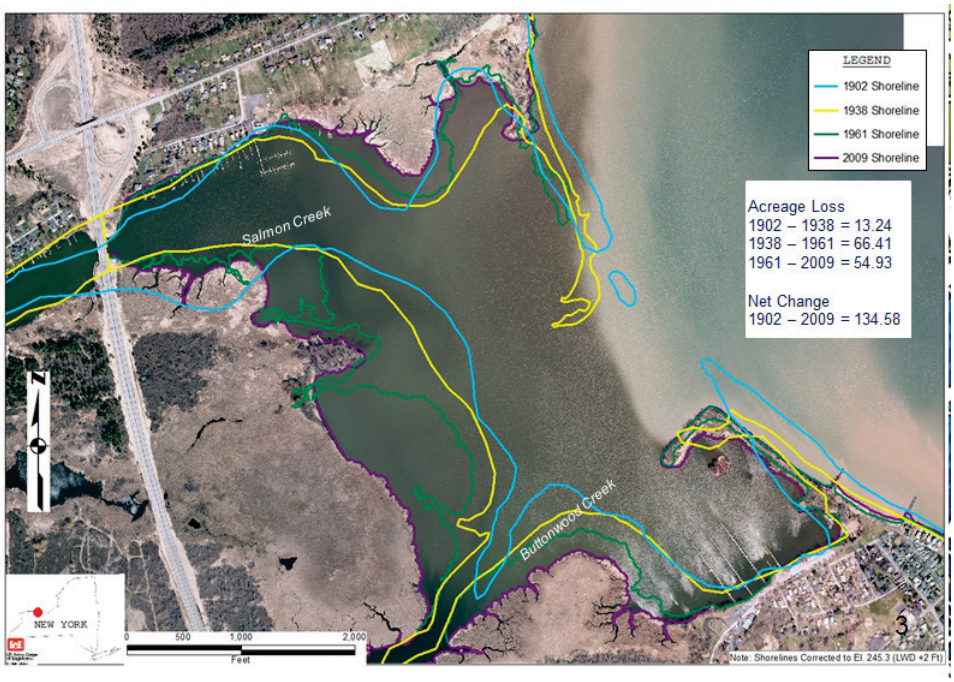

Figure 1-4. Central and southern shoreline change (1961-1979).

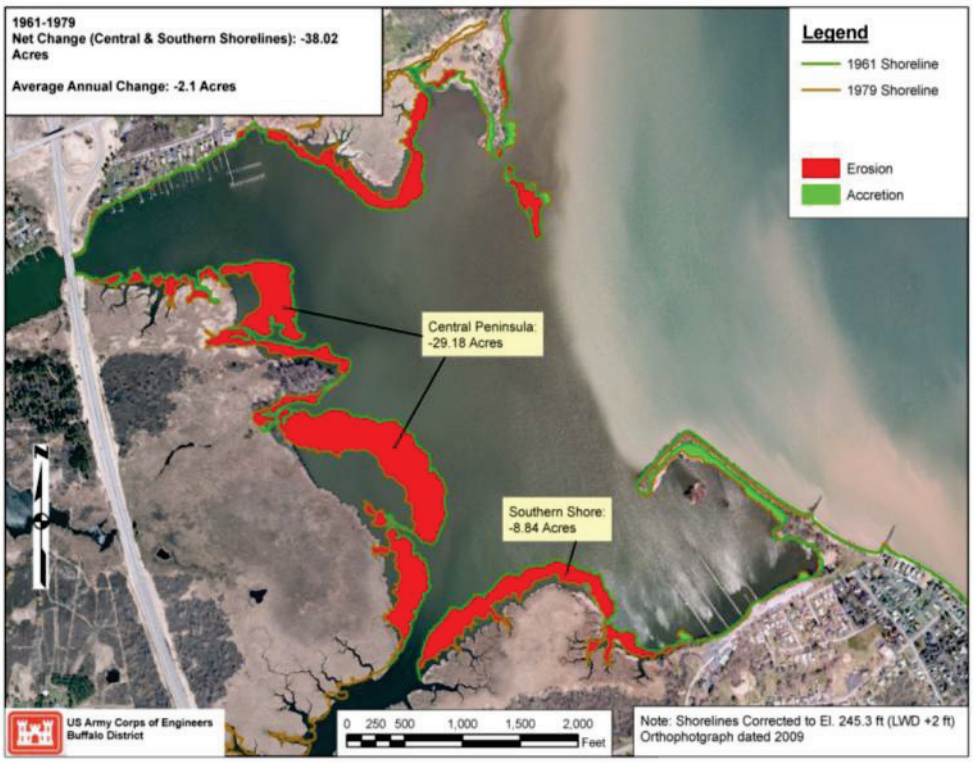

Figure 1-5. Central and southern shoreline change (1979-1994).

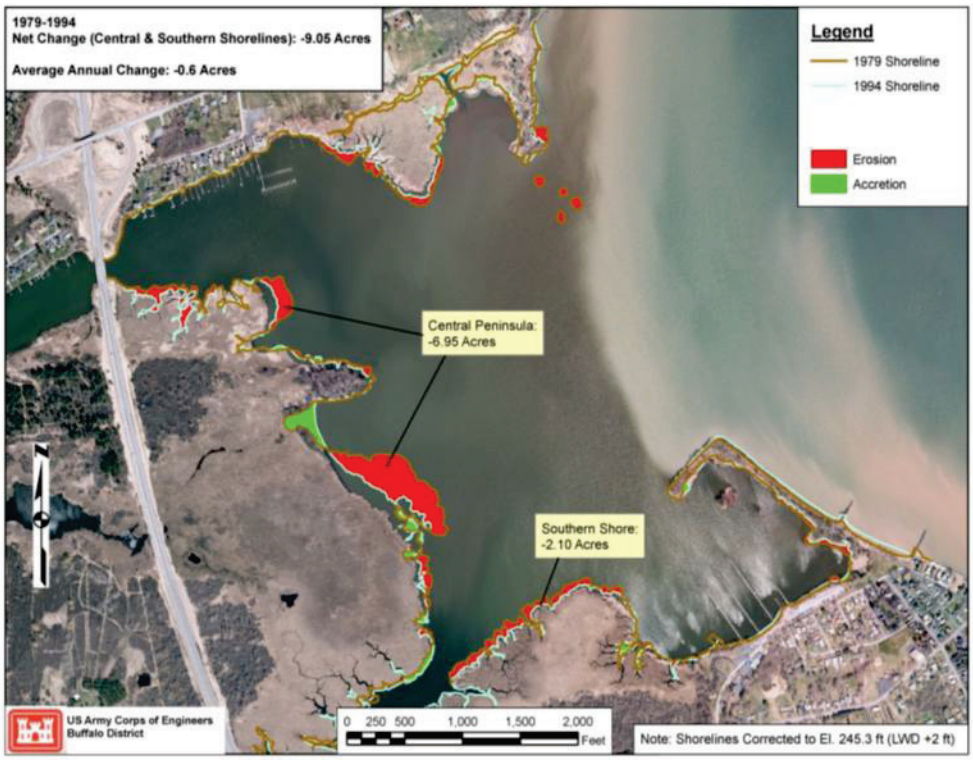

Figure 1-6 Central and southern shoreline change (1994-2009).

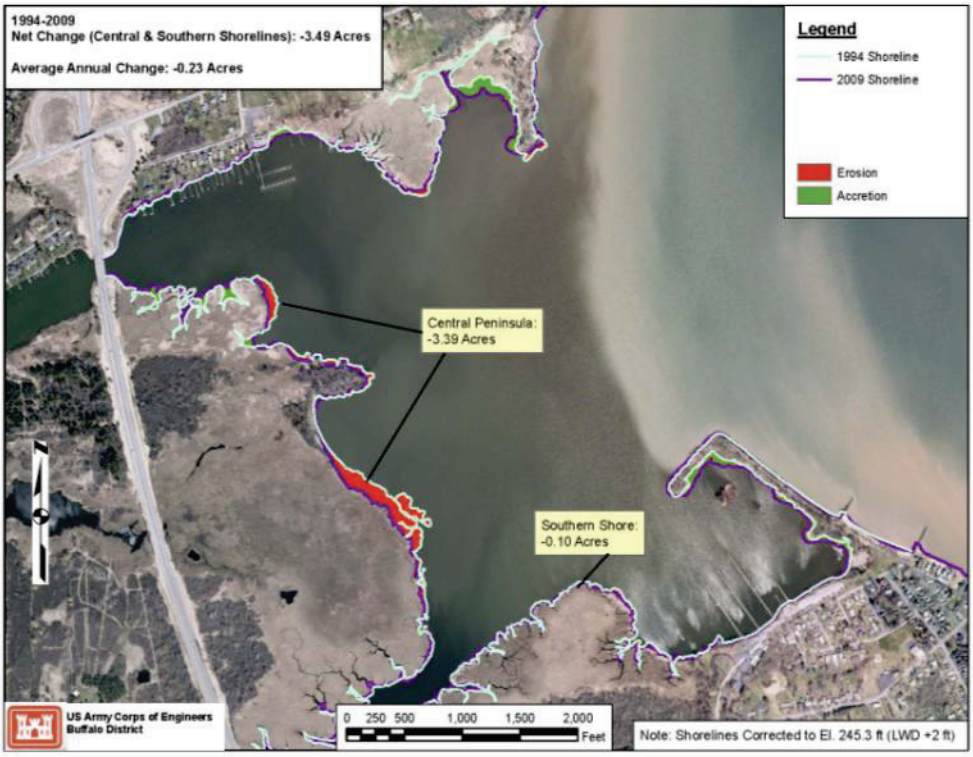

Because the barrier beach has eroded during the last century, the bay has lost significant coastal wetlands and ecological habitat. After the loss of barrier beach, the wetlands and interior marshes surrounding the bay have been exposed directly to the open lake side forcings (winds, waves, currents, and water levels), causing bay-wide shore erosion and decrease of total marsh acreage. The main goal of this study was to reduce wave energy and current in Braddock Bay to mimic the interior bay coastal conditions that had existed when the barrier bar was intact at the start of 1900.

Details of Braddock Bay barrier bar evolution are discussed in Chapter 2. A short synopsis is given here to highlight some major changes that have occurred during the last century. At the turn of the 20th century, a trolley line extended across the bay along the barrier bar that spanned the full length of the entrance as late as 1902. The trolley line was later abandoned as the barrier bar had gradually eroded away and shifted landward into the bay. The remnants of the barrier bar still exist at the northwestern and southeastern openings of the bay. In essence, Braddock Bay has gradually transformed from a barrier beach lagoon system in 1900 to an open embayment.

As the barrier bar continued to erode over the last century, the bay became further exposed to actions of waves and currents. A spit developing at the southeastern down-drift side was armored, and this has caused the shifting and erosion of the land and bar formation locally. A similar spit developed at the northwestern side, and it also eroded under continuous wave attack and strong nearshore currents. The barrier bar disappearance at the bay entrance combined with changes to the northwestern and southeastern spits have increased wave action within the bay. This led to a decrease in suitable aquatic habitat and damage to wetlands. The shorelines within the bay system have been retreating at an average rate of 1.3 acres per year (Figure 1-3) since 1902. Note that the rate of erosion varies with each time period.

Based on the historical shoreline change depicted in Figure 1-3, it is necessary to shelter the bay to the maximum extent possible from the lake-side waves and currents. This can be done by reducing the lake-bay connectivity at the entrance, which is the gateway for the exchange between the bay and lake. This can be achieved by practically joining the north and south barrier beaches with either continuous or segmented structures placed along the bay entrance. Such structural systems have been considered and

investigated numerically in this study. The primary purpose of the present study was to develop estimates of waves and currents that drive sediment pathways inside the bay and along the north and south barrier beaches. The results of this modeling could be used to identify the sources and sinks of sediment, and determine the magnitude and direction of transport processes that move sediments through different sections of the bay, including where the wetlands are present.

Water-quality modeling, including water exchange between the bay and Lake Ontario and total phosphorous loading is important to the socio-economics and health of the bay. It is being investigated in a separate study to determine water-quality characteristics of the existing bay and changes caused by the proposed structural systems.

1.2 Objective

The objective of the study was to analyze characteristics of waves, currents, and morphology change in relation to impacts of these on the wetlands located at the back side of the central bay. Various physical forcings affect the wetlands, navigation, and morphology change at Braddock Bay and vicinity. The contributing meteorological and oceanographic (metocean) forcings are winds, waves, water levels, and creek flows, which are considered in this modeling study.

It is emphasized that the objective of the study was neither to develop a detailed quantitative estimate of sediment transport or structural design. The goal was to characterize the combined effects of waves, currents, and sediment transport on wetlands and navigation issues at Braddock Bay by investigating individual roles of these contributing physical forcings. Final design calculations should be either validated with field data or checked by estimates from other two- or three-dimensional numerical models. This report presents details of numerical modeling tasks, results, and findings of the first-phase study. Although water quality and navigation were not in the scope of this study, modeling results are also applicable to addressing these issues in the bay.

2 Study Needs and Plan

2.1 Background

As a follow up to recently completed restoration feasibility investigation of Braddock Bay, the U. S. Army Corps of Engineers (USACE), Buffalo District, is conducting a study to evaluate shoreline protection measures for coastal wetlands at Braddock Bay. It includes approximately a 300-acre coastal wetland site, which is one of the largest and important coastal freshwater wetlands in the State of New York. Braddock Bay is located on the south shore of western part of Lake Ontario (Figure 2-1). It is not a federally maintained inlet. Dredging in parts of the bay has been done by local users.

Figure 2-1. Aerial photo showing main features of project location.

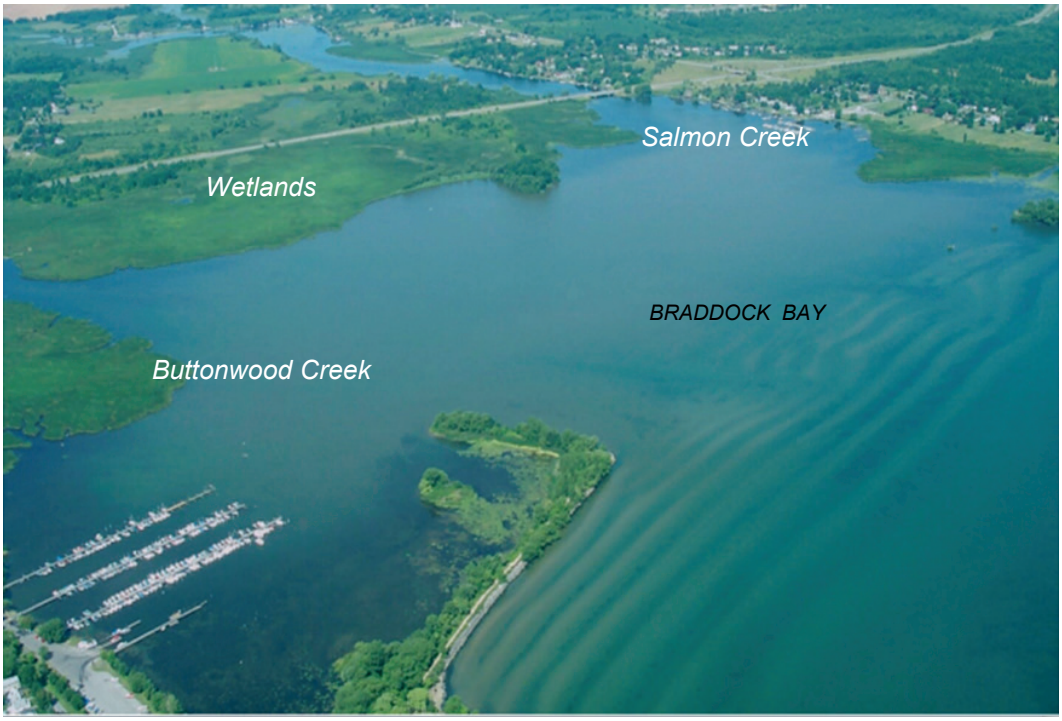

The loss of significant ecological habitat in Braddock Bay was attributed in the earlier LRB study by Baird & Associates to the erosion of a barrier beach used to protect the bay. The bay was once separated from Lake Ontario by a sandy barrier beach prior to 1900, so it was essentially a barrier beach-lagoon system in the 1800s. This nearly 5,000 ft (1,524 m) long barrier in 1890 has since diminished, and in 2009 it was less than half the original length. As a result, the bay has lost approximately 135 acres (1.3

acre/yr) from 1902 to 2009. Accordingly, the bay and habitat size has decreased, turning into a spit and embayment in the early 1900s. A history of barrier beach evolution at Braddock Bay spanning about 200 yrs is illustrated in Figure 2-2.

Figure 2-2. The historical change in acreage at Braddock Bay from 1811 to 1998.

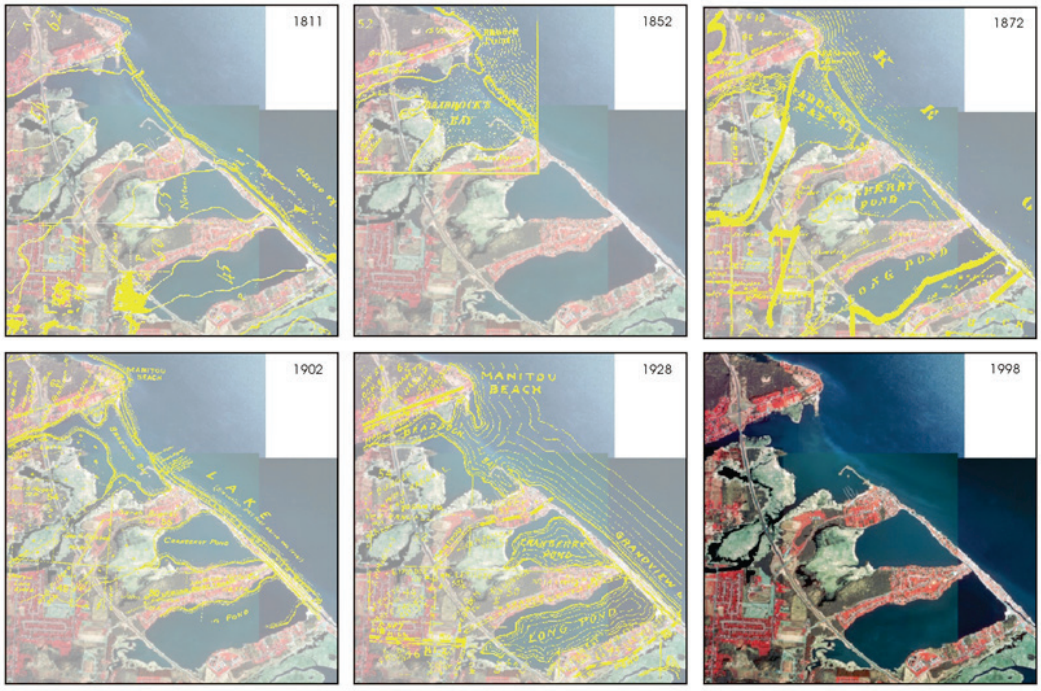

This erosional trend at Braddock Bay has continued in the second half of 1900s. The bay has, since the 1950s, become an open-lake embayment system, losing approximately 55 acres from 1961 to 2009. It is emphasized that this evolution occurring in the bay during the last two centuries is not a recent phenomenon, and continual erosion is expected. Figure 2-3 shows the acreage loss that has occurred in different areas of the bay in about last 50 yrs, from 1961 to 2009.

Figure 2-3. The change in acreage at Braddock Bay from 1961 to 2009.

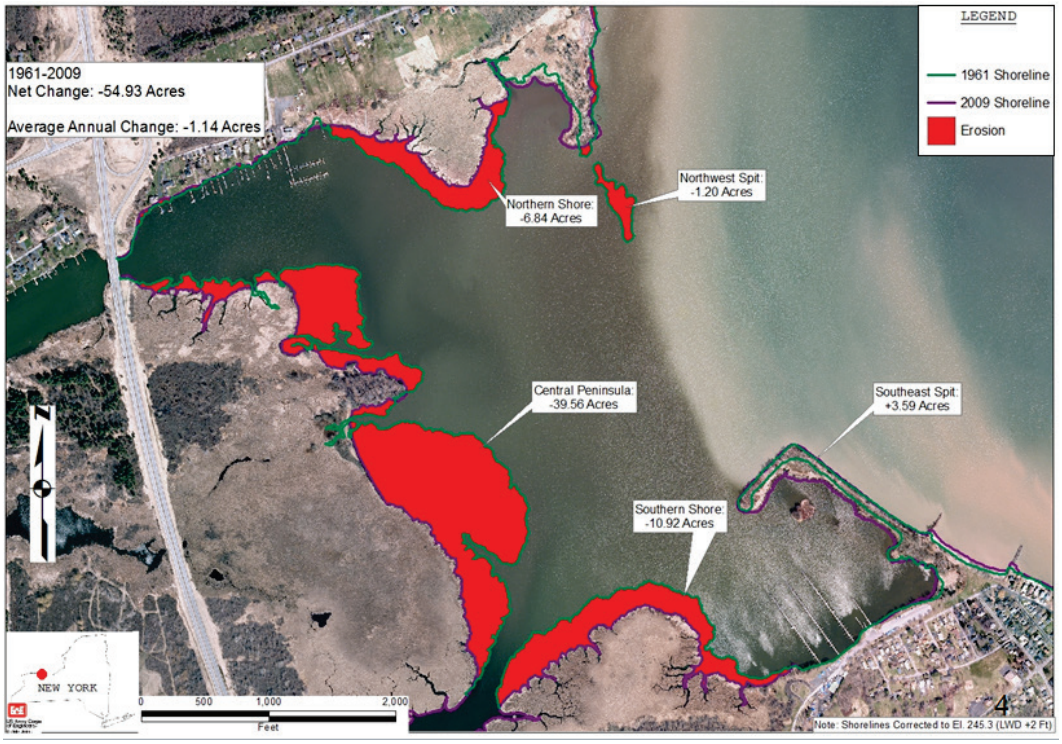

A 5,000 ft (1,524 m) long sandbar that spanned the entire length of bay entrance isolated the bay from the lake until 1902. The sandbar stretched the full length of entrance until the early 1900s, but gradually eroded and moved into the bay over ensuing decades. There used to be a railroad located on the sandbar, and a trolley line ran across the bay along this barrier bar, which was abandoned later. By the 1950s, most of the barrier bar had eroded and disappeared, and Braddock Bay became exposed to direct wave action.

The bay had also two natural spits at the northwestern and southeastern openings of the bay, and both of these also have gradually eroded away and shifted landward into the bay. With increasing residential developments along the beaches during the second half of 20th century, the armoring of southeastern and northern spits was sought by local residents. These armorings have slowed down erosion due to continuous nearshore breaking waves and strong currents emanating from Lake Ontario (Figure 2-4).

Figure 2-4. Armoring of north barrier shoreline at Braddock Bay.

The continued erosion of barriers increased the exposure of Braddock Bay to environmental forcings. The action of winds, waves, currents, and sediments mobilized by these had a toll on the entire embayment. Waves approach the bay from both the east and north directions. Larger storm waves are from the northwest, which refract and shoal around the edge of the north spit, and break as they enter the basin. The clockwise circulation within the bay produces erosional hot spots in the south and central regions. Generally, the longshore transport along the south shore of Lake Ontario in the vicinity of Braddock Bay is southward. The southern side of Braddock Bay has gained sand that consists of finer material as compared to the large grain sand and gravel found along the north shoreline. The south bar is not sheltered from storms, northeasters, and hurricanes.

The long fetch distances to Braddock Bay (Figures 1-1 and 2-1) allow for large wind waves to generate and grow, and waves developing in the lake move over the remnants of sandbars to get in to the bay to reach the wetlands. The direct exposure of the bay to lake waves must be minimized to reduce the effects of waves on the wetlands, which are situated in back of the central bay (Figure 2-5). As shown in Figures 1-4 through 1-6, the shorelines surrounding the bay have long experienced progressive flooding and erosion due to large wind waves approaching the bay from a half-

plane sector (E-N-W). Due to prevailing wind, wave, and current patterns, the longshore transport along the bay's outside barrier beaches is generally directed southerly.

Figure 2-5. Back side of central bay region with wetlands.

2.2 Objectives

The objectives of this study are to perform numerical modeling in support of a feasibility investigation of structural alternatives capable of reducing wave energy throughout the bay complex to minimize shoreline erosion, protect wetlands, and sustain navigation (e.g., potential shoaling at the bay entrance). Three structural alternatives are proposed and evaluated. The alternatives are named as S-1, S-2, and S-3 (with project), while S-0 represents the existing bay (without project). Figures 2-6 to 2-9 show the geometries of S-0, S-1, S-2, and S-3, respectively. The elevation presented in Figure 2-6 is a merged bathymetry dataset, which includes the following: 2011 offshore Lidar data from the Joint Airborne Lidar Bathymetry Technical Center of Expertise (JALBTCX), 2007 topographic data from JALBTCX Lidar, and July 2012 survey taken within the bay.

Figure 2-6. Existing configuration S-0 (without project) with bathymetric contours.

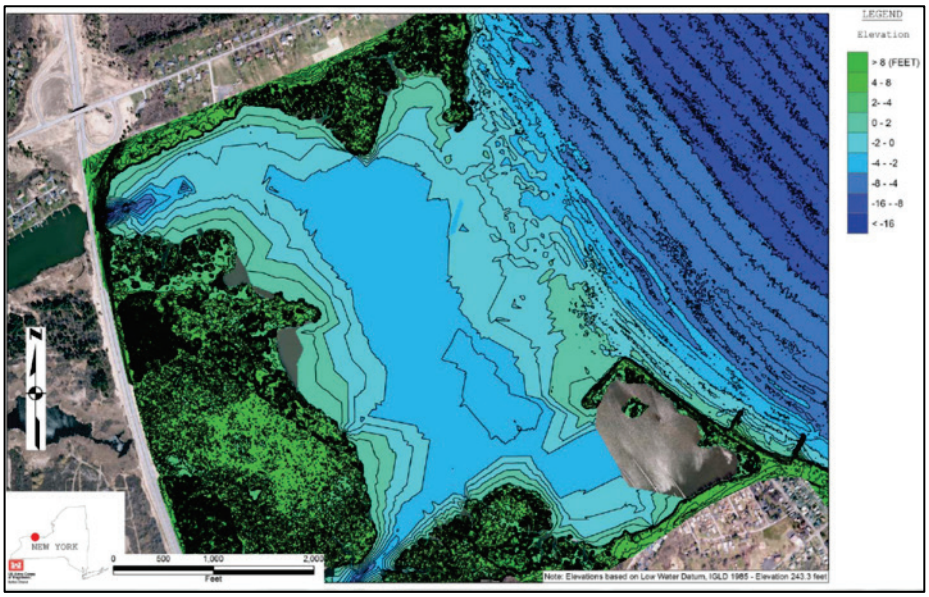

Figure 2-7. Alternative S-1 (with project), entrance blocked with four segmented breakwaters.

Figure 2-8. Alternative S-2 (with project), continuous breakwater with structured inlet.

Figure 2-9. Alternative S-3 (with project), entrance blocked partially with artificial headland breakwaters.

2.3 Metocean forcing types

The wave and hydrodynamic numerical modeling estimates have been developed for three meteorological and oceanographic (metocean) forcing types. This ensures that estimates include short- and long-term and extreme design conditions. The three forcing types considered were:

1. Tropical storm conditions were simulated with Hurricane Sandy for S-0, S-1, S-2, and S-3 configurations with three water level datums (WL = 0 ft, 2 ft, 4.7 ft) referenced to IGLD85 for Lake Ontario
2. Long-term conditions simulations were conducted for a 9-month period, March-November 2011, for S-0, S-1, S-2, and S-3 configurations.
3. Two design storm events were simulated with the associated winds and waves for S-0, S-1, S-2, and S-3 configurations at three specified water levels (WL = low, medium, high).

The effect of sea level rise is negligible for the Great Lakes. The sources of winds, water levels, and incident-wave bands used in the above simulations are described next in this chapter. A total of 40 conditions were simulated for these three groups of forcing types. An optimal design of three alternatives was performed and compared to the existing bay to determine

the maximum level of wave energy reduction in the bay. Estimates are provided for waves (wave height, period, and direction), water levels, currents, and morphology change along the footprints of the structural alternatives.

2.4 Data

Field data are required to set up and generate grids and other inputs for the numerical models used in this study. These data are grouped into two categories: (1) geo-spatial data, which include bathymetric and land elevation, shorelines, structures, and sediment characteristics, and (2) metocean data, which include meteorological and oceanographic inputs defining forcing conditions for models (e.g., winds, water levels, waves). LRB provided hydrographic survey data available for Braddock Bay and recent LIDAR (Light Detection and Ranging) data, past study reports, as well as other pertinent GIS (Geographic Information System) images and data files.

The ERDC and LRB team identified the pertinent metocean data available from various data sources, including previous studies conducted by Corps, other government agencies, and academic institutes. Land-based wind data were modified to over water conditions. The hurricane locally known as Superstorm Sandy (October 2012) and severe storm wind fields were assembled for input to numerical models.

2.4.1 Ice

Lake Ontario has the least amount of ice cover of the Great Lakes, with over 85% of the lake surface normally ice-free during the winter. Along the south shore of Lake Ontario, ice cover occurs over most of the smaller bays and ponds throughout western New York. Braddock Bay is relatively shallow and is one of the first of the larger bays in the lake to freeze each winter. The bay complex normally freezes in the period from middle December to early February.

2.4.2 Water levels

The lake water level fluctuates seasonally, and normal elevation of the lake surface varies irregularly from year to year. The water surface is subject to a consistent seasonal rise and fall. The lowest stage usually occurs in the late winter and the highest in the late summer.

Water-level measurements along the US shoreline are available from four NOAA (National Oceanic and Atmospheric Administration) coastal stations shown in Figure 2-10. These are Olcott, NY (Sta 9052076), Rochester, NY (Sta 9052058/RPRN6), Oswego, NY (Sta 9052030/OSGN6), and Cape Vincent, NY (Sta 9052000). Figure 2-11 and 2-12 show the water levels measured at Olcott and Rochester, and at Oswego and Cape Vincent, respectively, for 2008-2011. These figures clearly show consistent monthly change of water levels along the US side shoreline. The spatial variation of water levels is small at four NOAA stations. For this reason, the water-level data collected at Rochester, near Braddock Bay, were used in the present study.

Figure 2-10. NOAA coastal stations in Lake Ontario.

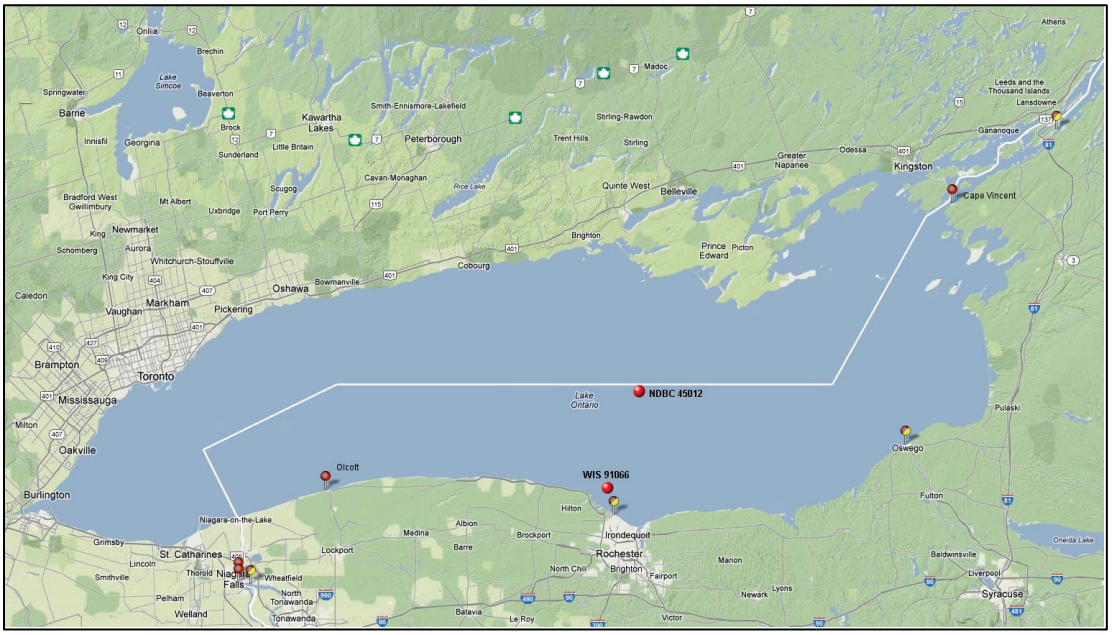

Figure 2-11. Water-level measurements from NOAA stations at Olcott and Rochester, NY, for 2008-2011.

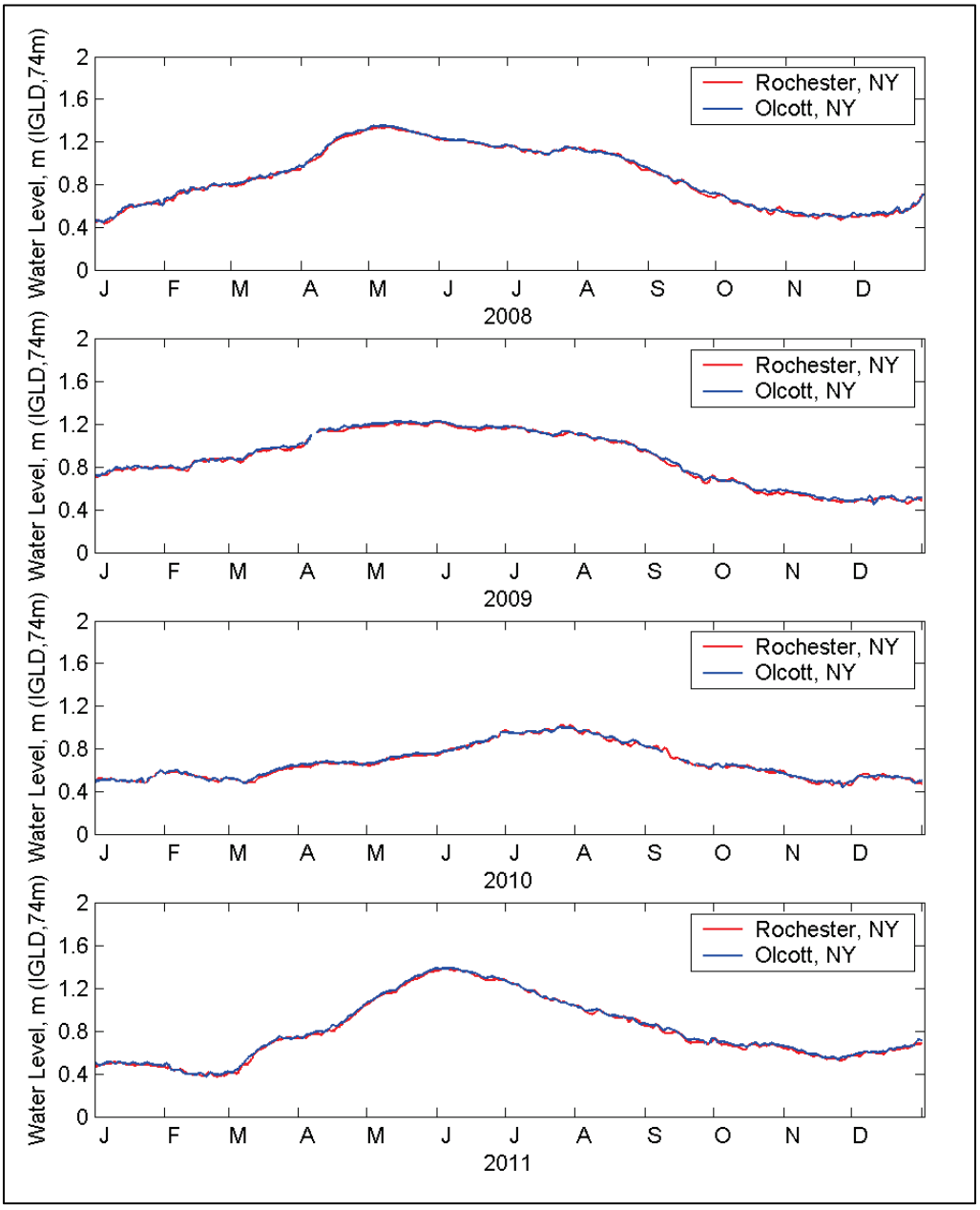

Figure 2-12. Water-level measurements at Oswego and Cape Vincent, NY, for 2008-2011.

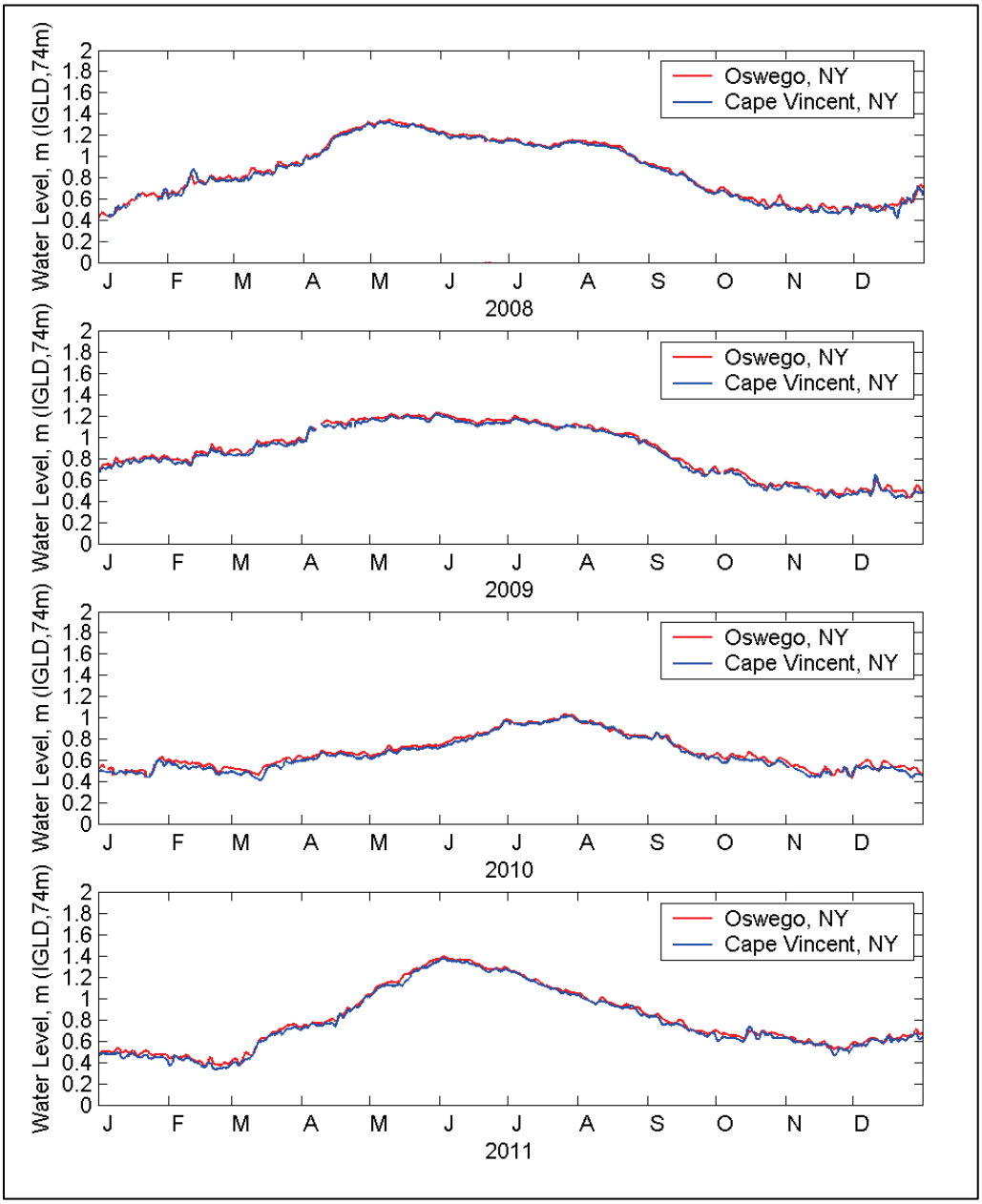

2.4.3 Winds and waves

Wind data are available from NOAA Stations Olcott, Oswego, Rochester, Cape Vincent, and from Buoy 45012 (Figure 2-10). Buoy 45012 is located in the middle of the lake and is normally deployed from late spring to late fall to avoid ice conditions. Wave data are also available from Buoy 45012. Figures 2-13 to 2-16 show the wind and wave data collected from Buoy 45012, and wind data from Oswego for 2008 to 2011, respectively. The

wave data from Buoy 45012 show a good range of wave height from 0.5 m to 6 m from late spring to late fall. The measured wave periods range from 2 to 9 seconds. The dominant wave direction is from west and is consistent with the prevailing wind direction in the same period. The wind at Buoy 45012 is similar to NOAA Oswego Coastal Station as both locations are geologically sensitive to strong wind from west. The Oswego Station data are more complete and available for the entire year. Wind data from both Oswego and Buoy 45012 are used in the present study.

Additional wave information for Lake Ontario is available from two databases: (1) approximately 40 yr hindcast data (1961-2000) from the Wave Information Study, WIS (http://wis.usace.army.mil), and (2) approximately the last 7 year (2006-2013) nowcast data from the Great Lakes Coastal Forecasting System, GLCFS (www.glerl.noaa.gov/res/glcfs). A coastal WIS Sta 91066 (77.67° W, 43.34° N) near Braddock Bay is shown in Figure 2-10. In the present study, the same WIS Sta 91066 is used as a GLCFS output location. Figure 2-17 shows the GLCFS output waves for 2011 at the same location as WIS Sta 91066. Figure 2-18 shows Buoy 45012 data and GLCFS output waves for 2012 with coastal wind data from Oswego Station. While wave heights from GLCFS and Buoy are similar, wave periods from GLCFS are overall smaller than the Buoy data. Figures 2-19 and 2-20 show the wind and wave roses, respectively, at WIS 91066 for 1961-2000. The wind rose shows the GLCFS dominant direction is from west while the wave rose shows the dominant wave direction is more from WNW as waves refract more toward the shoreline near Braddock Bay. Figure 2-21 shows the analyzed extreme waves for the 40 yr WIS data at Sta 91066.

2.4.4 River discharge

There are no direct flow measurements of Buttonwood Creek and Salmon Creek that discharge to Braddock Bay. However, the USGS measures flow rates at several rivers and creeks near Braddock Bay. These include Genesee River (Sta 04231600), Irondequoit Creek (Sta 04232205010), Allen Creek (Sta 042322050), West Creek (Sta 04220250), Oatka Creek (Sta 04230500), and Oak Orchard Creek (Sta 04220045). Among them, Genesee River is one of the major rivers emptying to Lake Ontario and Orchard Creek is the closest to Braddock Bay. Figure 2-22 shows the river discharges from Genesee River, Irondequoit Creek, Allen Creek, and West Creek for 2010. Figure 2-23 shows the flow rate of Oak Orchard Creek for 2010 and 2011.

Figure 2-13. Wind and wave data from Buoy 45012 and NOAA Stations 9052030 and RPRN6 for 2008.

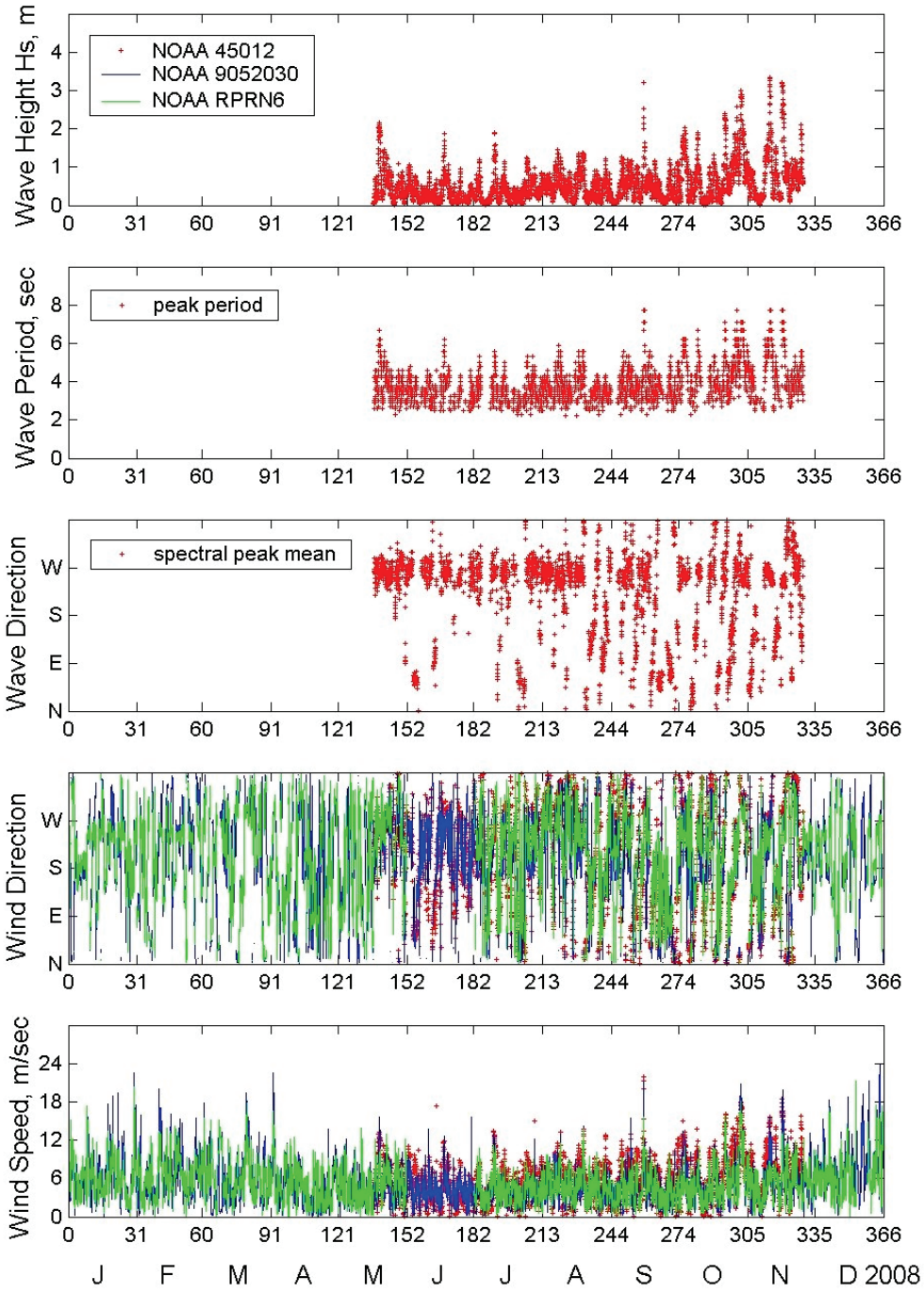

Figure 2-14. Wind and wave data from Buoy 45012 and NOAA Stations 9052030 and RPRN6 for 2009.

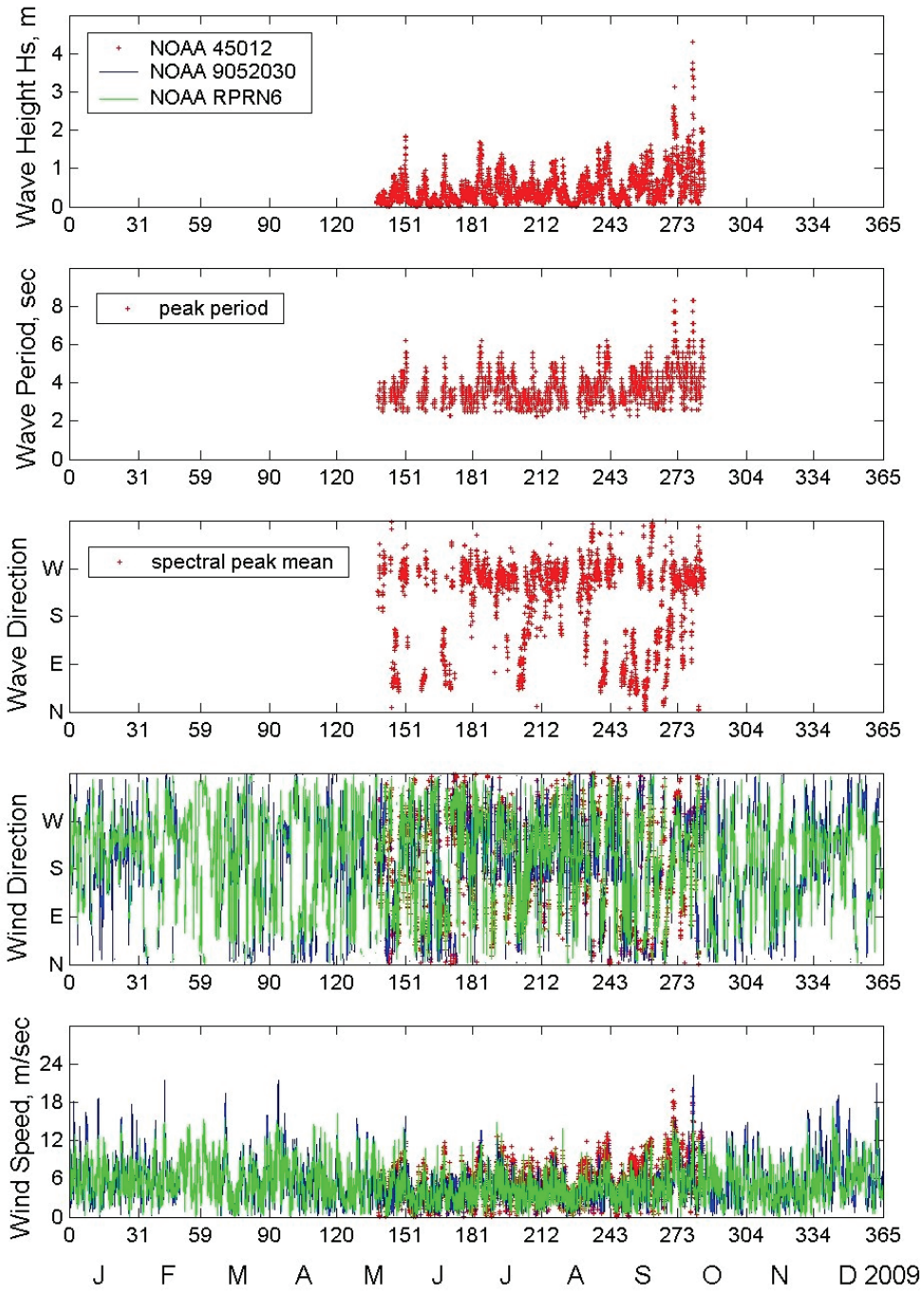

Figure 2-15. Wind and wave data from Buoy 45012 and NOAA Stations 9052030 and RPRN6 for 2010.

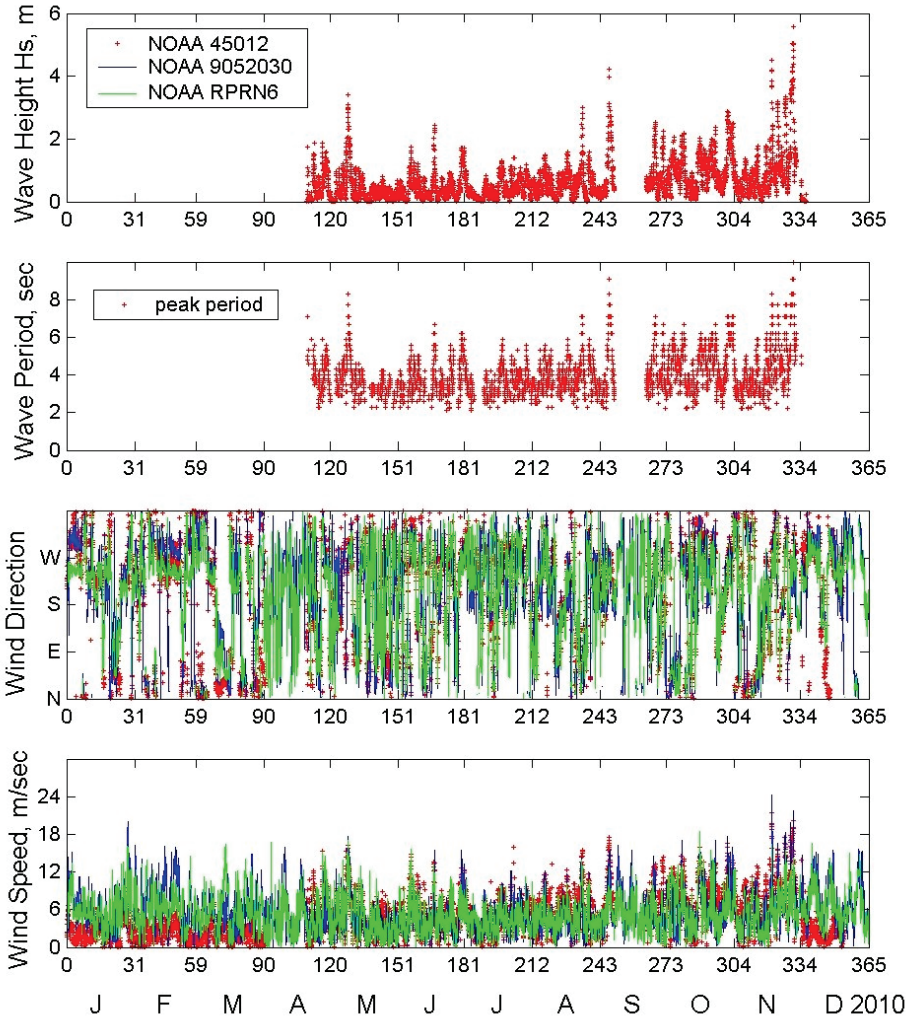

Figure 2-16. Wind and wave data from Buoy 45012 and NOAA Stations 9052030 and RPRN6 for 2011.

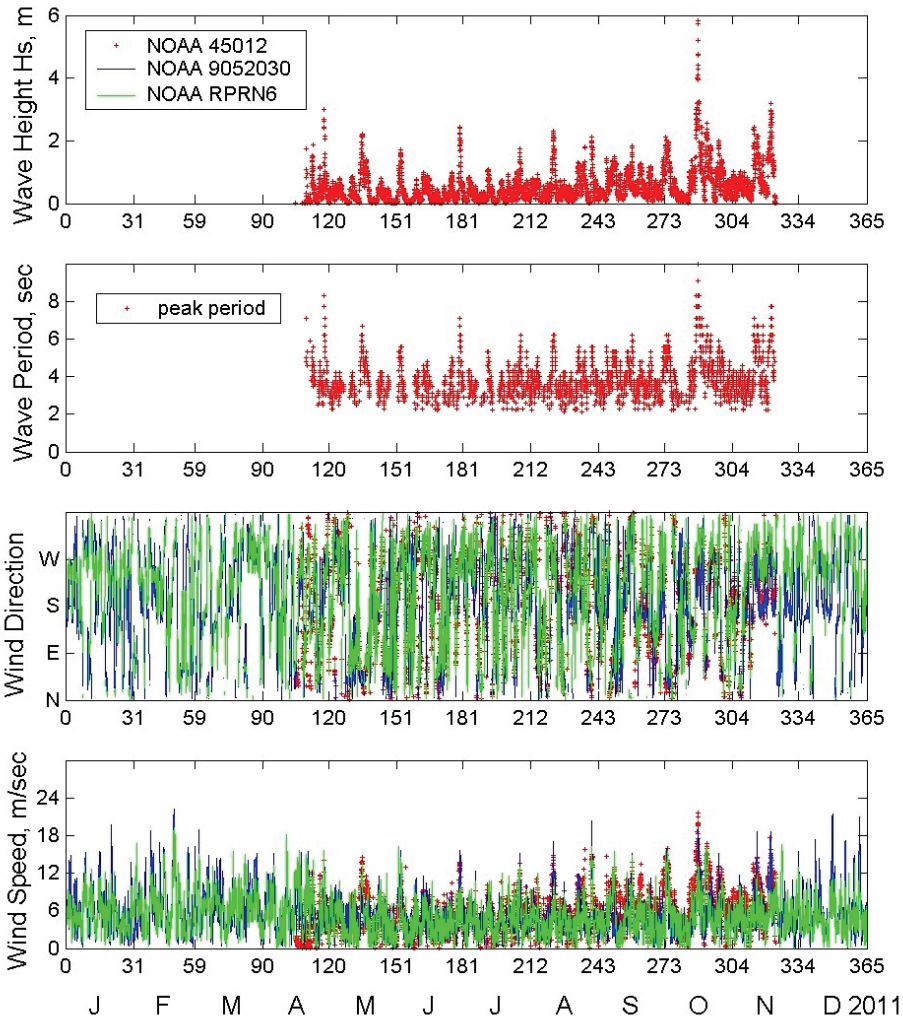

Figure 2-17. GLCFS nowcast waves for 2011 at the same location as WIS 91066.

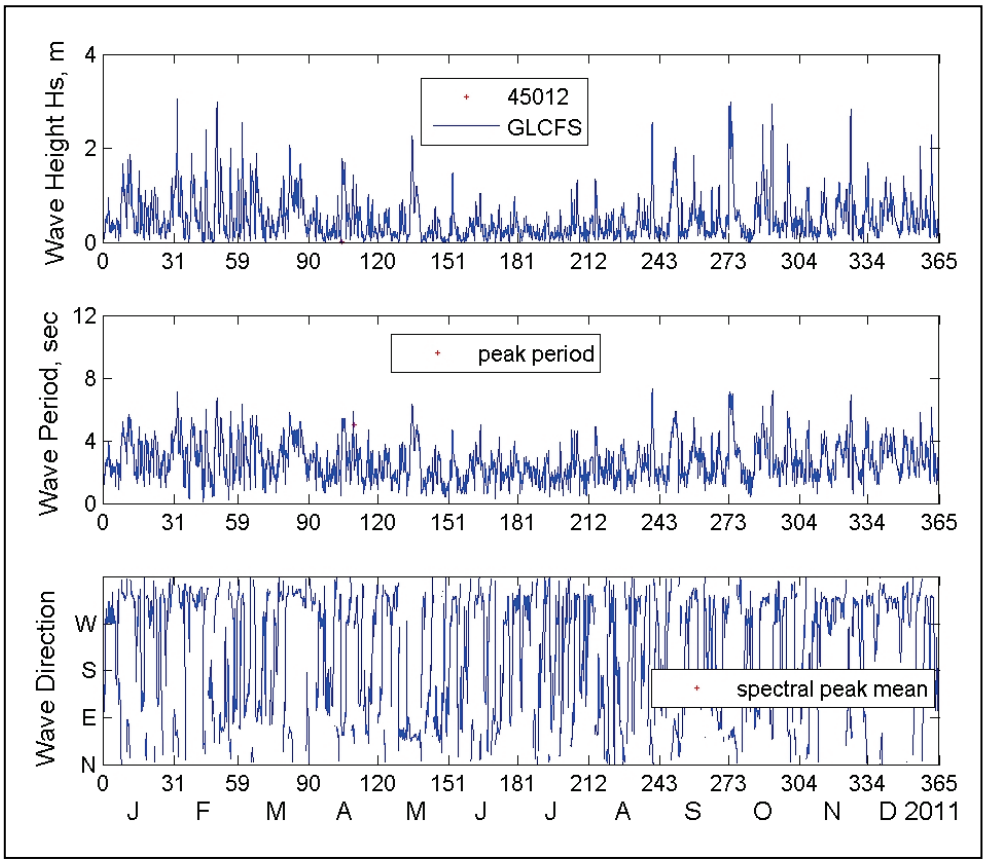

Figure 2-18. Buoy 45012, GLCFS, and Oswego data for 2012.

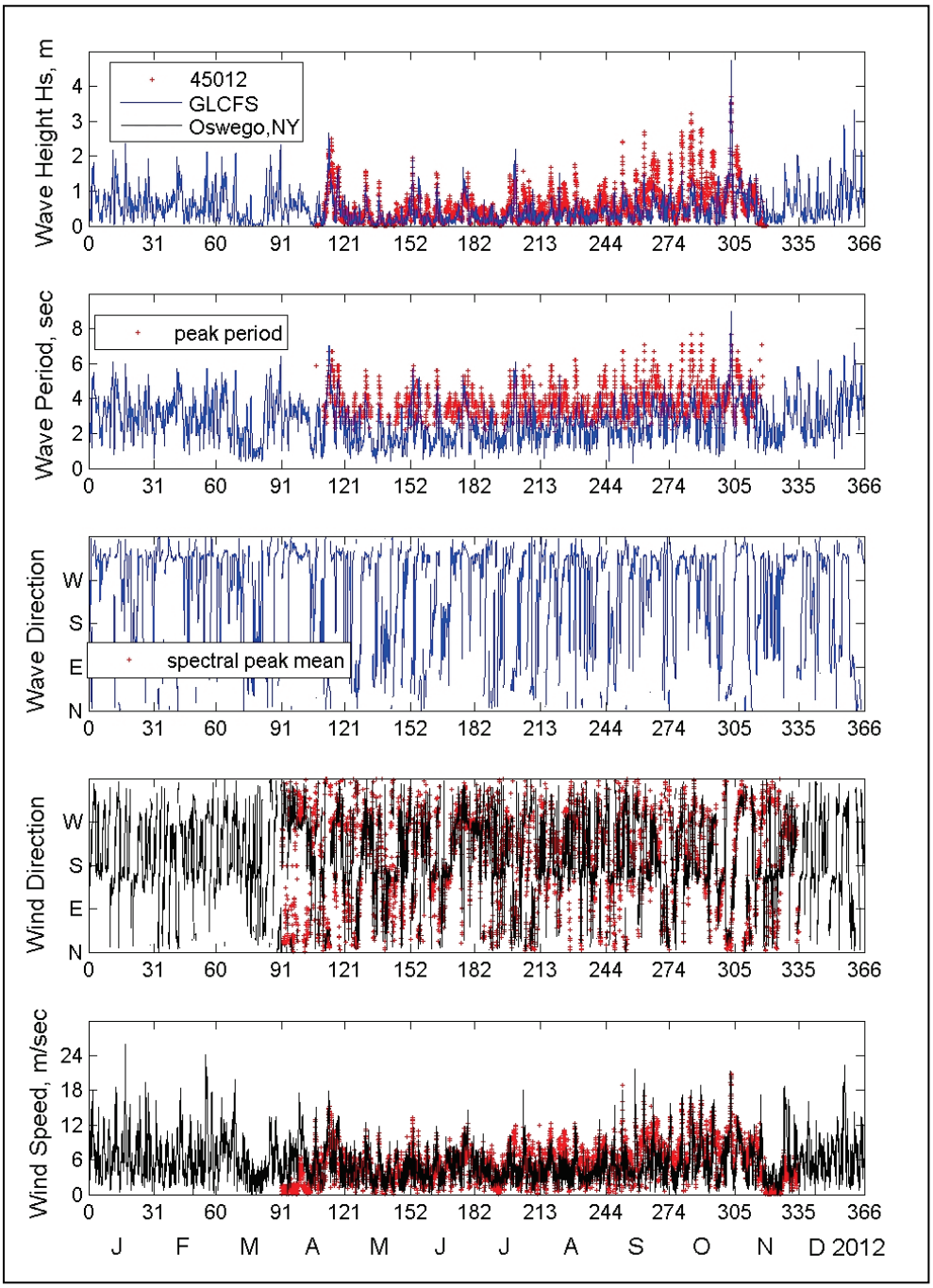

Figure 2-19. WIS Sta 91066 wind rose diagram for 1961-2000.

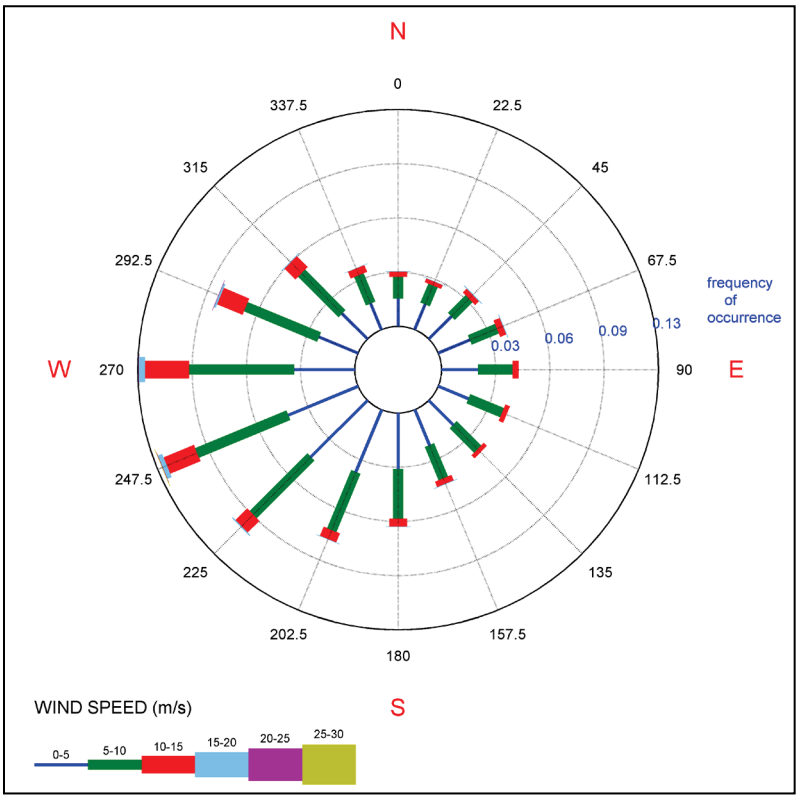

Figure 2-20. WIS Sta 91066 wave rose diagram for 1961-2000.

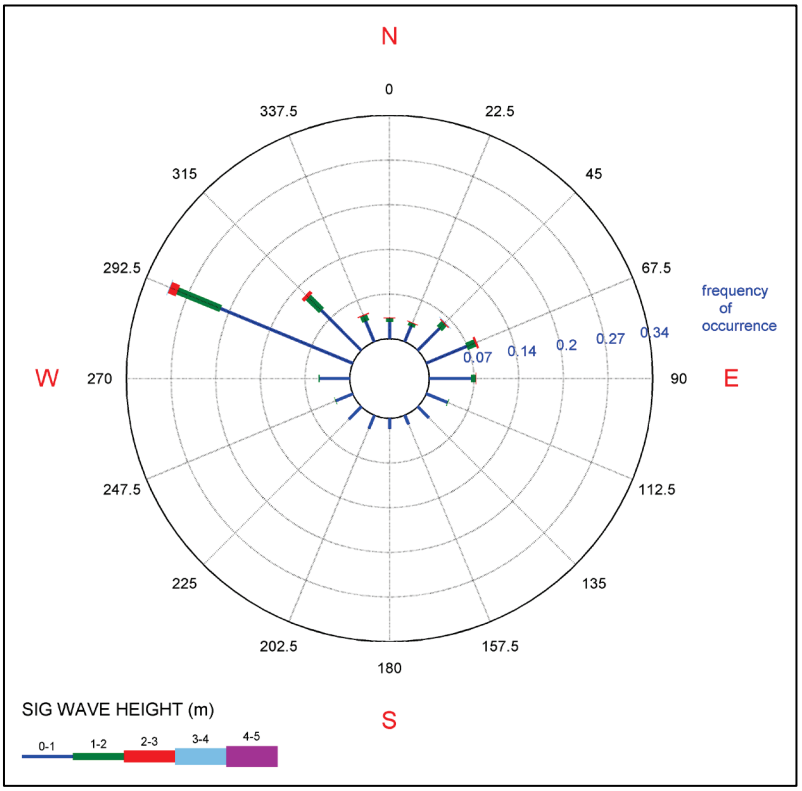

Figure 2-21. Extreme wave analysis for WIS Sta 91066.

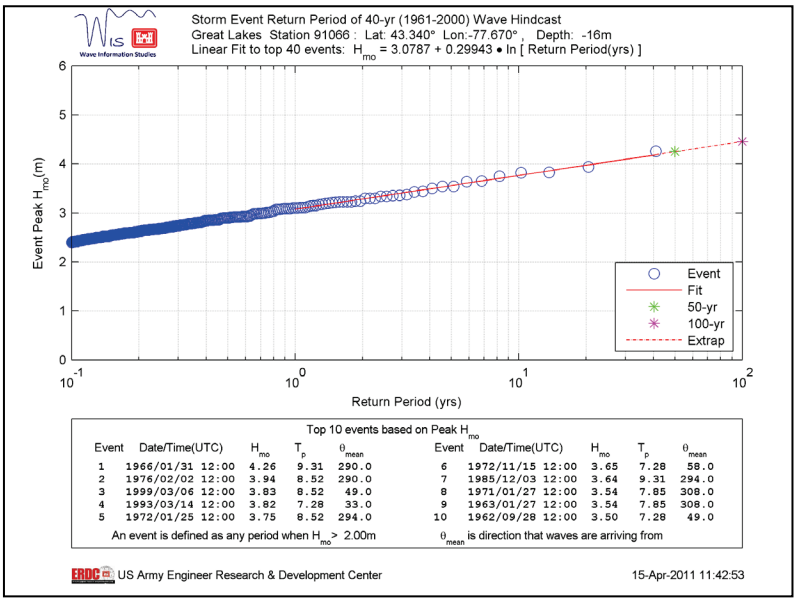

Figure 2-22. River discharges from Genesee River, Irondequoit Creek, Allen Creek, and West Creek for 2010.

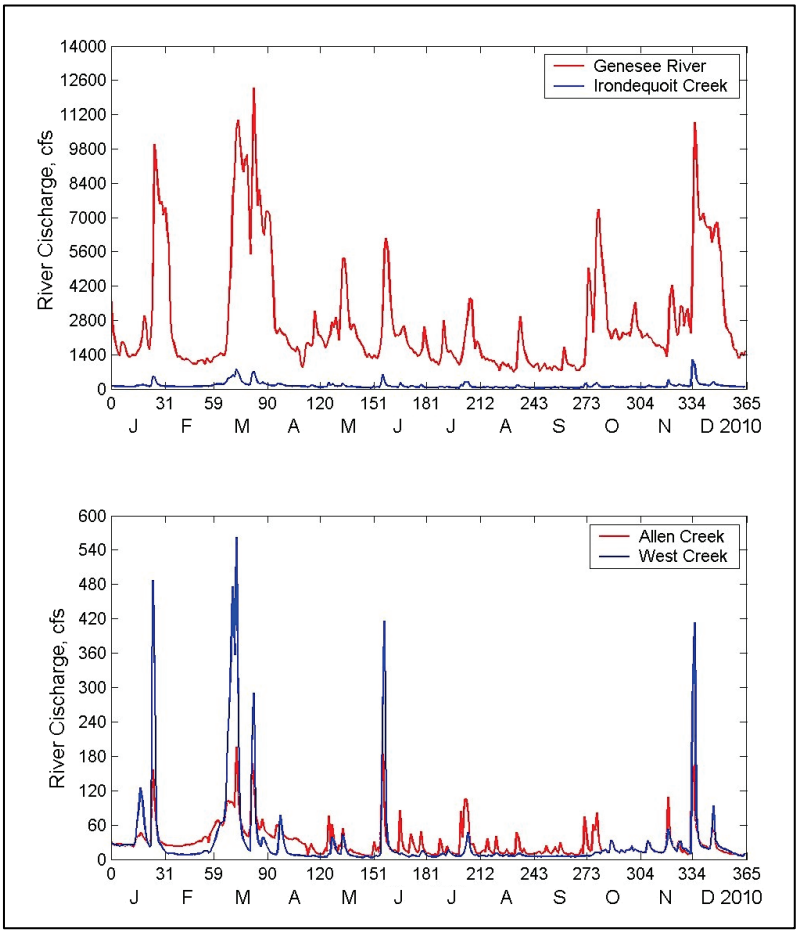

Figure 2-23. River discharges of Oak Orchard Creek for 2010 and 2011.

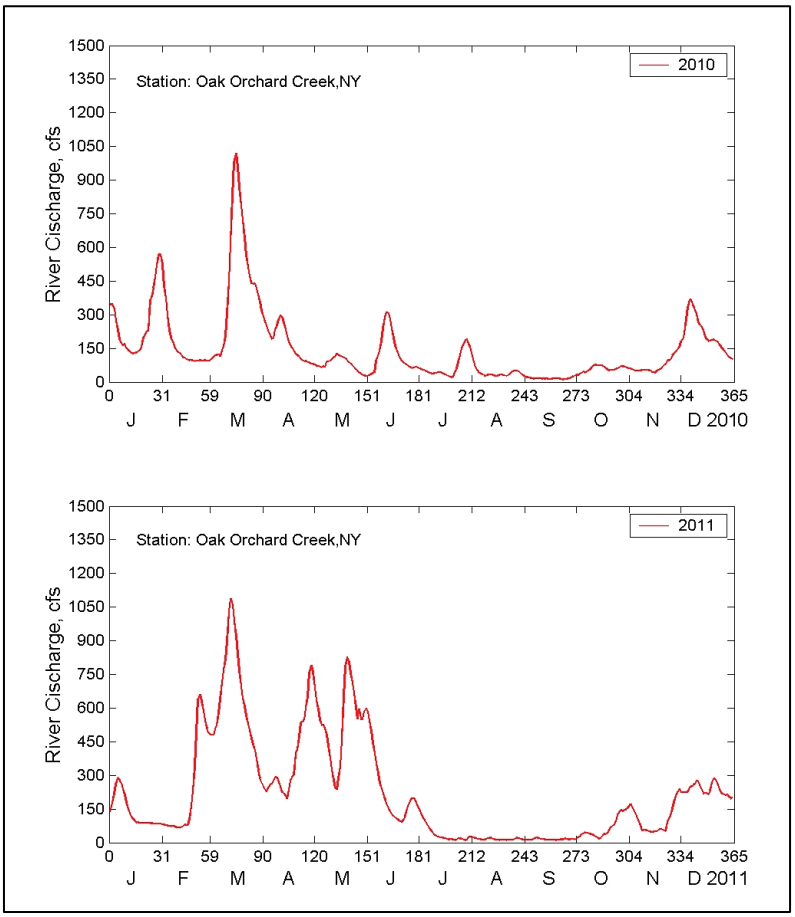

2.5 Tasks

The study plan and tasks included collection, analysis, formatting input data, and setting up and running numerical models for "with project" and "without project" conditions. Results of numerical models were analyzed and findings were discussed with the District on a regular basis, and necessary adjustments were made to the study plan as executed.

Assembling the wave data for modeling was a key element of the study plan as Braddock Bay is open to Lake Ontario and exposed to wind waves generated in the lake. Two wave climate databases used were the GLCFS and the Wave Information Studies, WIS. Wind data were available from WIS and NOAA Buoy 45012 and Coastal Sta 9052030 (Oswego, NY). Winds are used as input to wave generation and circulation models. Water levels were obtained from NOAA Sta 9052058 (Rochester, NY). River discharge data were provided by USGS (U. S. Geological Survey) at selected water-level gauge stations in the Monroe County, NY region. Details of

these metocean data are discussed in Chapter 3. A summary of specific tasks performed in the study is as follows:

2.5.1 Task 1. Develop metocean forcings (winds, waves, tides, currents, water levels, and river discharges)

This task involved assembly, analysis and preparation of wind, wave, current, water level, and river discharge data for the study. Details of the metocean data are provided in Chapter 3.

2.5.2 Task 2. Wave modeling

A spectral (phase-averaged) wave model CMS-Wave (Lin et al. 2011a; Lin et al. 2011b; Lin et al. 2008; Demirbilek et al. 2007; Lin and Demirbilek 2005; Demirbilek et al. 2005) was used to provide locally-generated wind wave estimates at the project site. This model can run on a grid with variable rectangular cells. It is suited to large area applications in which wider spacing cells can be specified in the far site, where wave-property variation is small and away from the area of interest, to save computational time. Wave diffraction, reflection, and transmission caused by structures are included in this class of wave models using empirical methods.

2.5.3 Task 3. Hydrodynamic modeling

Hydrodynamics (water levels and currents) were modeled with the Coastal Modeling System, CMS (Demirbilek and Rosati 2011). Model simulations were conducted for the existing bay (S-0) and three alternatives with structures (S-1, S-2, and S-3).

2.5.4 Task 4. Sediment transport modeling

One of the project design requirements was that the proposed structures at the entrance should not cause navigation problems within the bay. This includes a structured inlet that should require little or no long-term maintenance dredging, which should be self-scouring. The sediments in the modeling domain are a mixture of coarse gravel along the north barrier shoreline and mostly sands and fine-grained material in the south barrier shore and inside the bay. CMS is also used to calculate the sediment transport and morphology change by waves, currents, and water-level variation. Model results were used to identify potential depositional and ero-

sional areas in the bay, benefits to the wetlands, and possible impacts of proposed structures on the entrance, the entire bay, and shorelines.

2.5.5 Task 5. Study report

Document details of this modeling study are detailed in this Technical Report.

2.6 Report layout

Chapter 3 describes details of the numerical modeling study tasks, including model domain, bathymetry, grids, forcing types, structural alternatives, save stations, and conditions simulated. Chapter 4 provides modeling results, comparison of alternatives, and study findings. The conclusions and recommendations are presented in Chapter 5.

3 Numerical Modeling of Waves, Hydrodynamics, and Sediment Transport

3.1 Purpose

This chapter provides details of numerical modeling study for waves, hydrodynamics, and sediment transport at Braddock Bay. Estimates of wave parameters (height, period, and direction), hydrodynamics (water levels and currents), sediment transport, and morphology change are developed for without project, or existing bay (S-0) configuration, and three with project alternatives (S-1, S-2, and S-3). The modeling study was used to evaluate the appropriate location, size, and geometry of the structural alternatives and their effect on improving conditions within the bay. See Chapters 1 and 2 for the study plan, data needs, tasks, and the end product.

3.2 Numerical Models

The waves, hydrodynamics, sediment transport, and morphology change were simulated by CMS (Demirbilek and Rosati, 2011) in this study. The CMS (http://cirp.usace.army.mil/products/cms.php) provides advanced wave, flow, and sediment transport models for coastal inlets and navigation projects. The development and enhancement of CMS capabilities continues to evolve as a research and engineering tool for desk-top computers. The CMS uses the Surface-water Modeling System, SMS (Zundel 2006) interface for grid generation and model setup, as well as plotting and post-processing. Appendix A presents additional information of the CMS and its capabilities. The CMS is a "preferred model" in the list of coastal models by USACE (https://cops.usace.army.mil/sites/HHC/Lists/HHC%20Software%20Lists/AllItems.aspx).

CMS-Wave and CMS-Flow explicit models were used in this study to develop estimates of wave, current, and sediment transport in the bay. Several improvements to CMS were necessary to address the project's needs and enhance model's predictive capabilities, which were funded by the CIRP. The advances included a) an approach for developing 20-year design conditions (winds, waves, and water levels); b) a strategy for short- and long-term simulations of Superstorm Sandy, two northeasters, and

non-storm waves using the full- and half-plane metocean forcings and variable grid capability of CMS-Wave; c) a procedure for validating models with the lake buoys and tide gauges near the project site; d) development of the pre- and post-processing analysis codes for improving model setup; e) development of the Fortran and Matlab utilities for analyses of wind, wave, and river discharge data; and f) development of the codes for extracting boundary conditions for sediment transport and water-quality models.

It is important to note that calibration and validation of the CMS have been described in detail in a series of four reports (Demirbilek and Rosati 2011). The Grays Harbor, WA, and Matagorda Bay, TX cases were amongst the two cases in the calibration and validation for bays and estuaries with model settings similar to Braddock Bay. An application of the CMS for mixed sediment transport in a bay and estuary setting similar to Braddock Bay has been described in the Matagorda Bay study report (Lambert et al. 2013). The development of fine-grained and mixed sediment capabilities in the CMS is continuing. Consequently, preliminary modeling results were developed to assess general sediment pattern changes in Braddock Bay caused by introduction of the proposed structural alternatives. Because of the absence of field data at Braddock Bay, modeling estimates developed for this study are qualitative for a relative comparison of alternatives investigated. The goal of study was neither to develop a detailed quantitative estimate of sediment transport or estimates for the final structural design. The main goal was to characterize the combined effects of waves, currents, and sediment transport on wetlands and navigation issues at Braddock Bay by investigating individual roles of the key contributing environmental forcings.

3.3 Metocean forcings

The Lake Ontario IGLD85 Low Water Datum (LWD) is 243.3 ft (74.15 m). This datum is used as the reference lake level in the present modeling study. All water levels hereafter are referenced to this baseline datum.

NOAA maintains four water level gauges in Lake Ontario, located at Olcott, NY (9052076), Rochester, NY (9052058), Oswego, NY (9052030), and Cape Vincent, NY (9052000). The water level data from the Rochester gauge were used in the model simulations.

It was noted earlier that Salmon Creek and Buttonwood Creek connect to Braddock Bay. The drainage areas are 70 sq. miles for Salmon Creek and 20 sq. miles for Buttonwood Creek. Because there were no USGS gauges available for either creek, the discharges for these two creeks were estimated based on the USGS data at the Oak Orchard Creek (Sta 04220045) and Oatka Creek (Sta. 04230500), the nearest river gauge data that exist to this project site. The discharges for the two creeks were calculated using the ratios of their drainage areas to the drainage area of Oak Orchard Creek or Oatka Creek, depending upon the availability of data for the time period of interest. For Salmon Creek, the ratio to Oak Orchard Creek is approximately 48 percent, and 14 percent for Buttonwood Creek. The ratio to Oatka Creek is 34 percent for Salmon Creek and 10 percent for Buttonwood Creek.

3.4 Types of simulations

Three types of simulations were conducted using different metocean conditions: (1) a hurricane, (2) a 9-month long time period, and (3) a 20 yr design return period. Simulations for these conditions were performed to represent a strong tropical event, a typical non-tropical year, and 20 yr design storm conditions. The recent Superstorm Sandy (27-31 October 2012) was selected for the tropical storm simulation. Year 2011 was selected for the non-tropical year simulation. Because potential ice coverage at Braddock Bay is likely in December to February, the nine-month period of 1 March - 30 November 2011 was chosen for the non-tropical simulation. The 20 yr design storm conditions, which included two northeasters: (1) 26-30 January 1971, and (2) 36-16 March 1993, at low, average, and high water level scenarios The 20 yr design storms were selected based on the WIS Sta 91066 (77.67° W, 43.34° N).

For Superstorm Sandy simulations (27-31 Oct 2012), model input data for waves were obtained from the Great Lakes Coastal Forecast System (GLCFS, http://www.glerl.noaa.gov/res/glcfs/) at 77.67° W and 43.34° N. The hourly water level data from Rochester gauge 9052058 were used. The hourly wind data from Oswego gauge 9052030 were used. The daily discharge data for Oak Orchard Creek 04220045 (Shelby, NY) were used, which were 48 percent and 14 percent for Salmon Creek and Buttonwood Creek, respectively. It was no longer of hurricane strength when Superstorm Sandy passed through the area.

For the 9-month non-tropical simulation (March to November 2011), incident wave input data were obtained from the GLCFS. The 9-month simulation was a relatively calm period without significant storm events. Wind and water level input data were obtained from NOAA Oswego and Rochester stations, respectively. The discharge data for Salmon and Buttonwood creeks were based on USGS Oak Orchard Creek Station.

For the 20 yr design storms, the wind and wave forcing data were extracted from WIS Sta 91066. The water-level boundary data were obtained from the NOAA Rochester gauge. However, three different water levels were evaluated for each design storm: low, average, and high water levels. Essentially, the water levels were extracted from the monthly average all-year lake level frequency curve (NOAA Rochester Gage 9052058) period of record 1964 – 2012. The Salmon and Buttonwood Creek discharge data were pro-rated based on drainage area from the Oatka Creek USGS gage station 04230500.

3.5 Modeling domain and bathymetry

As shown in Figures 2-1 and 2-3, the primary area of interest in this modeling study was the Braddock Bay embayment, where wetlands are located on the back side of the central bay peninsula. Depths in the area of interest are relatively shallow, and generally less than 1 m within 500 ft (150 m) from the wetlands. The average water depth in the entire bay is less than 8 ft (2.5 m). Figure 3-1 shows bathymetric contours in the bay near the wetlands.

Figure 3-1. Bathymetric contours in the central bay peninsula.

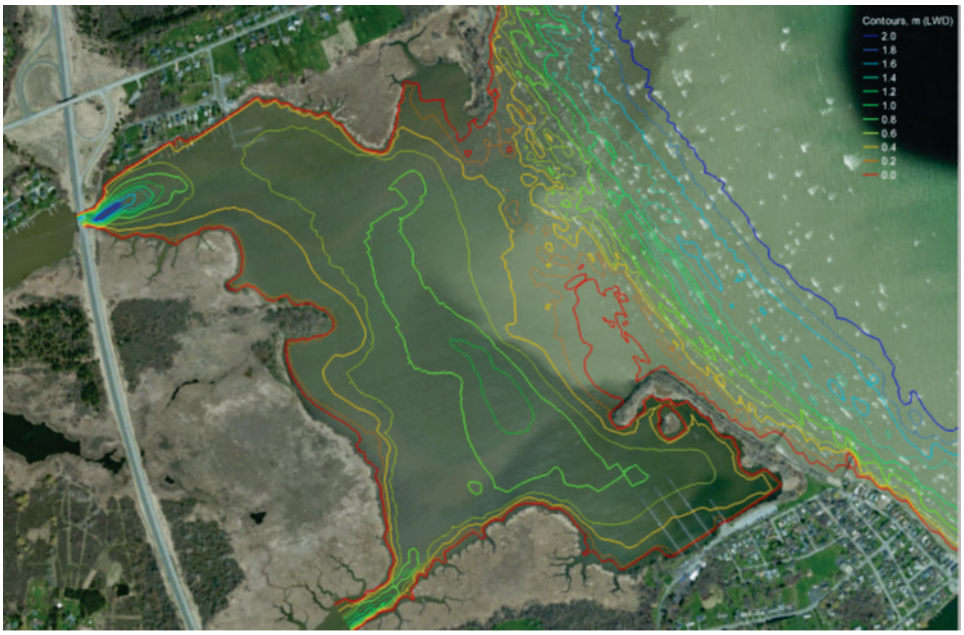

LRB provided available bathymetric survey data for Braddock Bay and adjacent areas. The data included high-resolution elevation and imagery data along the U.S. shorelines, and Lidar data collected in 2007 and 2011 for Lake Ontario. Additional data were obtained from the USGS coastal shoreline database, NOAA digital elevation maps (DEM) database, and an ADCIRC mesh for Lake Ontario using the GeoDas database.

The horizontal datum used for coordinate data input into the models was NAD83, State Plane, New York West (Federal Information Processing Standard state code: 3103 in meters). The vertical datum used in this study was the International Great Lakes Datum of 1985 (IGLD85). The Lake Ontario chart datum is 243.3 ft (74.15 m), which is the LWD. The IGLD85 is the joint benchmark approved by the USA and Canada for the entire Great Lakes region. All water levels used in this study have been referenced to the IGLD85. Figure 3-2 shows the composite depth contours for the entire modeling domain.

Figure 3-2. Composite bathymetry contours and modeling domain.

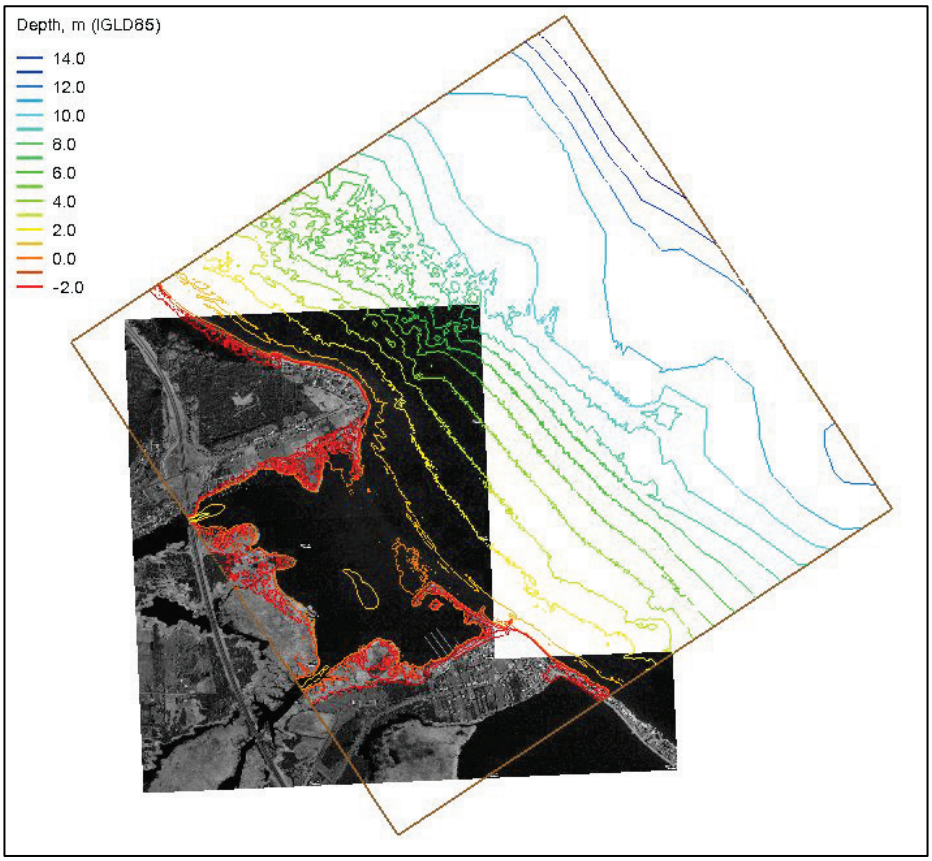

3.6 Existing bay and proposed alternatives

The existing bay geometry (S-0) and three alternatives (S-1, S-2, and S-3) were investigated in this study. The three alternatives were configured and sized per LRB requirements. Alternatives S-1 and S-2 had low-crested breakwaters connecting to north and south shorelines (Figures 2-7 and 2-8), whereas S-3 had artificial headland breakwaters connecting to the south shoreline (Figure 2-9). The location, length, and orientation of structures used in each alternative were determined in close consultation with the District. Because the primary study goal was to intercept the maximum wave energy getting into the bay, the structures were positioned as close to the bay entrance as possible.

The crest and width of berms of each breakwater segment were 6 ft (1.8 m) and 18 ft (5.4 m), respectively. The total length (linear foot) of structures in Alternative S-1 was approximately 2,600 ft (790 m), 2,800 ft (850 m) in S-2, and 2,200 ft (670 m) in S-3. Additional information about S-0, S-1, S-2, and S-3 is provided in the Numerical Model Grids section that follows the Sediment Distribution next.

3.7 Sediment distribution

Braddock Bay has mixed sediments, with coarser sand and gravel in the north side along the lake shore, and a mixture of mud and sand in the south and central back sides of the bay, and at the mouths of the two creeks. Fine sands dominating the nearshore and south lake shore have formed a distinct shallow sand bar in the southern part of the bay entrance. Sediment samples were collected during the period from 27-30 August 2012. Figure 3-3 shows a map of the sampling locations. The samples that consisted predominately of soil particles were subjected to grain-size analyses in general accordance with ASTM D422. Grain-size distributions are included as Appendix B.

Figure 3-3. Sediment sampling locations.

3.8 Numerical model grids

Figure 3-4 to Figure 3-6 show respectively the dimension and geometry of three alternatives (S-1, S-2, and S-3) used in the model grids. Alternative S-1 represented a segmented low-crested breakwater system consisting of four pieces of structures. In Alternative S-1, the lengths of the breakwater segments from north to south were 560 ft (170 m), 820 ft (250 m), 820 ft

(250 m), and 430 ft (130 m), respectively. From north to south, the three corresponding gaps between the breakwater segments were 213 ft (65 m), 213 ft (65 m), and 230 ft (70 m). The breakwater crest elevation was 6 ft (1.83 m), LWD.

Alternative S-2 was a dual-breakwater system, and it was connected to the north and south shorelines with a jettied inlet between two breakwaters. The lengths of north and south breakwater segments were 1,500 ft (450 m) and 1,410 ft (430 m), respectively. The width of inlet was 100 ft (30.5 m). The elevation and length of each jetty were 8 ft (2.44 m) and 410 ft (125 m). Both S-1 and S-2 also included a 500 ft (150 m) north shore revetment connected to the north breakwater segment.

Alternative S-3 was a breakwater system with beach-fill that consisted of a 1,860 ft (565 m) long breakwater attached to the south shoreline, one 80 ft (25 m) long groin connected to the middle of the long breakwater, and two headland breakwaters, 130 ft (40 m) long each, between the groin and south shoreline. The sand berm crest elevation is at 6 ft (1.8 m) LWD and 60 ft (18 m) wide; beach fill slope is 1:10 and the D_{50} = 0.7 mm. The sand berm covers the lakeside stability berm of the breakwater. Table 3-1 presents the coordinates of structural segments (breakwaters and groins) used in three alternatives (S-1, S-2, and S-3).

Figure 3-4. Geometry of Alternative S-1.

Figure 3-5. Geometry of Alternative S-2.

In numerical model grids, the distance of the present existing bay entrance (S-0) between north shore and south shore was 2,850 ft (870 m). The corresponding structural geometries for S-1, S-2, and S-3 are depicted in Figures 3-4 to 3-6. The cross-shore and along-shore dimensions of the model domain were 4 km x 4 km (Figure 3-2). The grid orientation was 213.55°, consisted of 120 rows and 166 columns. The grid had a variable cell resolution, with cell size of 10 x 15 m in the bay and 100 x 100 m at the lakeside boundary. The grid cell size for the structure was selected to represent the proper geometry and elevation of the structure to simulate the hydrodynamic and sediment transport. It is not intended for detailed structure design. The grids covered the entire footprint of Braddock Bay, and had resolution necessary to properly represent the key features of the bay

complex that could impact the dynamics of waves and circulation within the bay.

Figure 3-6. Geometry of Alternative S-3.

Table 3-1. Location and coordinates for alternatives (State Plane, NY West).

Number of Segments	Alternatives					
	S-1		S-2		S-3	
Coordinates	Easting (m)	Northing (m)	Easting (m)	Northing (m)	Easting (m)	Northing (m)
Revetment:						
Start Point	420540	368950	420540	368950	420601	368508
End Point.	420534	368842	420534	368842	420979	368086

Seg #1:						
Start Point	420534	368842	420534	368842	420757	368290
End Point.	420530	368693	420603	368362	420801	368323
Seg #2:						
Start Point.	420529	368622	420615	368330	420846	368283
End Point	420593	368382	420910	367968	420884	368233
Seg #3:						
Start Point	420623	368320			420922	368207
End Point	420768	368110			420969	368153
Seg #4:						
Start Point.	420818	368057				
End Point	420910	367968				

3.9 Metocean Forcing Conditions for Hurricane Sandy

The Superstorm Sandy simulation was conducted 27-31 October 2012. The incident waves were extracted from the GLCFS database. The wind input was based on NDBC Buoy 45012. Figure 3-7 shows the wind and wave forcings used in the simulation. The water-level forcing was obtained from the NOAA Rochester gauge (9052058), where the maximum observed water level above the LWD was 1.4 ft (0.4 m) during Sandy. The model simulations were conducted for three different pre-storm water levels: low (0 ft), medium (2 ft = 0.61 m), and high (4.7 ft = 1.43 m). Figure 3-8 shows the model input water-surface elevations for the three different water lev-

els. The river discharge forcing was based on USGS Orchard Creek gauge in the simulation.

3.10 Metocean forcing conditions for March-November 2011 simulation

For the March-November 2011 simulation, the hourly wind input is based on the NOAA Oswego station (9052030). The maximum observed wind speed was about 45 mph (20 m/sec) at Oswego station (see Figure 2-15). The water level forcing at the lakeside open boundary was supplied by the NOAA Rochester station (see Figure 2-10). The incident-wave input was based on the GLCFS data (see Figure 2-17). The river discharges for Buttonwood Creek and Salmon Creek are based on data from the USGS Oak Orchard station (Figure 2-23).

3.11 Metocean Forcing conditions for the design storms

Based on the hindcast wind and wave information from WIS Sta 91066, two 20 yr design waves (northeaster) were selected: (1) 26-31 January 1971 with the dominant wave direction from NW, and (2) 13-17 March 1993 with the dominant wave direction from NE (Figure 2-21). The design waves were selected at the 20 yr recurrence interval from the annual maximum wave heights from WIS data (1979 – 2012) for the two different dominant wave directions: NW and NE. Table 3-2 shows the wind and wave forcing data for the two design storms. For model simulations, the river discharge input is based on USGS Oatka Creek gauge. The water-level boundary data were extracted from NOAA Rochester gauge. For design storm waves with the dominant NW direction, the model-input water-surface elevations were adjusted by three water levels referenced to LWD: low (-1.3 ft = -0.4 m), medium (0.7 ft = 0.2 m), and high (2.95 ft = 0.9 m). For design storm waves with the dominant NE direction, the model input water surface elevations were adjusted by three water levels referenced to LWD: low (-3.23 ft = -0.98 m), medium (-1.23 ft = -0.38 m), and high (0.77 ft = 0.23 m).

Figures 3-9 and 3-10 show wind and wave forcings for the 20 yr design waves from NW and NE dominant directions, respectively. The water levels corresponding to the 20 yr design storms used in the model simulations are shown in Figure 3-11. The low (98% exceedance or 0 ft LWD), average (50% exceedance or +2 feet LWD), and high (2% exceedance or +4 feet LWD) water levels were obtained from the Rochester Harbor, NY

Gage 9052058 and based on a frequency curve for the monthly mean all-year water levels from 1964-2012.

Figure 3-7. Wind and wave forcings for Hurricane Sandy.

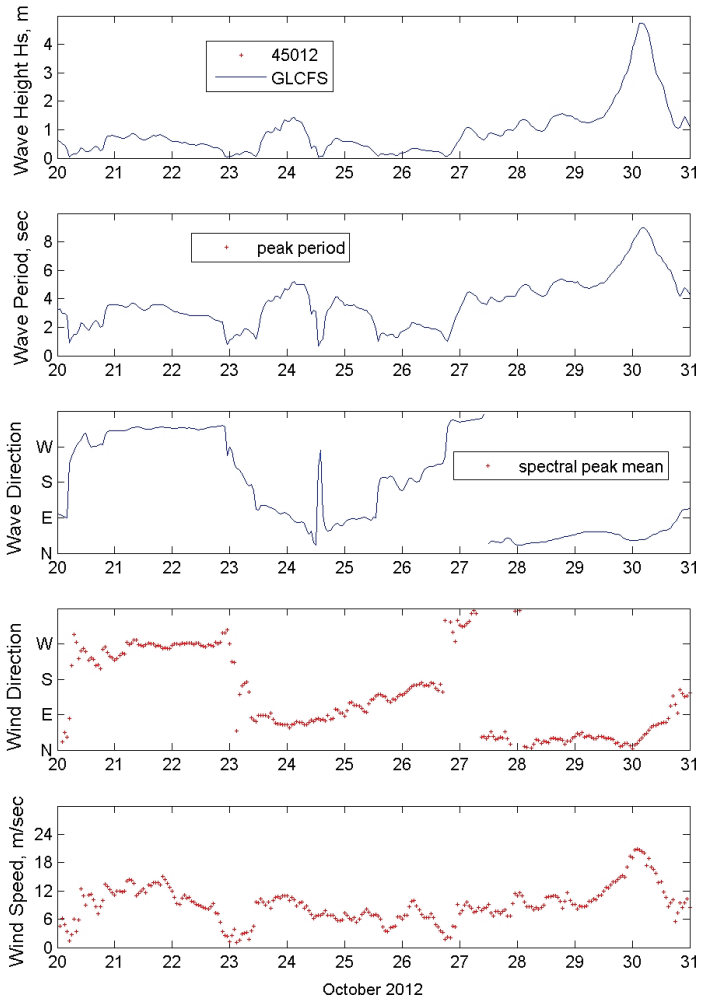

Figure 3-8. Model-input water levels for Hurricane Sandy.

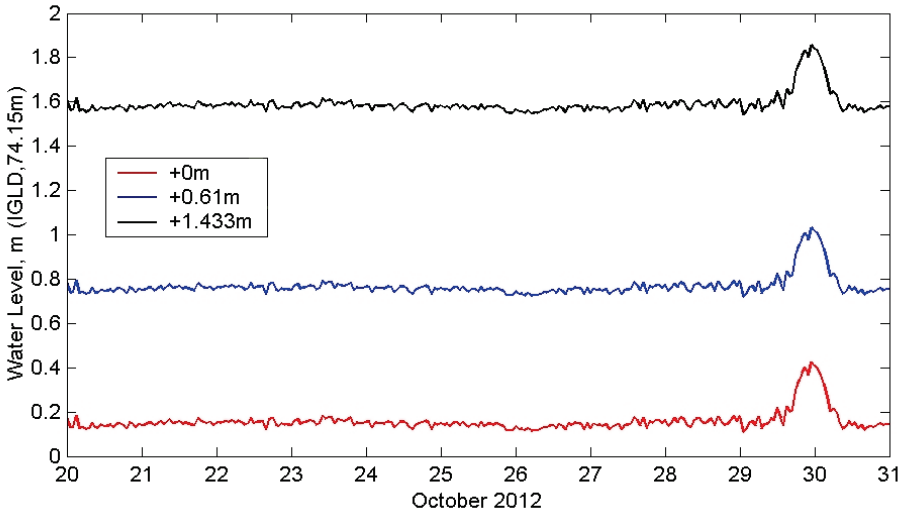

Table 3-2. 20 yr design storm conditions.

Storm Property	20 yr Design Storms	
Duration	26-30 Jan 1971	13-16 Mar 1993
Dominant wave direction	NW	NE
Max wave height(m)	3.05	3.85
Max wind speed (m/sec)	21	25
Max water level (m)	1.45	1.45
Min Water level (m)	-0.05	-0.05

Figure 3-9. 20 yr design wind waves from dominant NW direction.

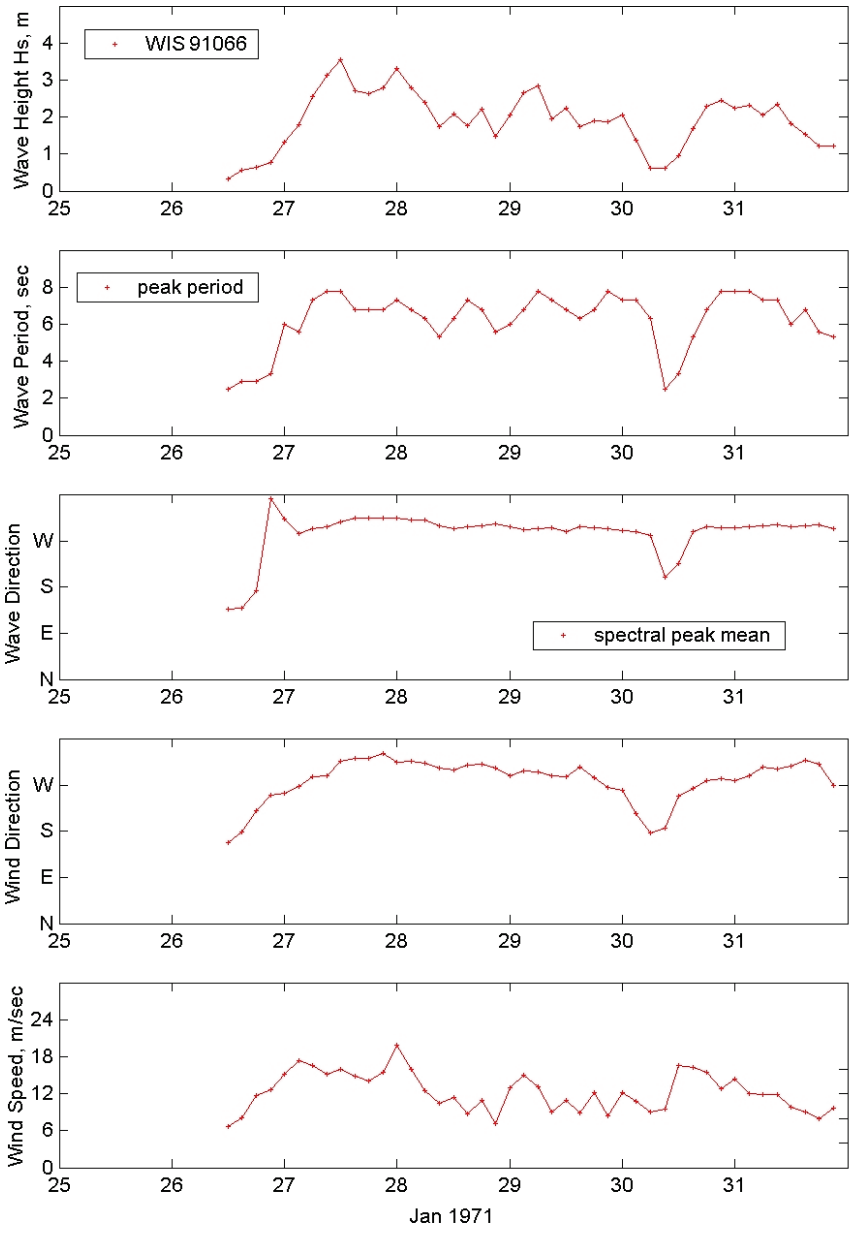

Figure 3-10. 20 yr design wind waves from dominant NE direction.

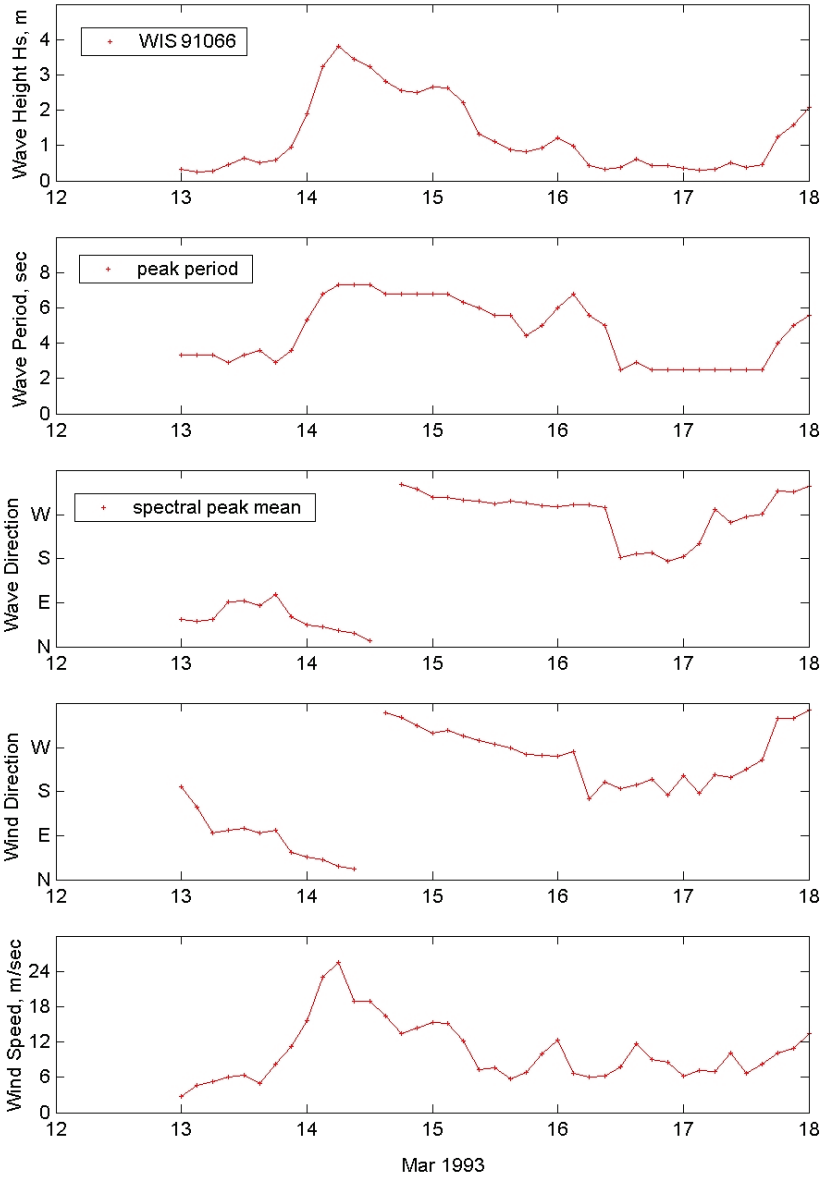

Figure 3-11. Model input water levels for 20 yr design storms.

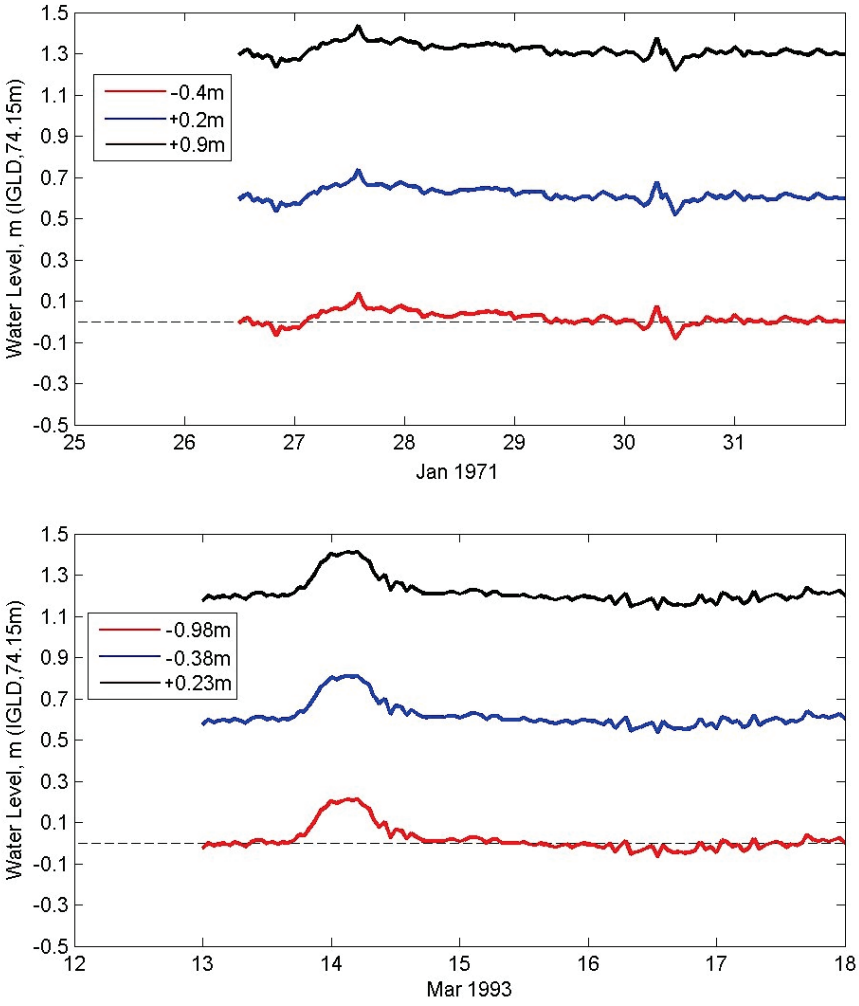

4 Modeling Results

4.1 Production runs

For Superstorm Sandy, numerical simulations for S-0, S-1, S-2, and S-3 were conducted with the storm surge at three different water levels (0 ft, 2 ft, and 4.7 ft). The long-term simulations (Mar-Nov 2011) for S-0, S-1, S-2, and S-3 were conducted using the measured winds, waves, river discharges, and water levels data described in Chapter 3. The simulations for 20 yr design storms were made with two incident wave events that had occurred on 26-31 Jan 1971 and 13-17 Mar 1993. These are referred to as the extreme NW and NE wave events, signifying the direction of forcing. For the extreme NW event, the maximum wave height was 10 ft (3.05 m) occurring at 1200 GMT (Greenwich Mean Time) on 27 Jan 1971. For the extreme NE event, the maximum wave height was 12.6 ft (3.85 m), occurring at 0600 GMT on 14 Mar 1993. The design storm simulations were conducted for the low, medium, and high water levels.

The sediment in Braddock Bay is a mixture of coarse gravel along the north barrier shoreline and mostly sands and fine-grained material in the south barrier shore and inside the bay. Outside the bay, the sediment is primarily fine sands. Inside the bay, the sediment contains more organic material with mixed silt and clay. The sediment median grain size is provided to the model based on the sample data collected in the field during the period from 27-30 August 2012 (Appendix B). Figure 4-1 shows the median grain size distribution used in the model. Figure 4-2 shows the coarse grain size (D_{50} = 0.7 mm) used for beach fill in Alternative S-3.

4.2 Model output

The results from wave and hydrodynamic models included wave height, wave period, wave direction, water-surface elevation, current magnitude and direction, and morphology change. These have been saved for all cells in the computational grids. The spatial or temporal variation of wave, flow, and morphology change fields can be extracted using the SMS from the saved results for any specific times coinciding with the peak of a storm or at any other desired times of interest.

Figure 4-1. The median grain size distribution used in the model.

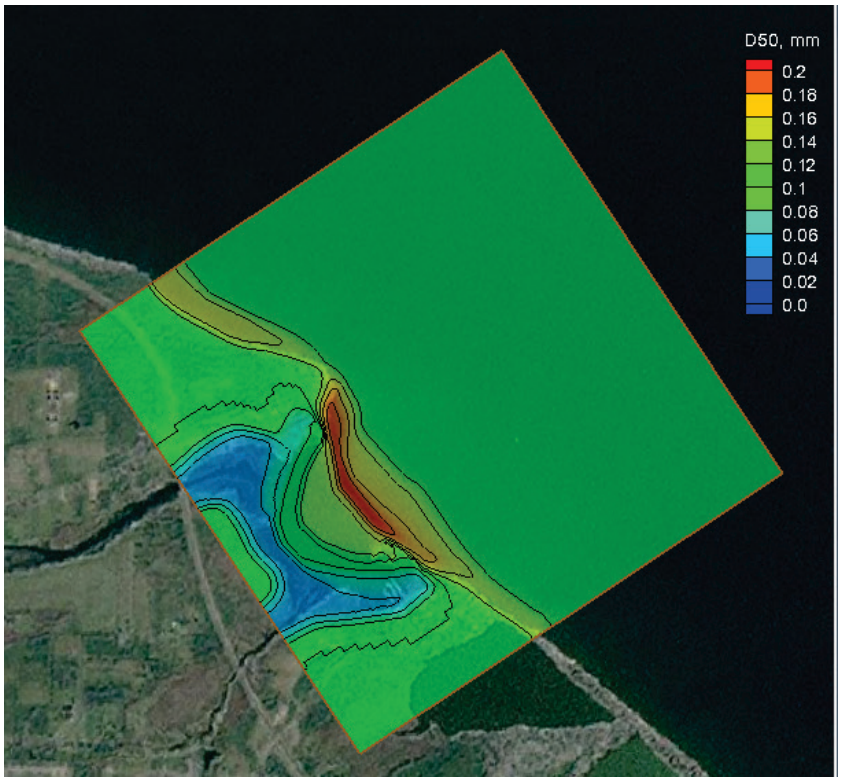

Figure 4-2. The median grain size distribution for Alternative S-3.

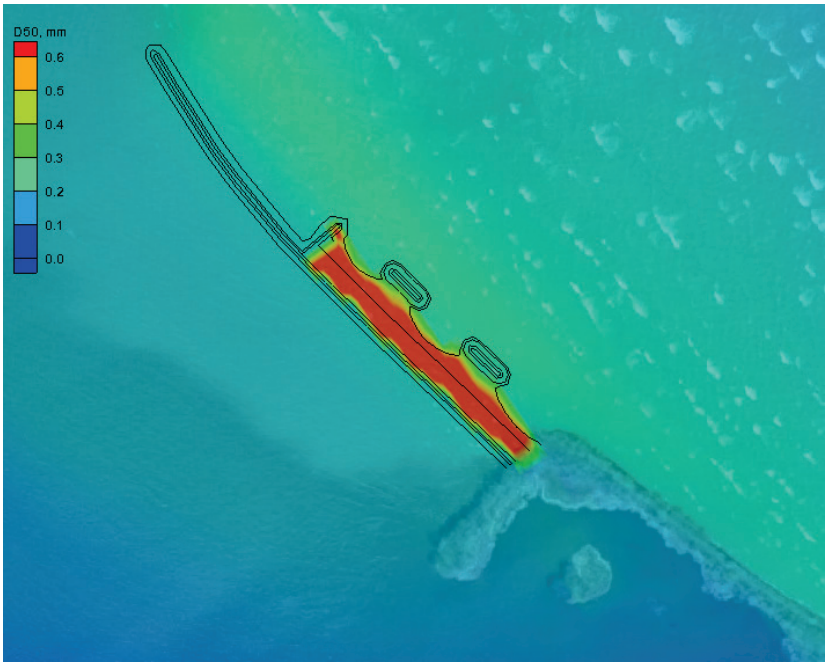

4.3 Comparison of alternatives

4.3.1 Hurricane Sandy simulations

The largest waves during Sandy occurred at 0300 GMT on 30 Oct 2012, with the wave height reaching 14 ft (4.3 m). Figures 4-3 to 4-6 show the model maximum wave fields during Sandy for S-0, S-1, S-2, and S-3, respectively. S-0 (without project) serves as the baseline to determine relative performance of Alternatives S-1, S-2, and S-3. There is a substantial reduction in calculated wave heights throughout the bay, and the largest reduction is for S-2. The wave fields outside the bay in the east of the Braddock Bay entrance are practically identical for S-0, S-1, S-2, and S-3. At higher water levels, incident waves may overtop S-1 and S-2 structures and this will increase wave transmission into the bay. For example, Figure 4-7 to Figure 4-9 compare wave-height contours for S-0 and S-1 during the maximum wave condition in Hurricane Sandy at three water levels, 0 ft, + 2 ft (0.61 m), and + 4.7 ft (1.43 m). Figure 4-10 to Figure 4-12 show the corresponding difference of wave-height fields between S-0 and S-1 for three water levels.

Figure 4-3. Calculated maximum wave height field for S-0 during Hurricane Sandy.

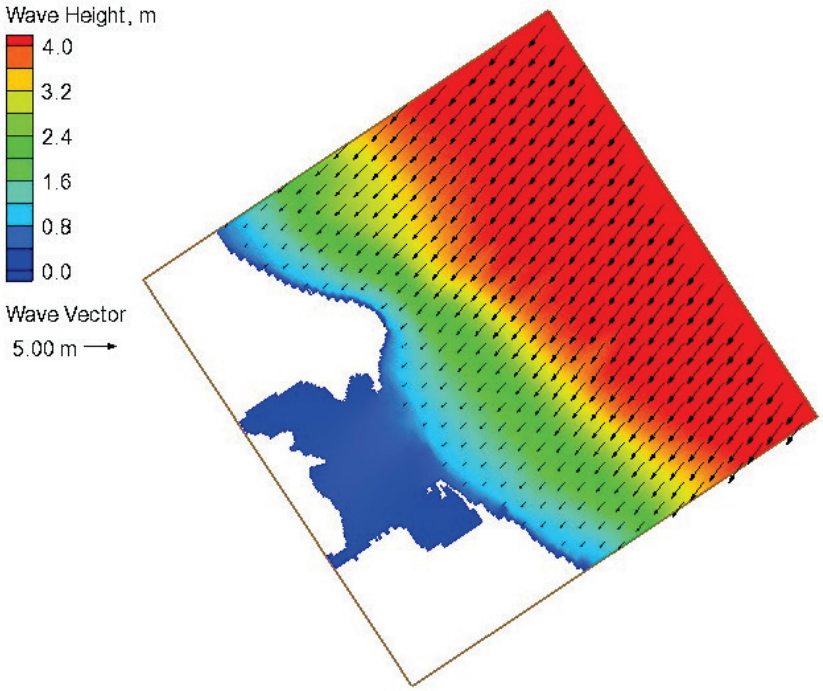

Figure 4-4. Calculated maximum wave height field for S-1 during Hurricane Sandy.

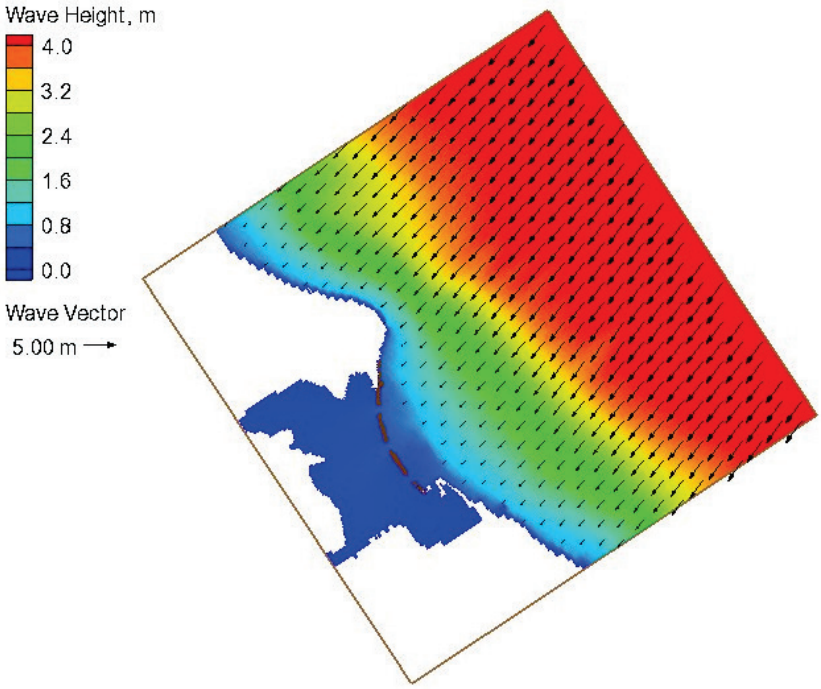

Figure 4-5. Calculated maximum wave height field for S-2 during Hurricane Sandy.

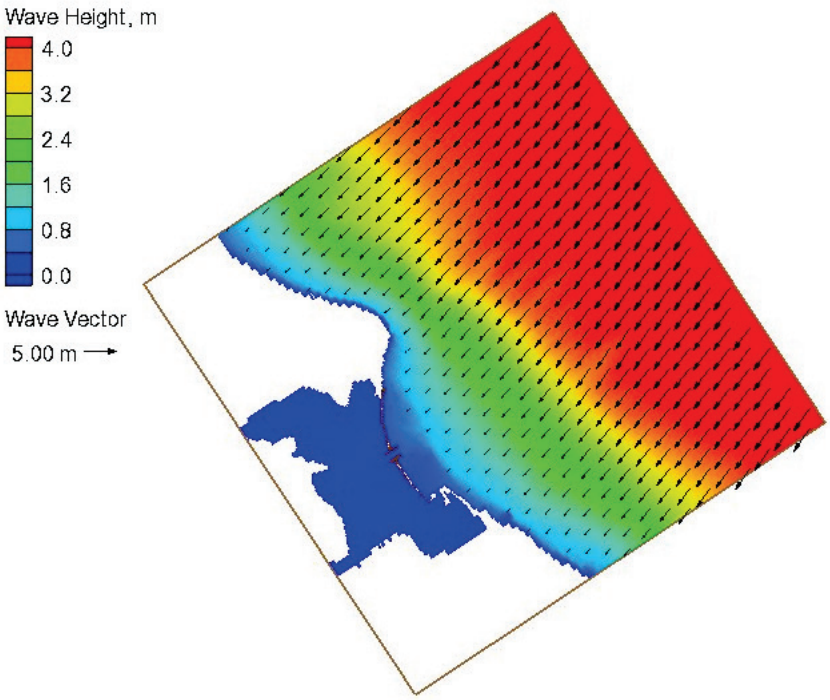

Figure 4-6. Calculated maximum wave height field for S-3 during Hurricane Sandy.

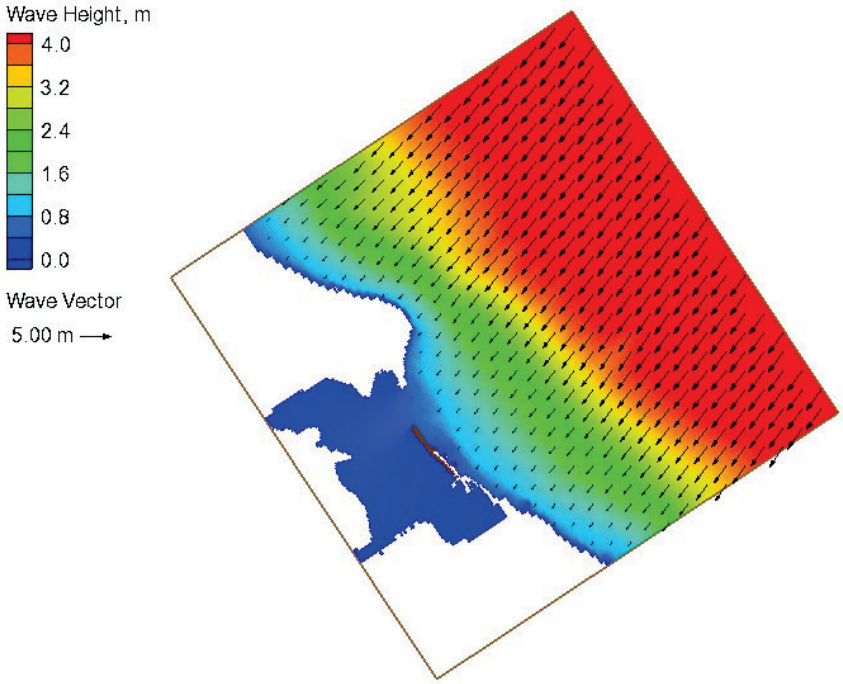

Figure 4-7. Model wave contours during Hurricane Sandy peak wave condition for S-0 and S-1 (WL= 0 m).

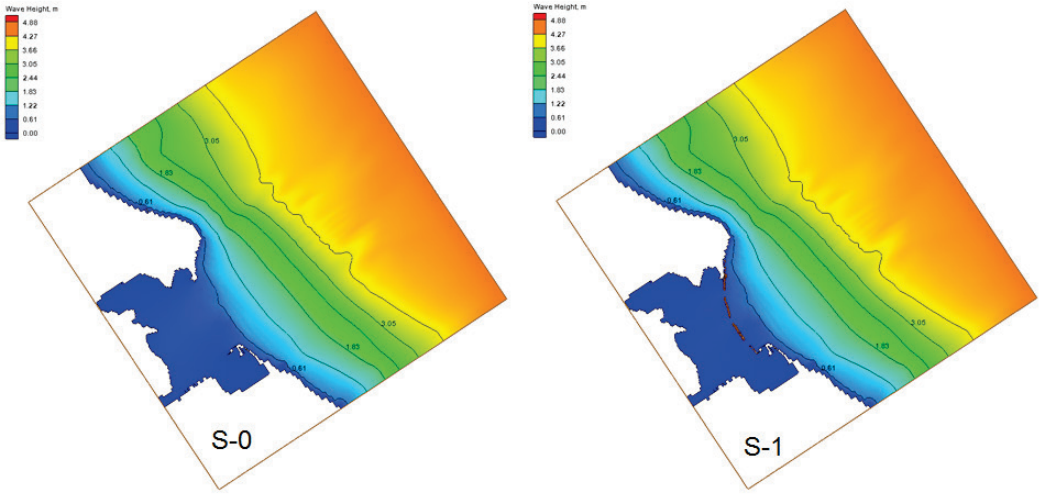

Figure 4-8. Model wave contours during Hurricane Sandy peak wave condition for S-0 and S-1 (WL= 0.61 m).

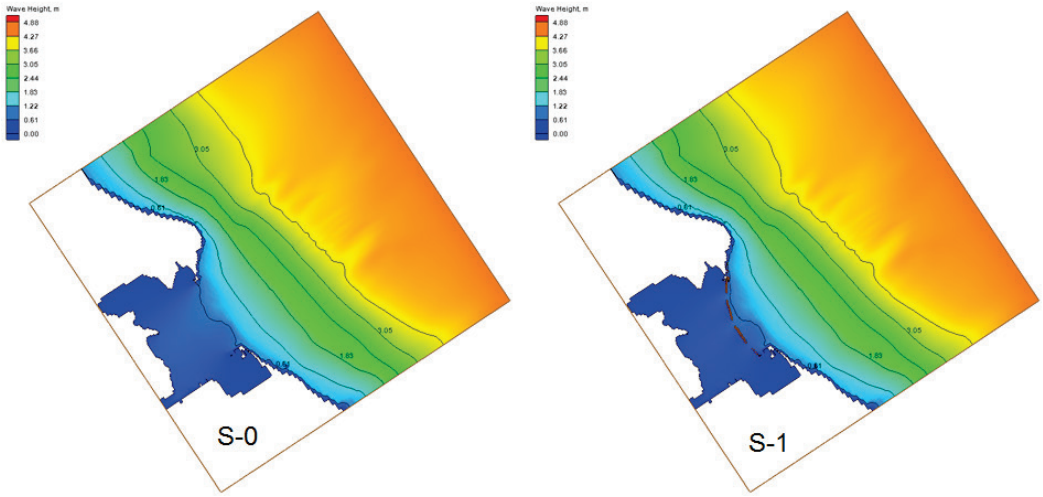

Figure 4-9. Model wave contours during Hurricane Sandy peak wave condition for S-0 and S-1 (WL= 1.43 m).

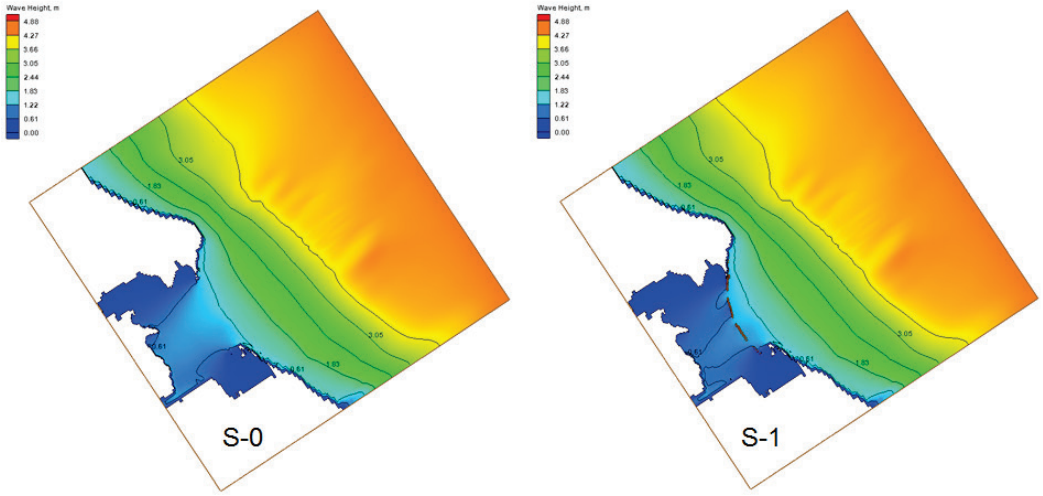

Figure 4-10. Calculated wave-height difference for S-0 and S-1 during Hurricane Sandy peak wave condition (WL= 0 m).

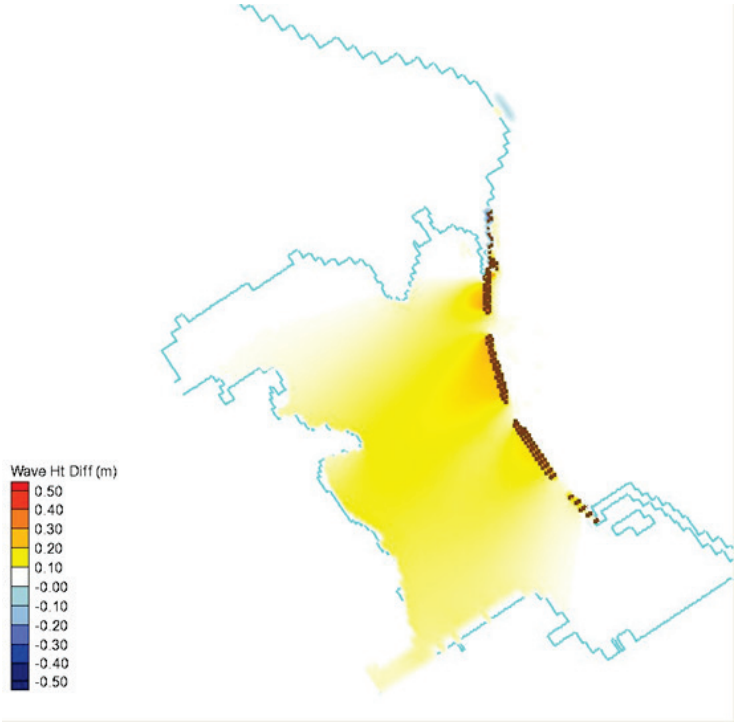

Figure 4-11. Calculated wave-height difference for S-0 and S-1 during Hurricane Sandy peak wave condition (WL= 0.61 m).

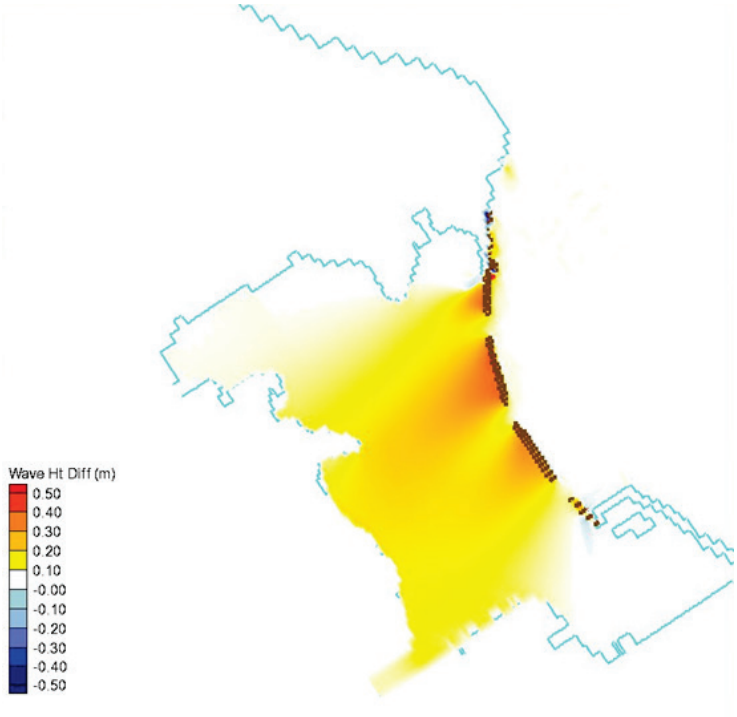

Figure 4-12. Calculated wave-height difference for S-0 and S-1 during Hurricane Sandy peak wave condition (WL= 1.43 m).

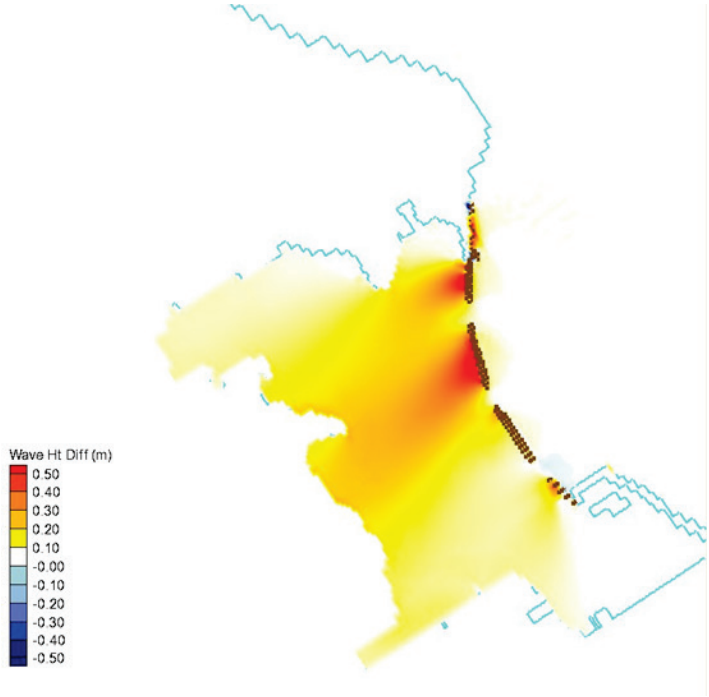

Model results indicated that Alternatives S-1 and S-2 performed well, achieving a significant reduction in the wave energy, flow, and morphology change in the lee of low-crested breakwater systems. Figures 4-13 to 4-16, for example, show the calculated morphology change fields from Hurricane Sandy for S-0, S-1, S-2, and S-3, respectively, for WL = 0 m. Figure 4-17 shows the morphology change fields in the bay for S-0, S-1, S-2, and S-3 for WL = 0 m. There is an increase in the current speed around the perimeters of low-crested breakwaters, in the gap areas between the breakwaters, and in the inlet. Alternative S-2 provides a comparatively greater reduction in wave heights, currents, and morphology change. Table 4-1 presents the calculated maximumwave heights near the backbay shoreline during the peak wave condition of Hurricane Sandy for S-0, S-1, S-2, and S-3. Table 4-2 presents the calculated morphology changes near the backbay shoreline from Hurricane Sandy for S-0, S-1, S-2, and S-3. Alternative S-3 is less effective than other alternatives, as it provides only a partial protection to the south side of the bay entrance.

Figure 4-13. Calculated morphology-change field for Hurricane Sandy for S-0 (WL = 0 m).

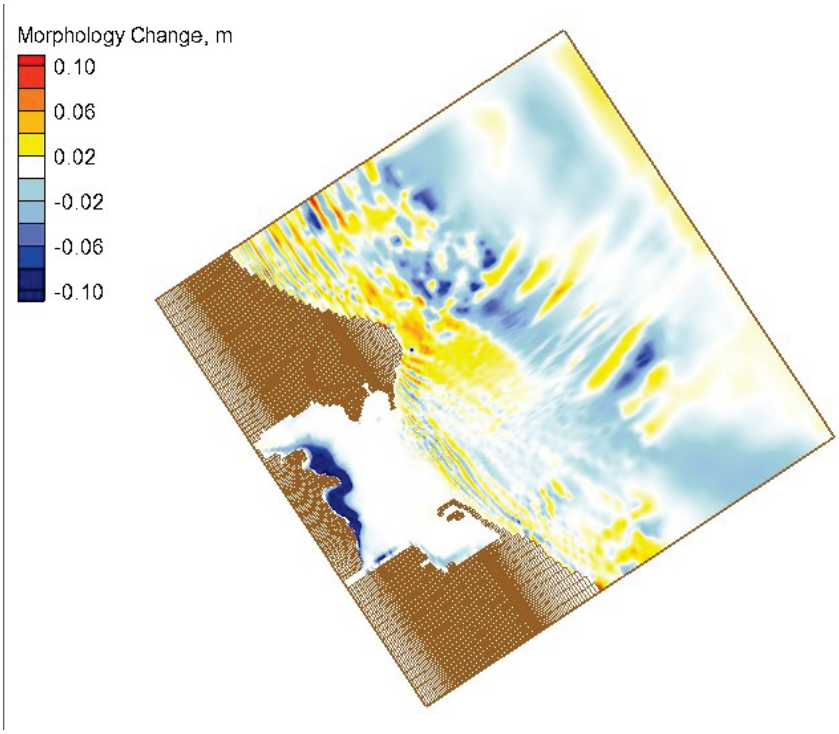

Figure 4-14. Calculated morphology-change field for Hurricane Sandy for S-1 (WL = 0 m).

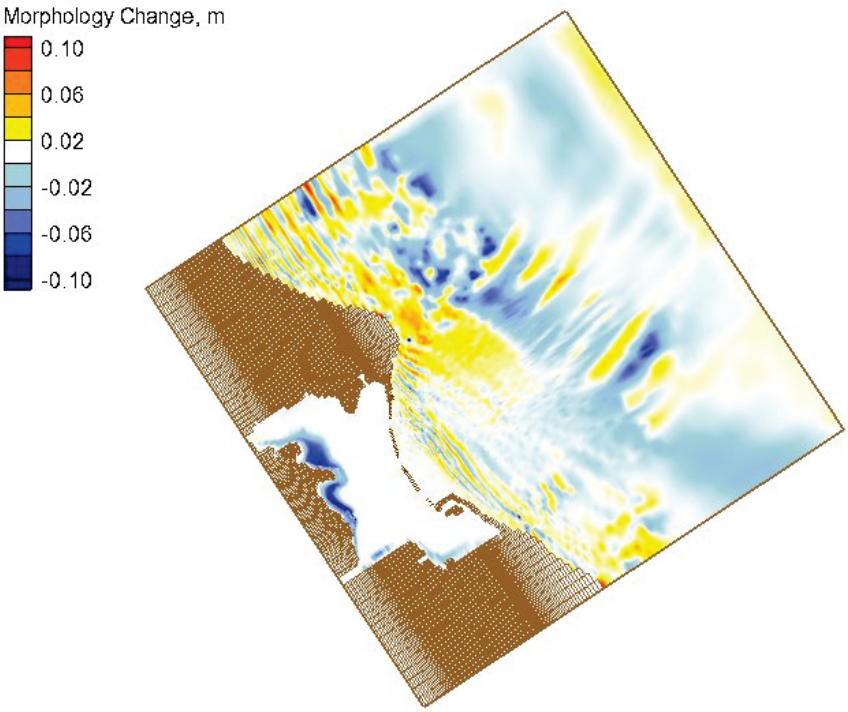

Figure 4-15. Calculated morphology-change field for Hurricane Sandy for S-2 (WL = 0 m).

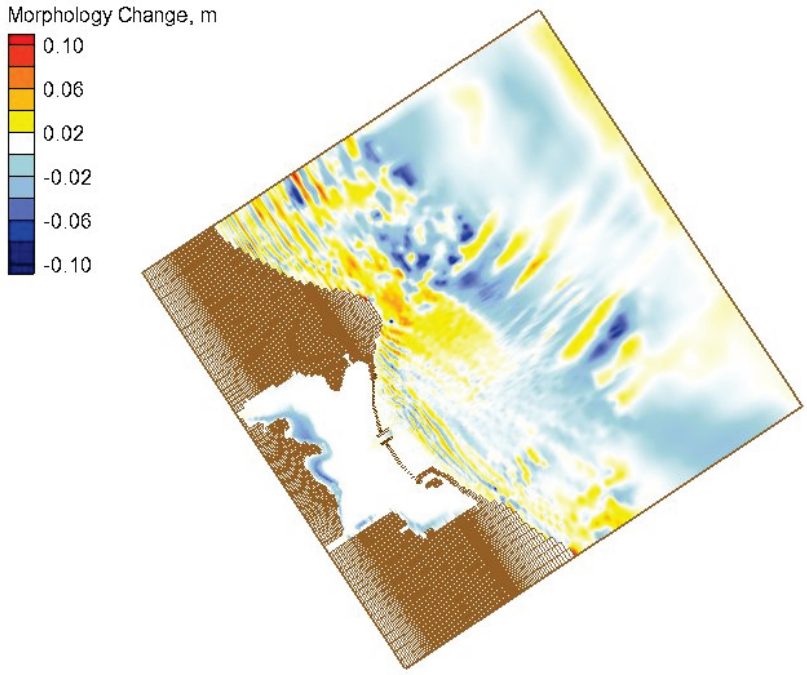

Figure 4-16. Calculated morphology-change field for Hurricane Sandy for S-3 (WL = 0 m).

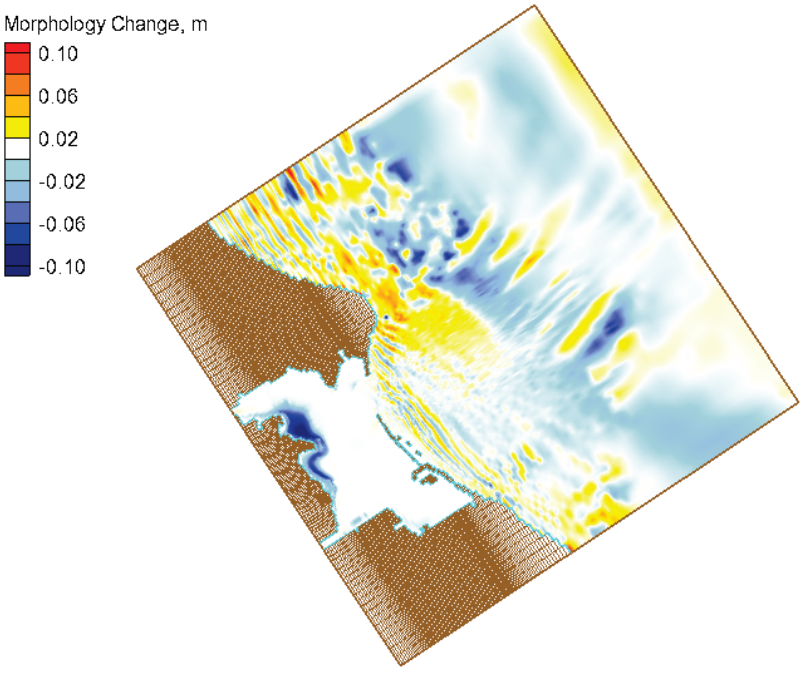

Figure 4-17. Calculated morphology-change fields in the bay for S-0, S-1, S-2, and S-3 for Hurricane Sandy simulation (WL = 0 m).

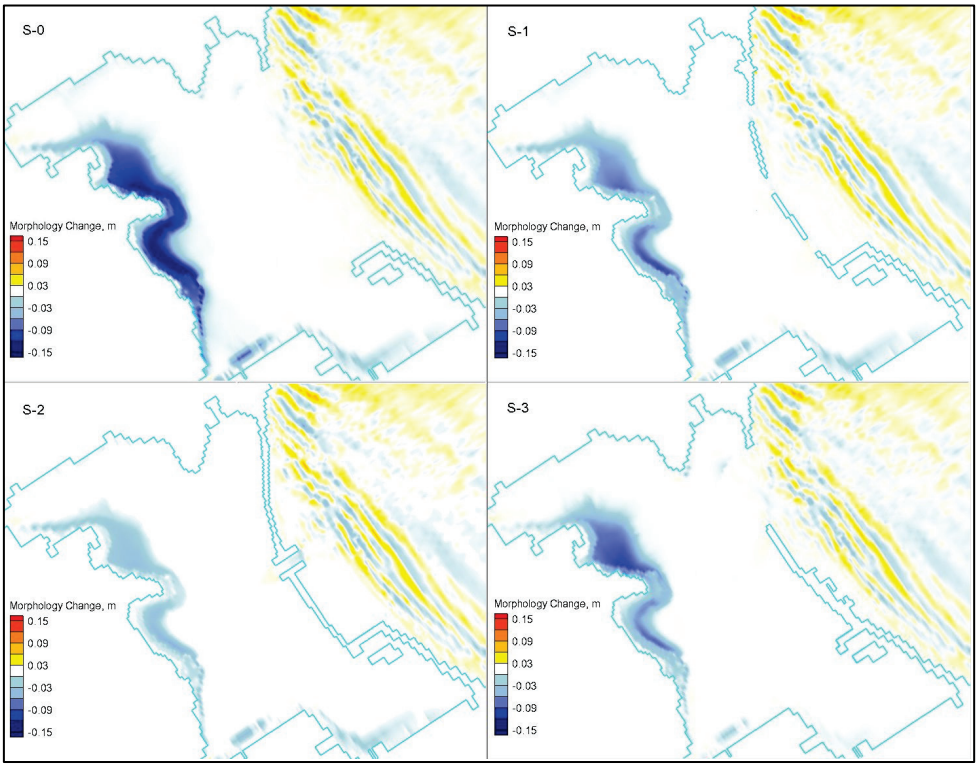

Table 4-1. Calculated maximum wave heights (m) for S-0, S-1, S-2 and S-3, and percent reduction of wave heights near the backbay shoreline during Hurricane Sandy.

WL / Datum / Scenario	+ 0 m (low)	+ 0.61 m (medium)	+ 1.433 m (high)
S-0	0.25	0.48	0.86
S-1	0.16 (-36%)*	0.32 (-33%)	0.63 (-27%)
S-2	0.11 (-56%)	0.23 (-52%)	0.50 (-42%)
S-3	0.16 (-36%)	0.34 (-29%)	0.72 (-16%)
* Percent difference (in parentheses) relative to S-0 (negative values indicate reduction).			

Table 4-2. Calculated maximum morphology change (m) for S-0, S-1, S-2 and S-3, and percent reduction of morphology change near the backbay shoreline during Hurricane Sandy.

WL / Datum Scenario	+ 0 m (low)	+ 0.61 m (medium)	+ 1.433 m (high)
S-0	-0.19	-0.51	-0.75
S-1	-0.11 (-42%)*	-0.34 (-33%)	-0.59 (-21%)
S-2	-0.06 (-68%)	-0.32 (-37%)	-0.42 (-44%)
S-3	-0.12 (-37%)	-0.40 (-22%)	-0.65 (-13%)
* Percent difference (in parentheses) relative to S-0 (negative values indicate reduction).			

4.3.2 Nine-month simulations

The largest waves during the 9-month (Mar-Nov 2011) simulation occurred at 0900 GMT on 1 Nov 2011, with wave height reaching 9.5 ft (2.9 m). Figures 4-18 to 4-21 show the corresponding wave fields for S-0, S-1, S-2, and S-3, respectively. It is noted that these simulations used measured (field gauge) water-level data varying in time during the simulation period. Comparison of results indicates a similar performance by alternatives as described in the previous section for Hurricane Sandy simulations. Due to increased dissipation of waves prior to reaching the structures in S-1, S-2, and S-3, much less wave energy remains from high- incident waves to penetrate into the bay. Figures 4-22 to 4-25 show the calculated morphology-change fields from 9-month simulations for S-0, S-1, S-2, and S-3, respectively. Figure 4-26 shows the calculated morphology changes in the bay for these alternatives. Table 4-3 presents the calculated maximum wave heights near the backbay shoreline during the 9-month simulations for S-0, S-1, S-2, and S-3. Table 4-4 presents the calculated morphology changes near the backbay shoreline from the 9-month simulations for S-0, S-1, S-2, and S-3. Morphology change for Alternative S-3 is comparable to those for S-1 and S-2. However, comparatively more sand transport occurs with Alternative S-3, given that it spans only half of the bay entrance.

Figure 4-18. Calculated maximum wave-height fields for S-0 with 9-month simulation.

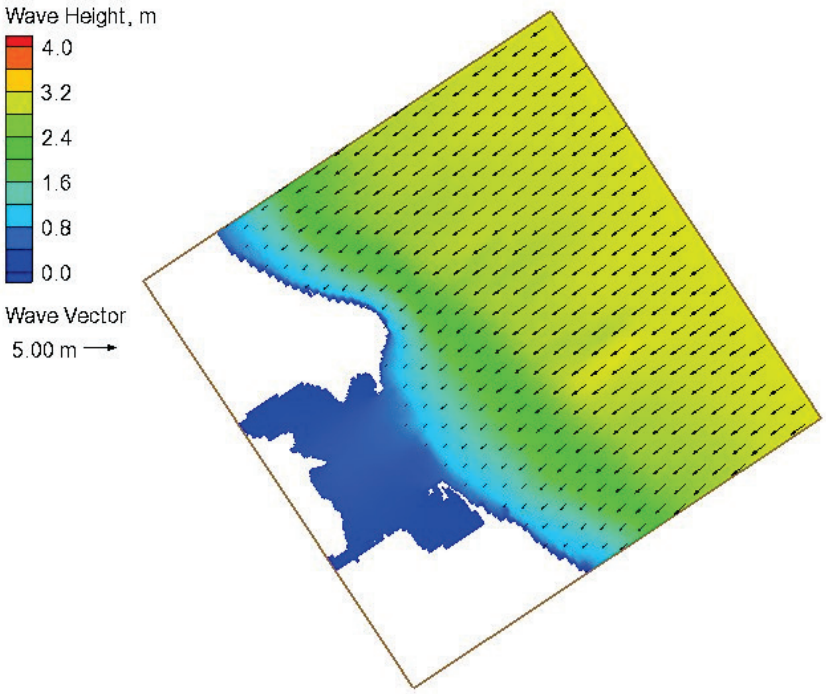

Figure 4-19. Calculated maximum wave-height field for S-1 with 9-month simulation.

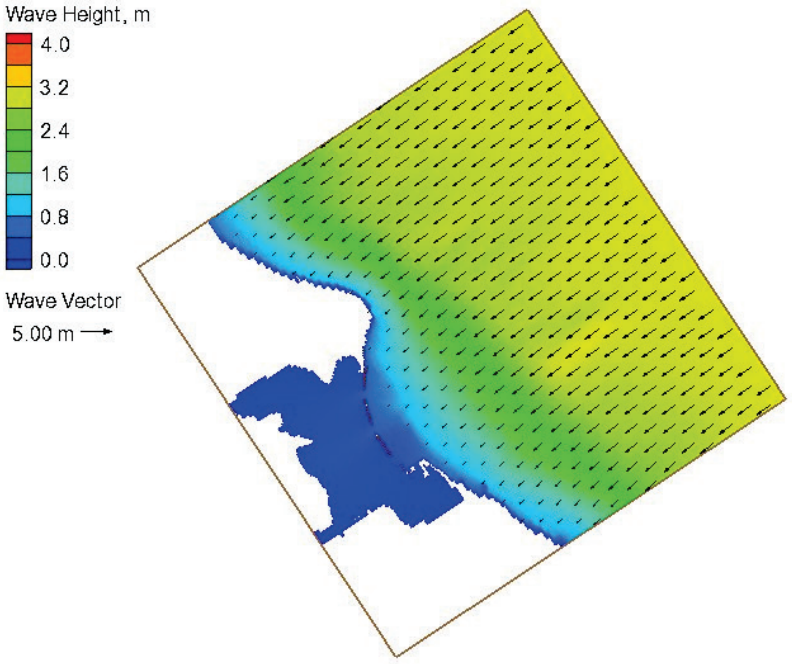

Figure 4-20. Calculated maximum wave-height field for S-2 with 9-month simulation.

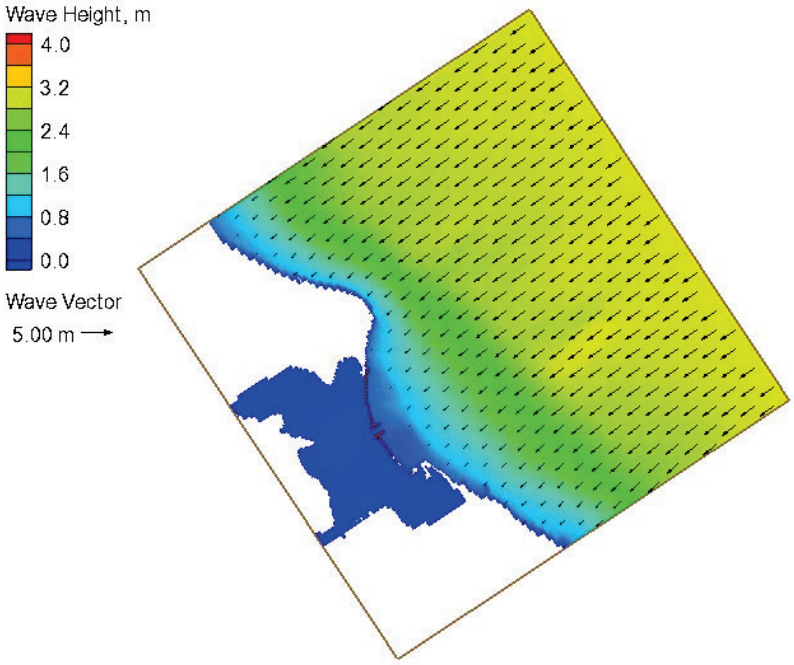

Figure 4-21. Calculated maximum wave-height field for S-3 with 9-month simulation.

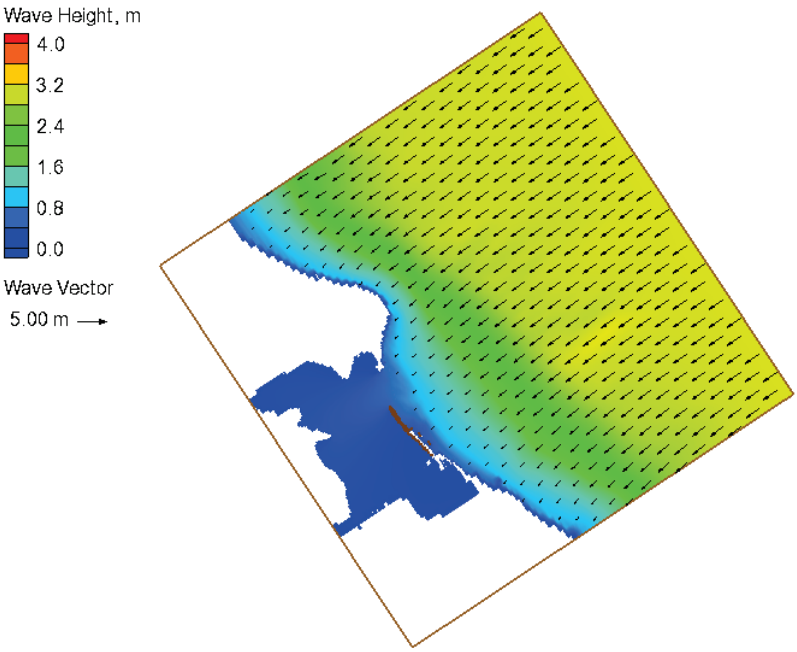

Figure 4-22. Calculated morphology-change field for S-0 with 9-month simulation.

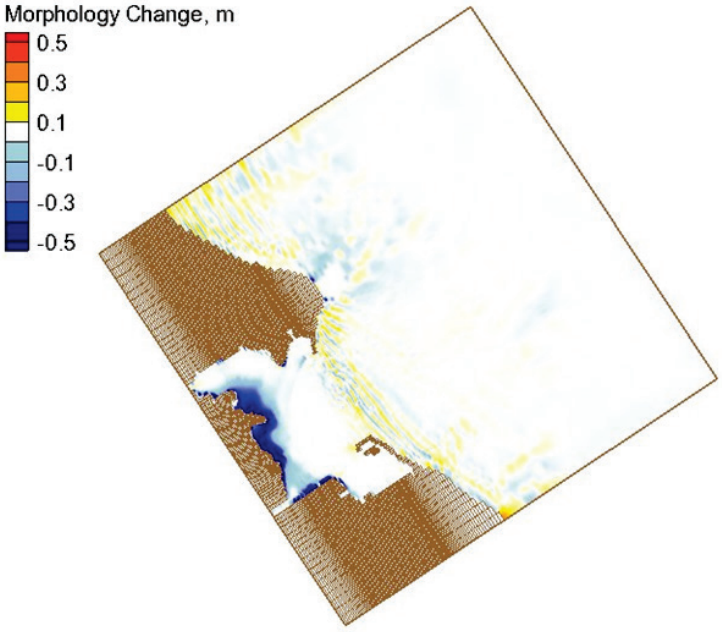

Figure 4-23. Calculated morphology-change field for S-1 with 9-month simulation.

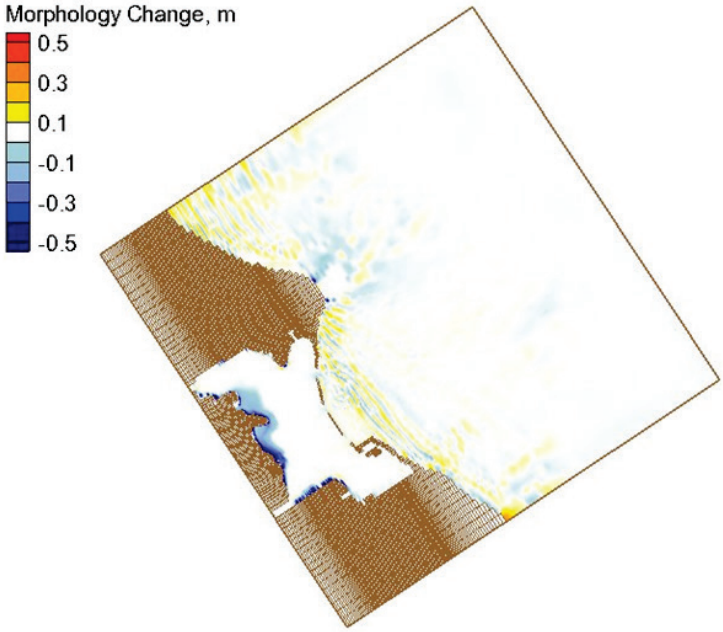

Figure 4-24. Calculated morphology-change field for S-2 with 9-month simulation.

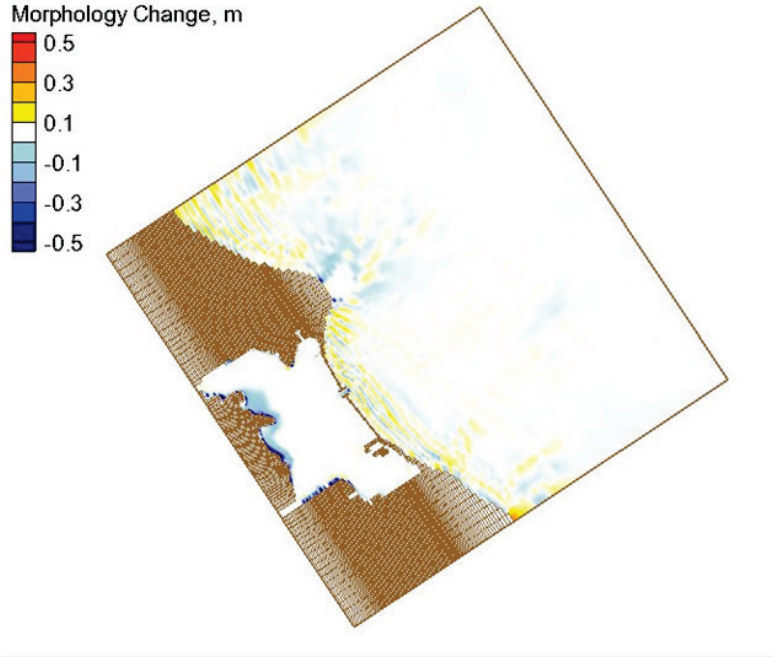

Figure 4-25. Calculated morphology-change field for S-3 with 9-month simulation.

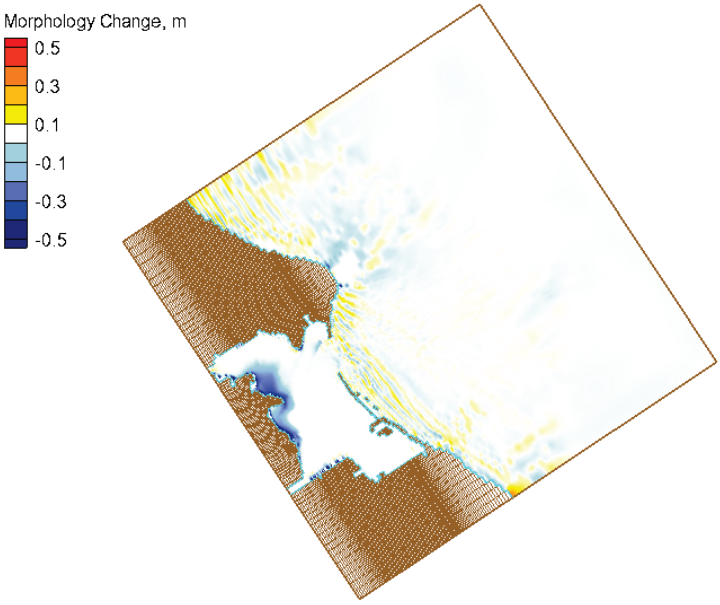

Figure 4-26. Calculated morphology-change fields in the bay for S-0, S-1, S-2, and S-3 for 9-month simulation.

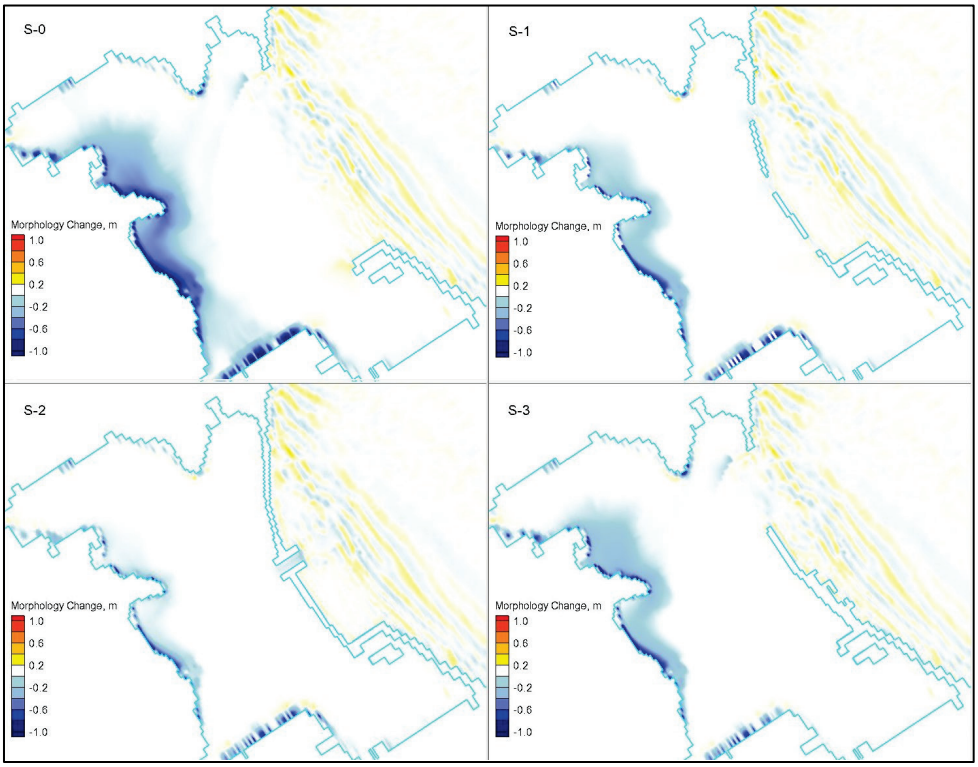

Table 4-3. Calculated maximum wave heights (m) and percent reduction in wave height near backbay shoreline during 9-month simulation.

WL Datum / Scenario	+ 0 m (low)
S-0	0.26
S-1	0.17 (-35%)*
S-2	0.11 (-58%)
S-3	0.22 (-15%)
* Percent difference (in parentheses) relative to S-0 (negative values indicate reduction)	

Table 4-4. Calculated maximum morphology change (m) and percent reduction in morphology change near backbay shoreline during 9-month simulation.

WL Datum / Scenario	+ 0 m (low)
S-0	-1.83
S-1	-1.24 (-32%)*
S-2	-1.07 (-42%)
S-3	-1.14 (-38%)
* Percent difference (in parentheses) relative to S-0 (negative values indicate reduction)	

4.3.3 20 yr Design storm simulations

Simulations were conducted for two design storms in Jan 1971 and Mar 1993 with three water levels (low, medium, high). The largest waves during the Jan 1971 storm occurred at 1200 GMT on 27 Jan 1971, and wave height reached 10 ft (3.05 m). The largest waves during the Mar 1993 storm occurred at 0600 GMT on 14 Mar 1993, and wave height reached 12.6 ft (3.85 m). Figures 4-27 to 4-30 show the calculated maximum wave fields during the Jan 1971 storm for S-0, S-1, S-2, and S-3 respectively, with the WL of 3 ft (0.9 m). Figures 4-31 to 4-34 show the calculated maximum wave fields during Mar 1993 storm for S-0, S-1, S-2, and S-3 respectively, with the WL of 0.8 ft (0.23 m). Table 4-5 presents the calculated maximum wave heights near the backbay shoreline from the Jan 1971 storm for S-0, S-1, S-2, and S-3. Table 4-6 presents the calculated maximum wave heights near the backbay shoreline from the Mar 1993 storm for S-0, S-1, S-2, and S-3.

There are no surprises from examination of results for the 20 yr design storm, where three alternatives have similar performance outcomes as in two previous sections. The 20 yr design storms represent the most severe conditions simulated so far. All three alternatives (S-1, S-2, and S-3) improve the conditions within the bay by reducing waves and morphology change. Like the simulations in two previous sections, because Alternative S-2 breakwaters are continuous (without gaps), waves can only move into the bay through a narrow (100 ft or 30.5 m) jettied inlet. For this reason, Alterative S-2 reduced waves more than Alternatives S-1 and S-3. Howev-

er, we should note that there is also a noticeable increase in the current magnitude in the jettied inlet of Alternative S-3.

Figures 4-35 to 4-38 show the morphology-change fields corresponding to S-0, S-1, S-2, and S-3, respectively, for the Jan 1971 storm with the WL = 3 ft (0.9 m). Figure 4-39 shows the calculated morphology changes in the bay for these alternatives. Figures 4-40 to 4-43 show the morphology change fields corresponding to S-0, S-1, S-2, and S-3, respectively, for the Mar 1993 storm with the WL = 0.8 ft (0.23 m). Figure 4-44 shows the calculated morphology changes in the bay for these alternatives. Table 4-7 presents the calculated morphology changes near the backbay shoreline from the Jan 1971 storm for S-0, S-1, S-2, and S-3. Table 4-8 presents the calculated morphology changes near the backbay shoreline from the Mar 1993 storm for S-0, S-1, S-2, and S-3. Alternative S-3 provides the least wave reduction at three water levels as compared to S-1 and S-2, and its morphology change is about half those of S-1 and S-2.

Figure 4-27. Model maximum wave-height field for S-0 during Jan 1971 storm (WL = 0.9 m).

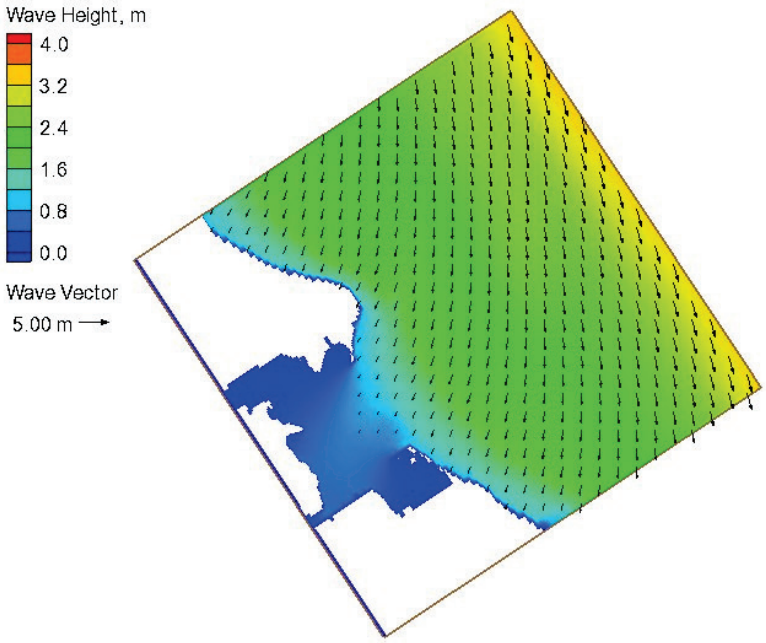

Figure 4-28. Model maximum wave-height field for S-1 during Jan 1971 storm (WL= 0.9 m).

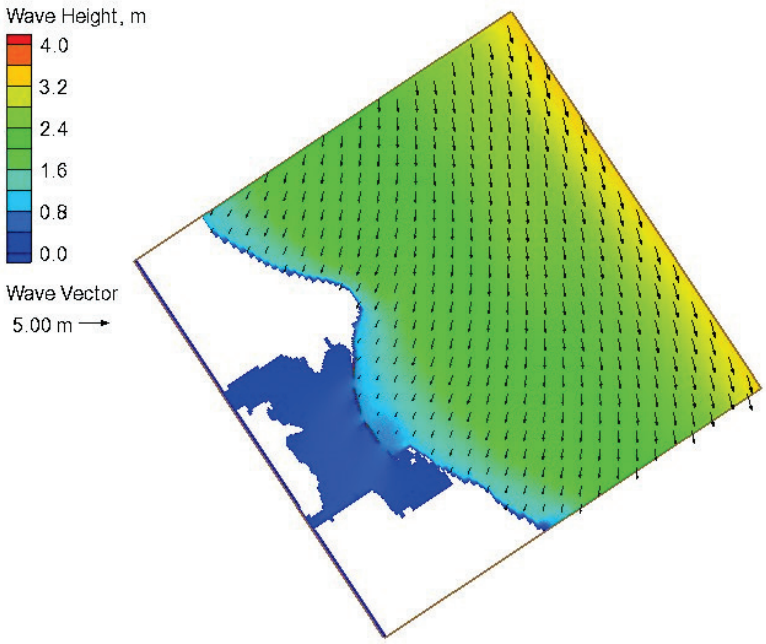

Figure 4-29. Model maximum wave-height field for S-2 during Jan 1971 storm (WL= 0.9 m).

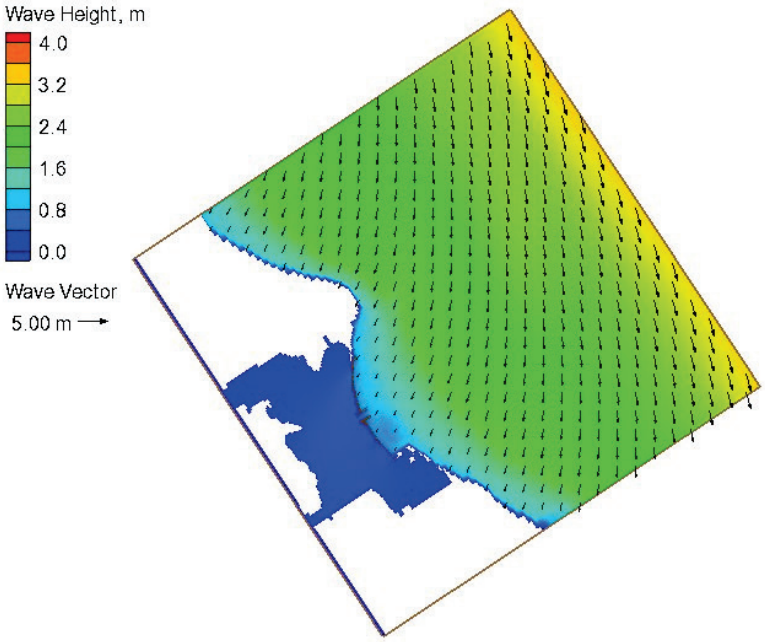

Figure 4-30. Model maximum wave-height field for S-3 during Jan 1971 storm (WL= 0.9 m).

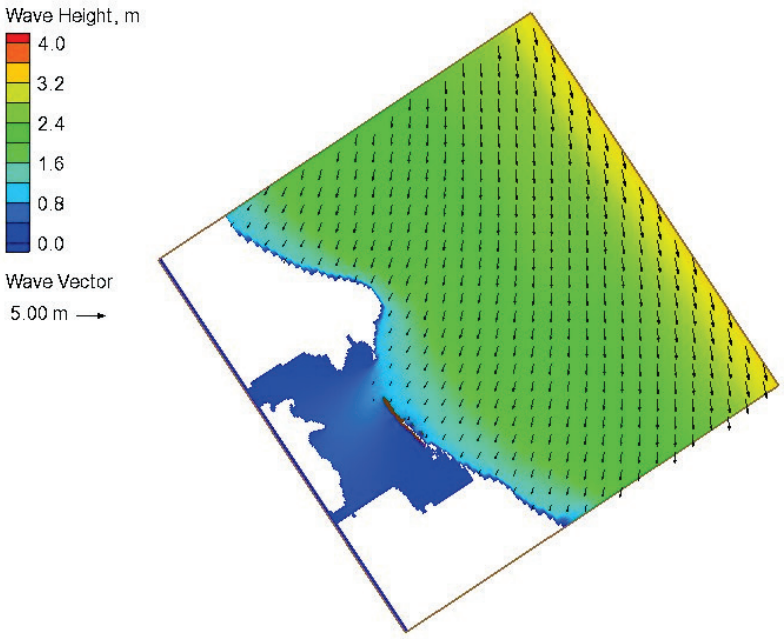

Figure 4-31. Model maximum wave-height field for S-0 during Mar 1993 storm (WL= 0.23 m).

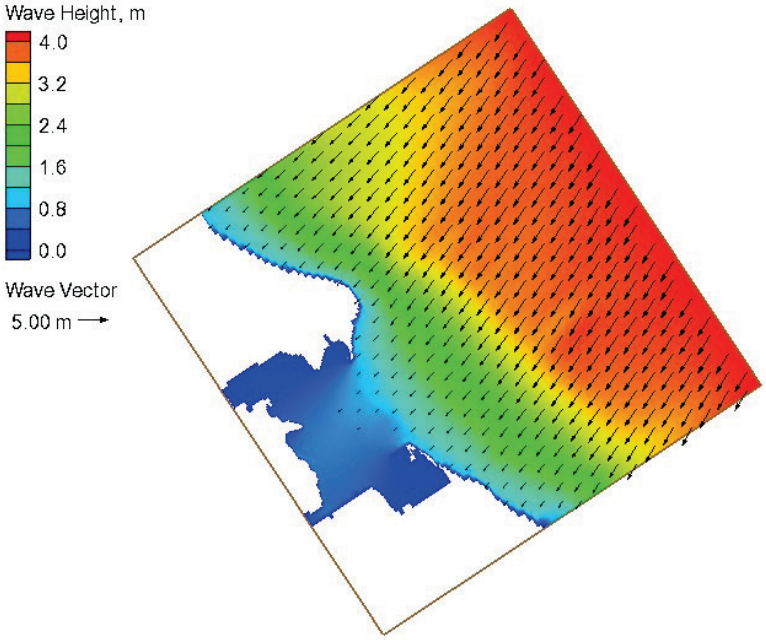

Figure 4-32. Model maximum wave-height field for S-1 during Mar 1993 storm (WL = 0.23 m).

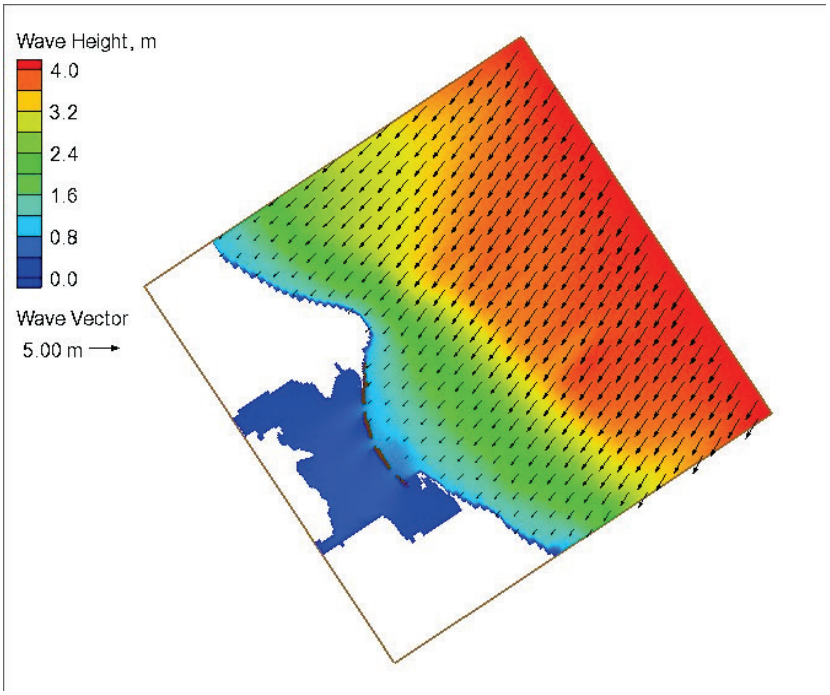

Figure 4-33. Model maximum wave-height field for S-2 during Mar 1993 storm (WL= 0.23 m).

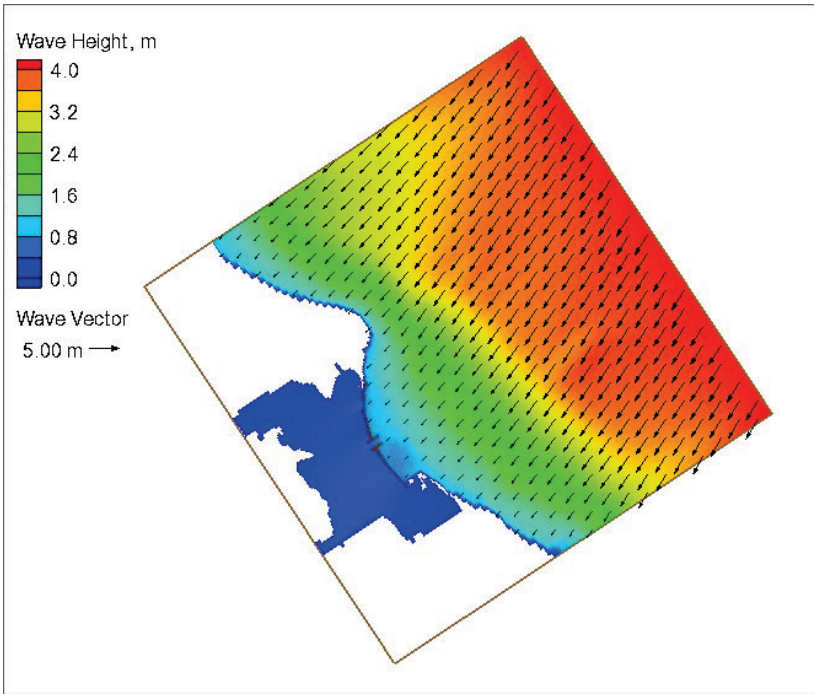

Figure 4-34. Model maximum wave-height field for S-3 during Mar 1993 storm (WL= 0.23 m).

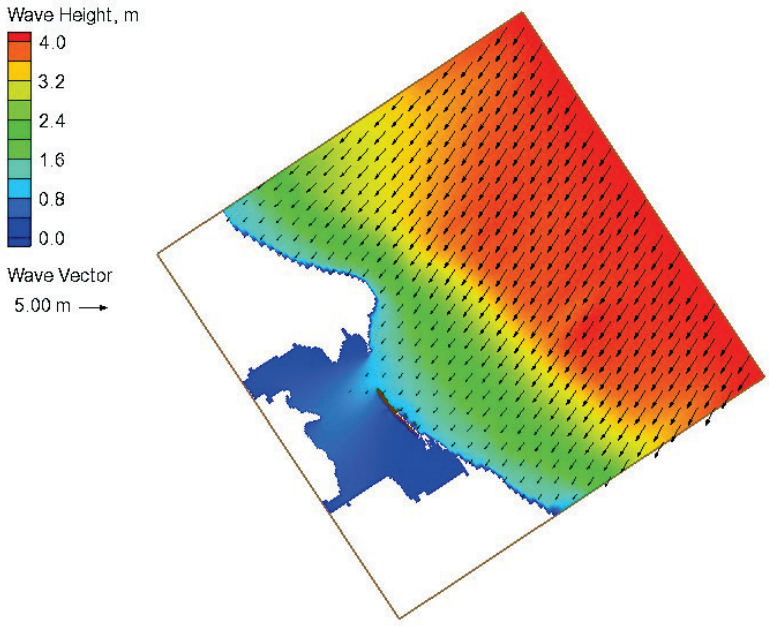

Figure 4-35. Model morphology changes for S-0 during Jan 1971 storm (WL= 0.9 m).

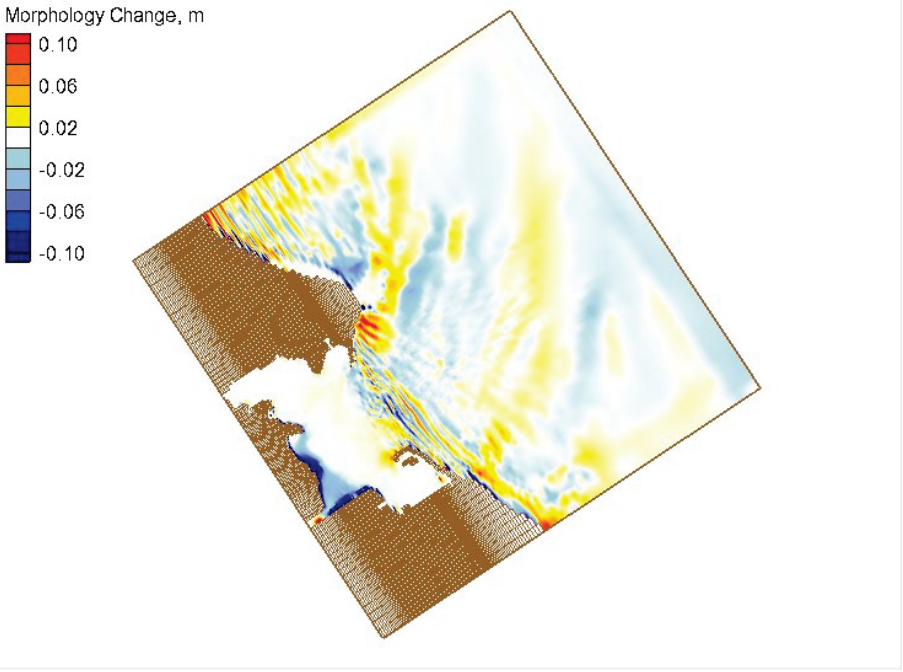

Figure 4-36. Model morphology changes for S-1 during Jan 1971 storm (WL = 0.9 m).

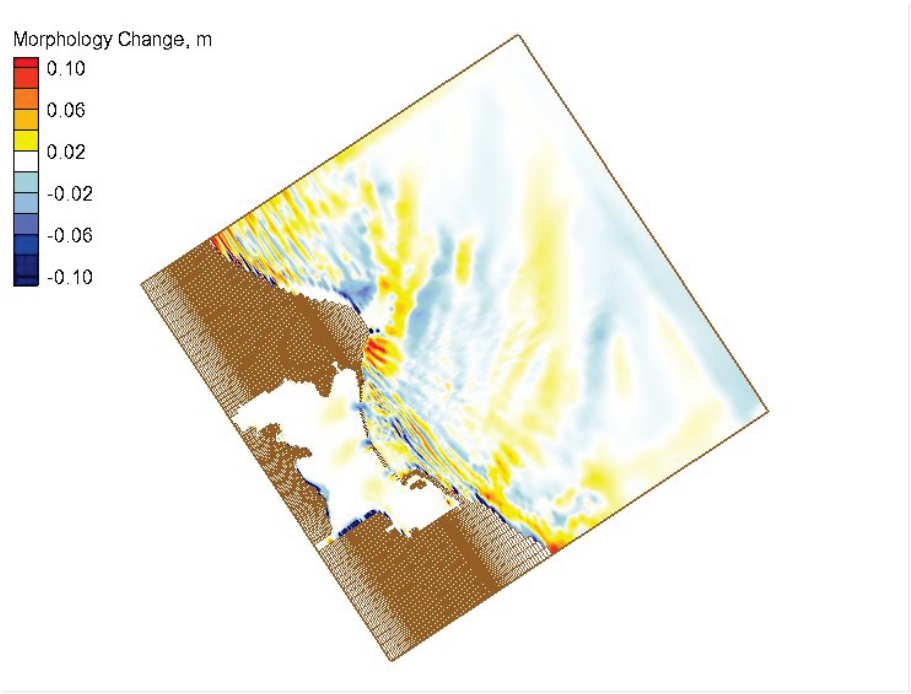

Figure 4-37. Model morphology changes for S-2 during Jan 1971 storm (WL = 0.9 m).

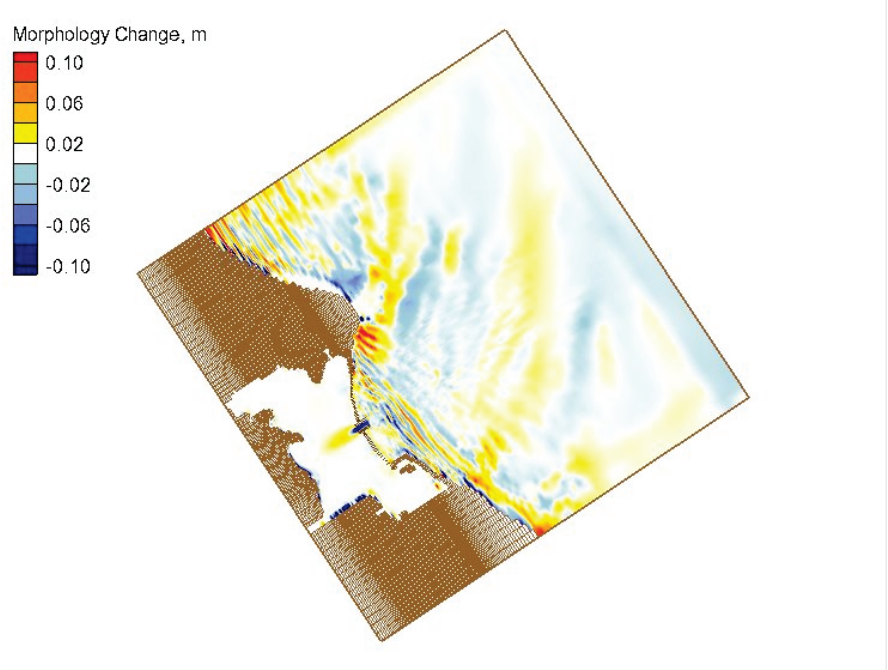

Figure 4-38. Model morphology changes for S-3 during Jan 1971 storm (WL = 0.9 m).

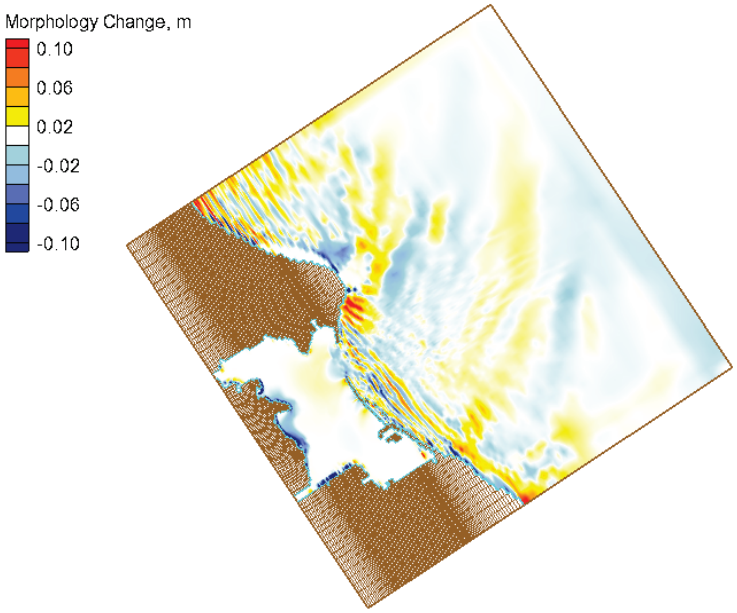

Figure 4-39. Model morphology changes in the bay for S-0, S-1, S-2, and S-3 during Jan 1971 storm (WL = 0.9 m).

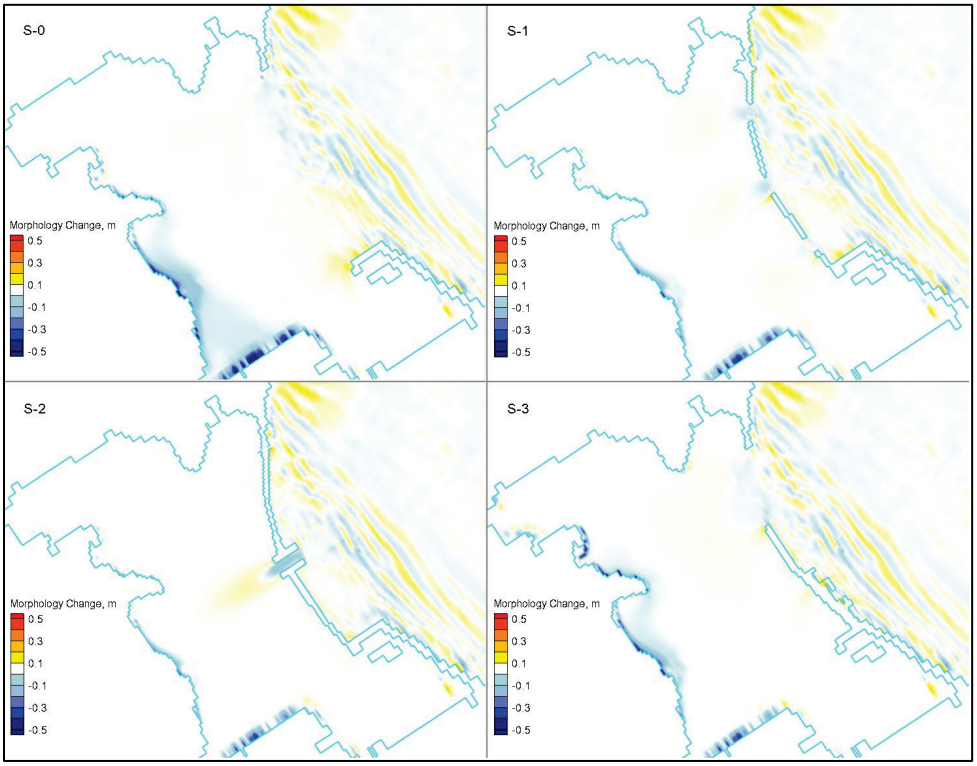

Figure 4-40. Model morphology changes for S-0 during Mar 1993 storm (WL= 0.23 m).

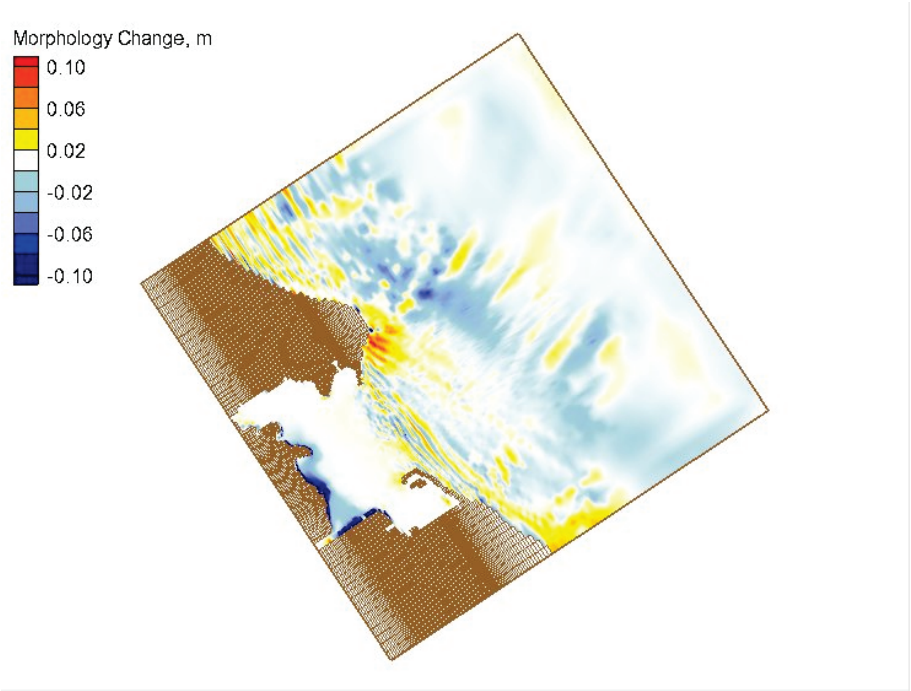

Figure 4-41. Model morphology changes for S-1 during Mar 1993 storm (WL= 0.23 m).

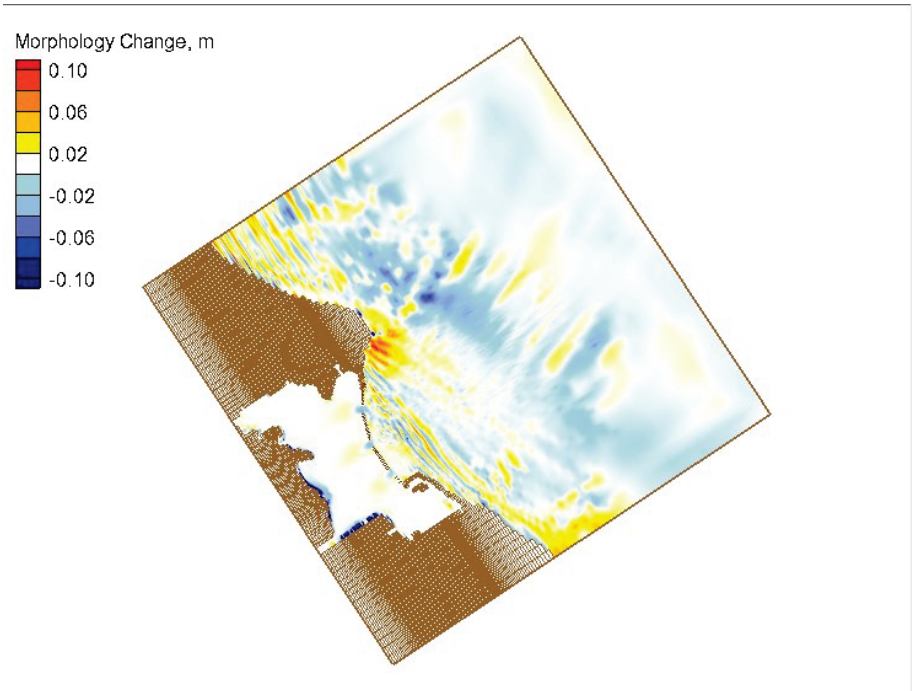

Figure 4-42. Model morphology changes for S-2 during Mar 1993 storm (WL= 0.23 m).

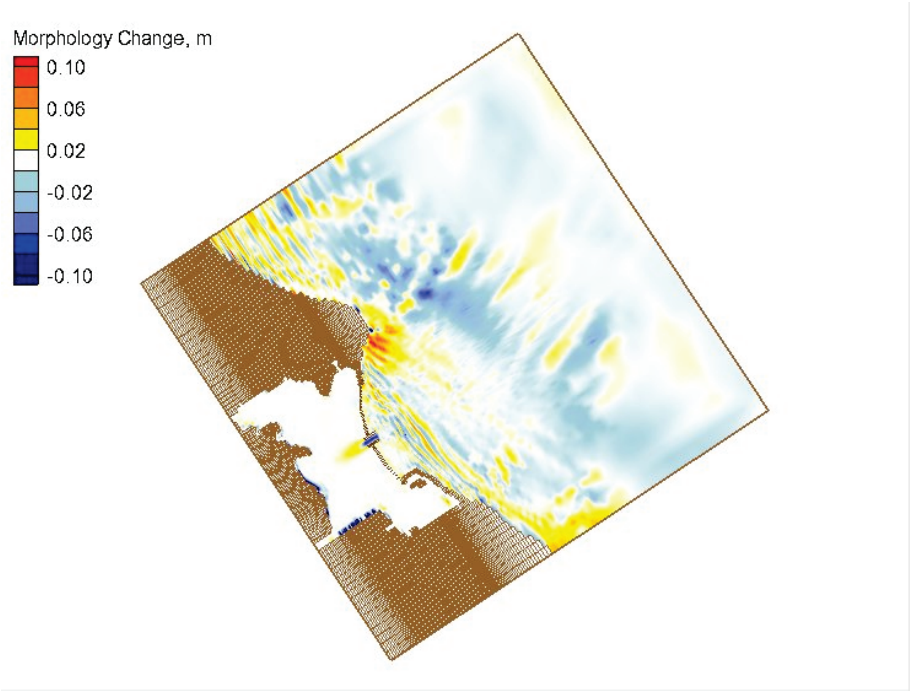

Figure 4-43. Model morphology changes for S-3 during Mar 1993 storm (WL= 0.23 m).

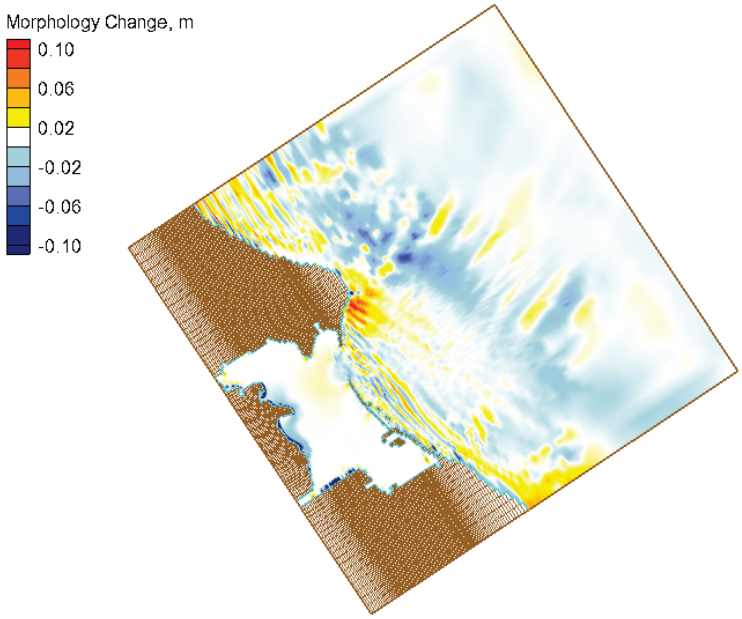

Figure 4-44. Model morphology changes in the bay for S-0, S-1, S-2, and S-3 during Mar 1993 storm (WL= 0.23 m).

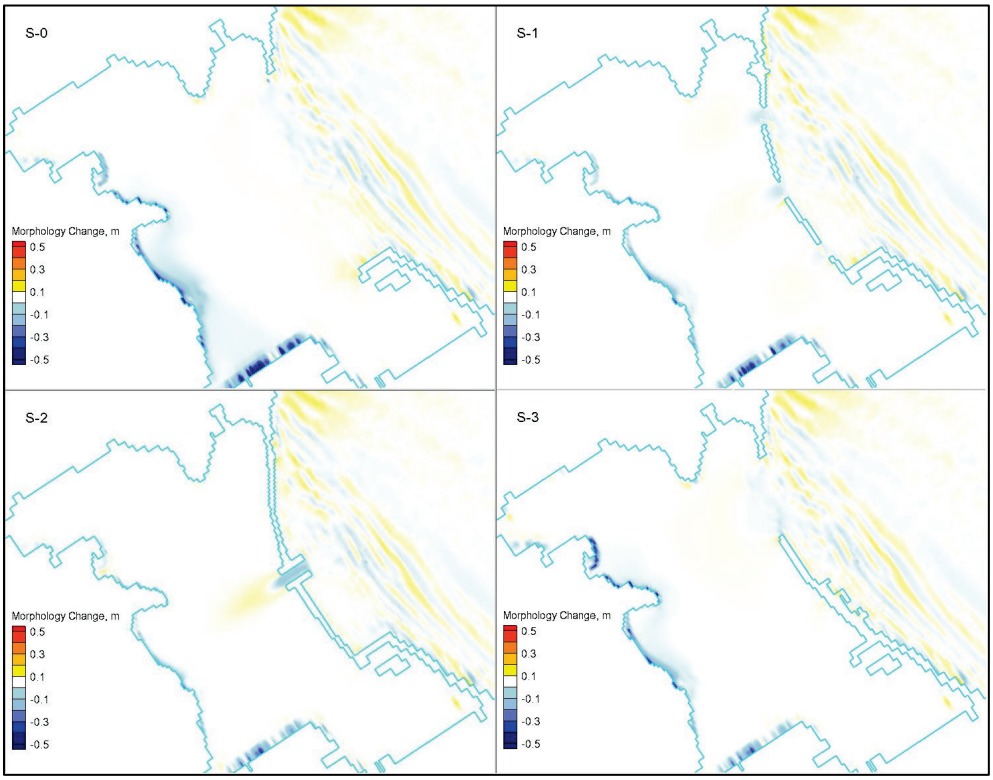

Table 4-5. Calculated maximum wave height (m) during Jan 1971 storm, and percent reduction in wave height near the backbay shoreline.

WL / Datum / Scenario	-0.4 m (low)	+ 0.2 m (average)	+ 0.9 m (high)
S-0	0.09	0.27	0.48
S-1	0.06 (-33%)*	0.15 (-44%)	0.27 (-44%)
S-2	0.05 (-44%)	0.10 (-63%)	0.24 (-50%)
S-3	0.08 (-11%)	0.21 (-22%)	0.38 (-20%)
* Percent difference (in parentheses) relative to S-0 (negative values indicate reduction)			

Table 4-6. Calculated maximum wave height (m) during Mar 1993 storm and percent reduction in wave height near the backbay shoreline.

WL / Datum Scenario	-0.98 m (low)	-0.38 m (average)	+ 0.23 m (high)
S-0	0.22	0.41	0.67
S-1	0.15 (-32%)*	0.29 (-29%)	0.40 (-40%)
S-2	0.13 (-41%)	0.21 (-49%)	0.27 (-60%)
S-3	0.18 (-18%)	0.35 (-15%)	0.54 (-19%)
* Percent difference (in parentheses) relative to S-0 (negative values indicate reduction)			

Table 4-7. Calculated maximum morphology change (m) during Jan 1971 storm and percent reduction in morphology change near the backbay shoreline.

WL / Datum Scenario	-0.4 m (low)	+ 0.2 m (average)	+ 0.9 m (high)
S-0	-0.11	-0.49	-0.75
S-1	-0.04 (-64%)*	-0.29 (-41%)	-0.54 (-28%)
S-2	-0.04 (-64%)	-0.14 (-71%)	-0.46 (-39%)
S-3	-0.05 (-55%)	-0.37 (-24%)	-0.53 (-29%)
* Percent difference (in parentheses) relative to S-0 (negative values indicate reduction)			

Table 4-8. Calculated maximum morphology change (m) during Mar 1993 storm and percent reduction in morphology change near the backbay shoreline

WL Datum / Scenario	-0.4 m (low)	+ 0.2 m (average)	+ 0.9 m (high)
S-0	-0.08	-0.62	-0.67
S-1	-0.03 (-63%)*	-0.31 (-50%)	-0.36 (-46%)
S-2	-0.03 (-63%)	-0.19 (-69%)	-0.29 (-56%)
S-3	-0.04 (-50%)	-0.41 (-34%)	-0.59 (-12%)
* Percent difference (in parentheses) relative to S-0 (negative values indicate reduction)			

4.4 Results for current fields

A few samples of current fields are provided in this section for the Hurricane Sandy simulation for all three configurations (S-0, S-1, and S-2). Because the current fields for the 9-month and 20 yr design storm simulations were similar, they are not included. The spatial variation of current fields near the peak of storm is shown for the S-0, S-1, and S-2 bay configurations at three water levels. Results indicated that maximum current magnitude for three bay configurations at three water levels did not exceed 1 m/sec. Details can be found in the sections that follow.

4.4.1 Currents for S-0 from Hurricane Sandy simulations

The current fields for S-0 at three water levels are shown in Figures 4-45 to 4-47. These are the snapshots near the largest waves (14 ft =4.3 m) occurring during Sandy at 0300 GMT on 30 Oct 2012. These plots indicate circulation pattern is influenced not just by waves, but also by wind speeds, wind direction, and water levels. The change in the circulation pattern both in the lake and inside the bay is apparent for three water levels. With increasing water level, current vectors diminish in magnitude and change direction inside and outside the bay. Generally, a weakening of current occurs as the water level increases. S-0 (without project) is the baseline to assess relative merits of three alternatives (S-1, S-2, and S-3). The structures introduced in each alternative alter circulation patterns near them, but have no effect on currents away from the structures. Changes in the current occurring away from the structures signify the effects of the wind- and wave-induced currents. Changes to currents seen on the up-wind side of the entrance (lake side) are caused by wave processes (e.g., wave shoaling, breaking, wave-current interaction). Overall, stronger currents occurred for Alternative S-0 at low water level than the intermediate and high water levels.

Figure 4-45. Calculated current field for S-0 during Hurricane Sandy (WL= 0 m).

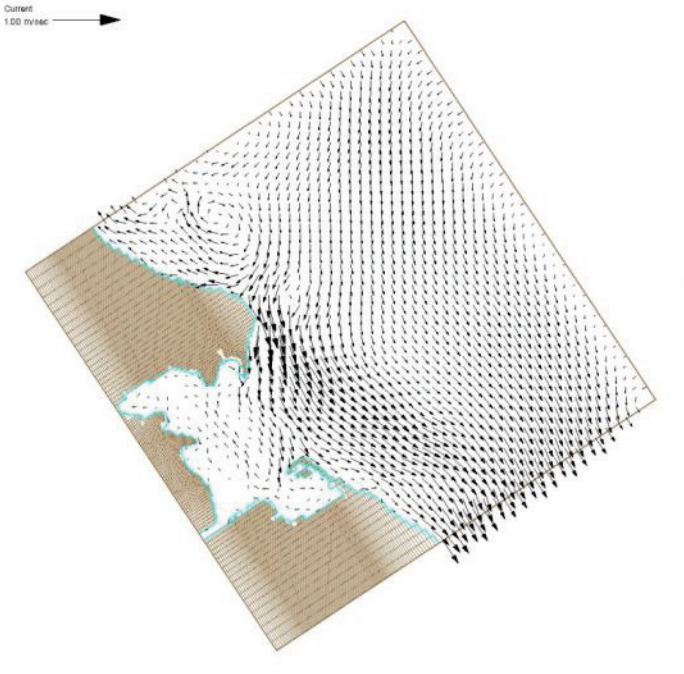

Figure 4-46. Calculated current field for S-0 during Hurricane Sandy (WL= 0.61 m).

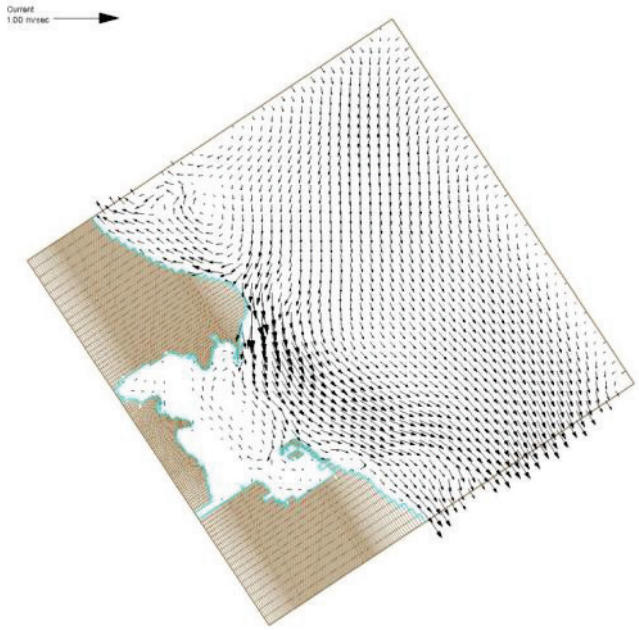

Figure 4-47. Calculated current field for S-0 during Hurricane Sandy (WL= 1.433 m).

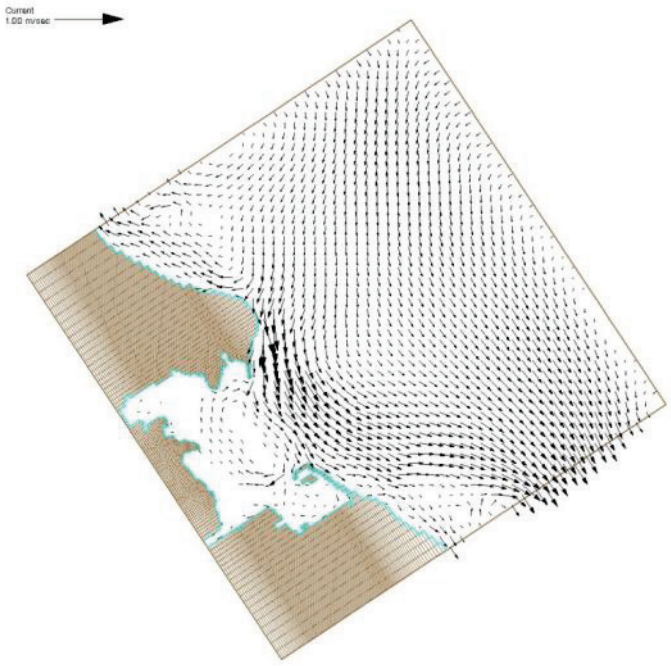

4.4.2 Currents for S-1 from Hurricane Sandy simulations

The S-1 current fields are shown in Figures 4-48 to 4-50 for three water levels (WL = 0 m, 0.61 m, 1.433 m). The observations made for S-0 in the previous section apply to Alternative S-1. In this case, the wave-structure interaction plays a significant role in changing the circulation and current fields. As the water level increases, the magnitude of current decreases, especially inside the bay, with smaller currents at higher water level. The change in the circulation near the structures of S-1 is seen on the upwind side of the structures (lake-ward in front of structures). This change is caused by wave-structure interactions (e.g., wave reflection, diffraction, runup and overtopping, breaking, wave-current interaction calculated in CMS-Wave by using CEM-type empirical equations). These interactions contribute to strong currents developing in the gaps between structures, and in the immediate vicinity of structures. Comparatively stronger currents occur for Alternative S-1 at the lowest water level than those that occur at the two other water levels.

Figure 4-48. Calculated current field for S-1 during Hurricane Sandy (WL= 0 m).

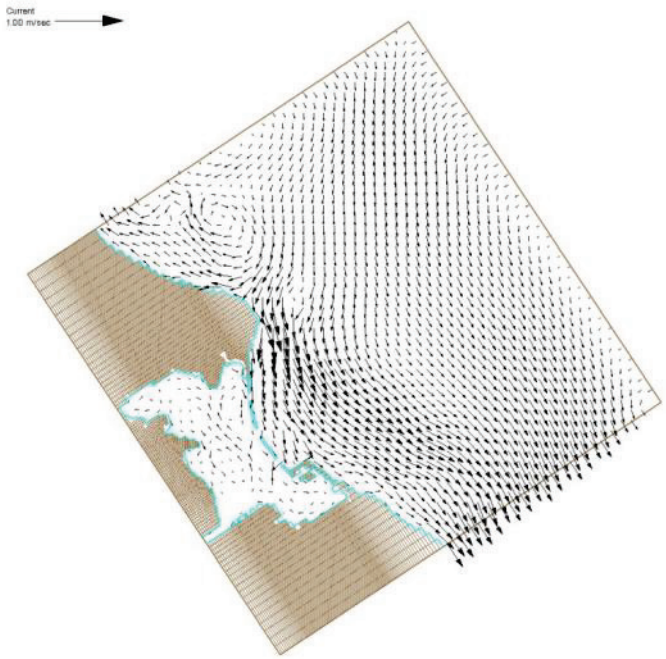

Figure 4-49. Calculated current field for S-1 during Hurricane Sandy (WL= 0.61 m).

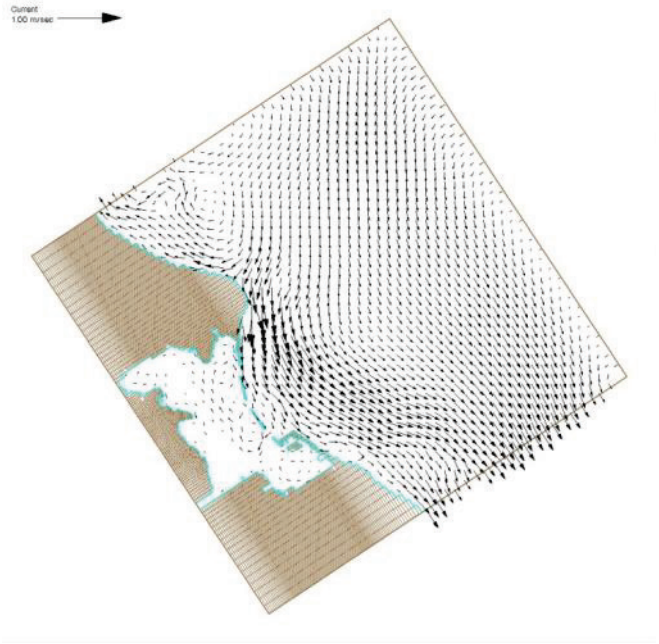

Figure 4-50. Calculated current field for S-1 during Hurricane Sandy (WL= 1.433 m).

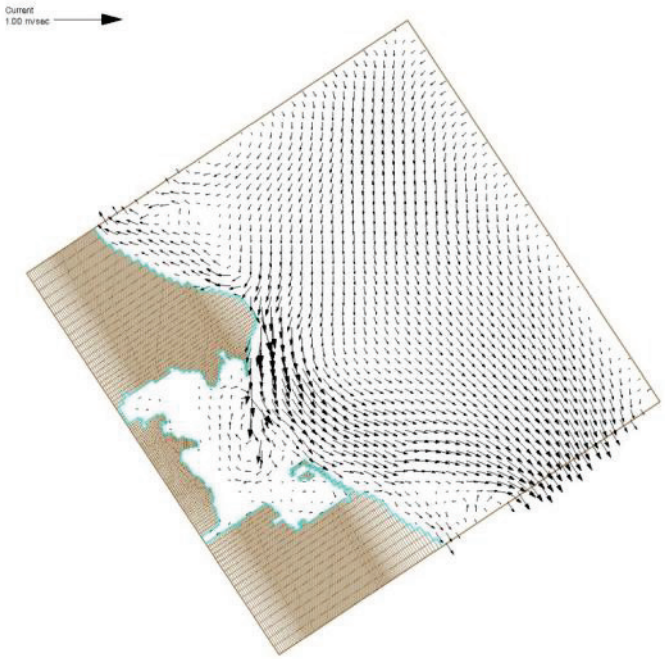

4.4.3 Currents for S-2 from Hurricane Sandy simulations

The current fields for S-2 at three water levels (WL = 0 m, 0.61 m, 1.433 m) are shown in Figures 4-51 to 4-53. Results are similar to S-1, except that there is only one gap in the middle where an inlet is configured. The figures for S-2 show the role of wave-structure interaction on the circulation field. With increasing water level, the magnitude of current decreases inside the bay. At the high water level, it appears wave overtopping produces more flow in the lee of two structures, but flows are weak at higher water levels. Because the structures for this alternative are nearly continuous, the change in the circulation up-wind of the structures (lake-ward in front of structures) closest to the S-2 structures is more pronounced than S-1. This is an indication of the presence of stronger wave-structure interactions in S-2. Because of these interactions, the strongest currents occur for S-2 at and around the inlet (and channel) area. Such currents have both beneficial and detrimental consequences, e.g., may naturally scour and flush the inlet, but these currents could also undermine the foundation of structures and cause excessive channel shoaling and in-filling. These concerns can be investigated using a 3-D wave-hydro-sediment transport model to study details of waves, flow, and transport in the immediate vicinity of structures.

Figure 4-51. Calculated current field for S-2 during Hurricane Sandy (WL= 0 m).

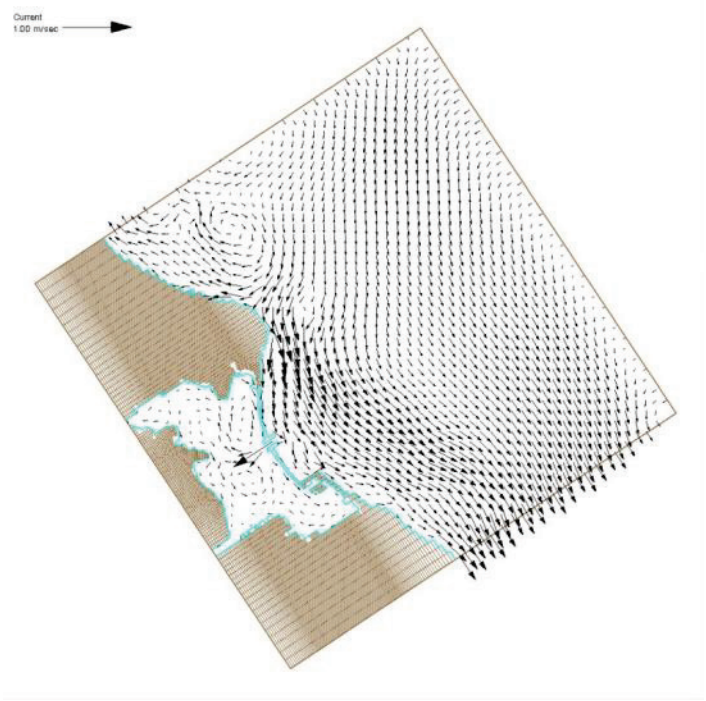

Figure 4-52. Calculated current field for S-2 during Hurricane Sandy (WL= 0.61 m).

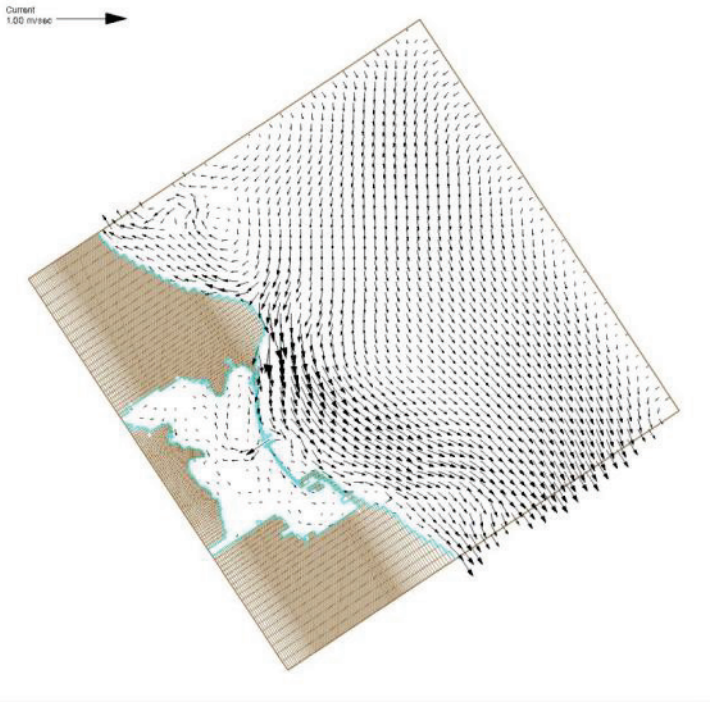

Figure 4-53. Calculated current field for S-2 during Hurricane Sandy (WL= 1.433 m).

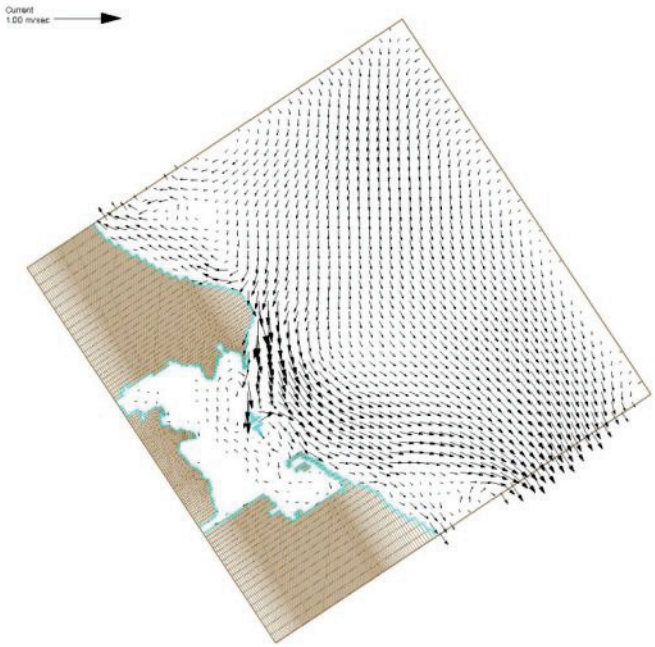

4.4.4 Currents for S-3 from Hurricane Sandy simulations

The current fields for S-3 at three water levels (WL = 0 m, 0.61 m, 1.433 m) are shown in Figures 4-54 to 4-56. Results are similar to the S-0, except the current magnitude inside the bay is much smaller than S-0 configuration. As was the case for S-0, and Alternatives S-1 and S-2, with increasing water level, the magnitude of current in Alternative S-3 decreases inside the bay. At the highest water level, there is a much higher chance for wave runup/overtopping of breakwaters and groins than at the two lower water levels. This would require use of the BOUS-2D, a Boussinesq wave model, to determine and optimize the side slopes and crest height of structures, and to calculate estimates of wave runup and overtopping of the final alternative selected for design.

Figure 4-54. Calculated current field for S-3 during Hurricane Sandy (WL= 0 m).

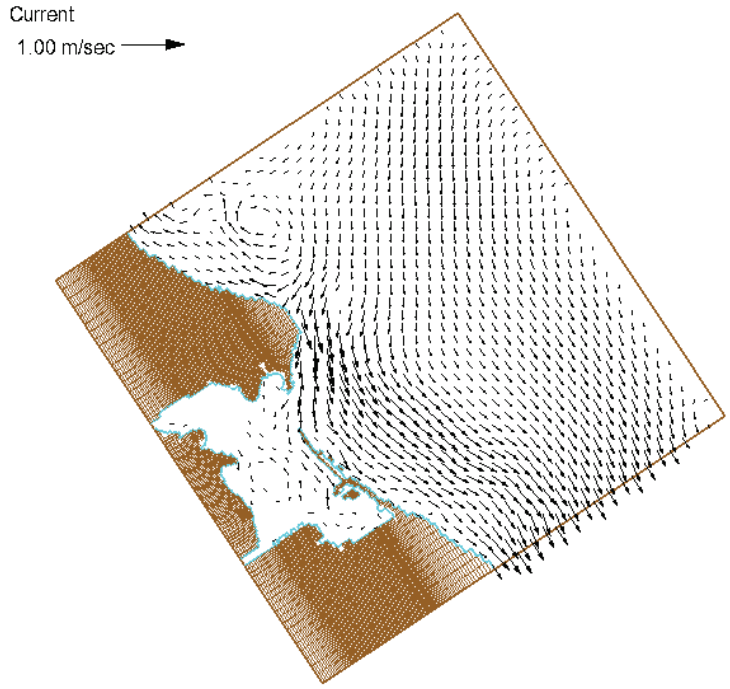

Figure 4-55. Calculated current field for S-3 during Hurricane Sandy (WL= 0.61 m).

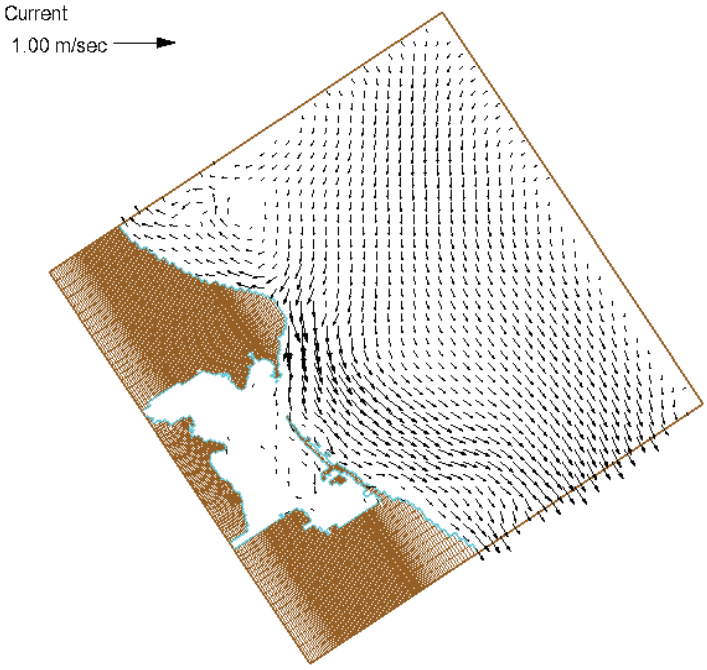

Figure 4-56. Calculated current field for S-3 during Hurricane Sandy (WL= 1.433 m).

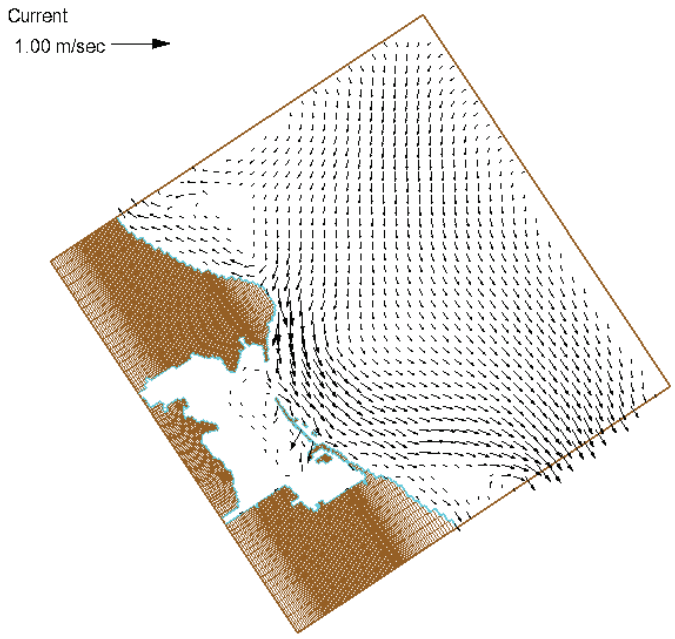

4.5 Results for local areas of interest

The solution fields presented so far provide an overall picture of the modeling results over the entire computational grid domain for each configuration (S-0, S-1, S-2, and S-3), and conditions that have been simulated. If required, results can be extracted in any particular area of interest within the bay to determine the degree of reduction attained in that local area. In principle, this analysis can be applied to any location of interest in the modeling domain, and is not limited to areas inside the bay. The selected area may be in close proximity of breakwaters or away from the structures. This additional analysis can shed more light into the benefits of a specific alternative to different regions in the bay. For example, the wetlands area located behind the central peninsula water region of the bay may be selected for this analysis. The leeward entrance areas of breakwaters are also candidate regions to consider. Additional information about the methodology follows.

The details of a solution field can be examined using the SMS at a user-selected set of points, lines (transects), or areas (polygons). As an example, the analysis can be applied to the leeward regions of breakwater pieces in S-0, S-1, S-2, and S-3, or to central bay water region in front of wetlands. This is done here by using a number of transects (T1, T2, T3, etc) in the areas of interest. An in-water transect may be placed behind or in front

of a structure, or it could be configured to follow the trace of backbay shoreline at a desired distance bayward. A transect can be a straight or curved line consisting of multiple segments. Each segment can be sub-divided by distributing points along a segment or over the entire transect.

Once transects for local output have been defined in the SMS, these may be saved into a SMS map file which can be revised and re-used later as needed with any simulation. The map features in SMS are GIS objects in a conceptual model framework. Because there are several GIS feature types in SMS, it is necessary to define the output points, lines, and areas in the map file as the "observation" type for extracting model results. To extract results from a global solution file in SMS, the Data Menu is used to select Plot Wizard and the Observation Type. Users may follow detailed instructions available from the SMS website, ERDC wiki, or the Help Menu.

As an example, Figure 4-57 illustrates the utility of SMS map in a local analysis for S-2. In this demonstration, three cross-shore transects (T1, T2, and T3) are lined up to pass through three structural gaps of S-1. These transects connect the lake and bay sides of the grid domain. Transect T4 is positioned in the lee of structures S-1, S-2, and S-3. Transect T5 in the backbay follows the shoreline contour and curves both at the north and south ends. Users can control the location, length, shape, and other characteristics of transects. The SMS allows users to construct and modify such preferred conceptual map objects. Figure 4-58 shows the extracted water depth that depicts the variation of depth along each of five transects or arcs for S-2. Any other model solution or grid feature may be extracted along one or more of these transects in the same manner.

Figure 4-57. Transects T1 to T5 for local analysis of model S-2 grids and solution fields.

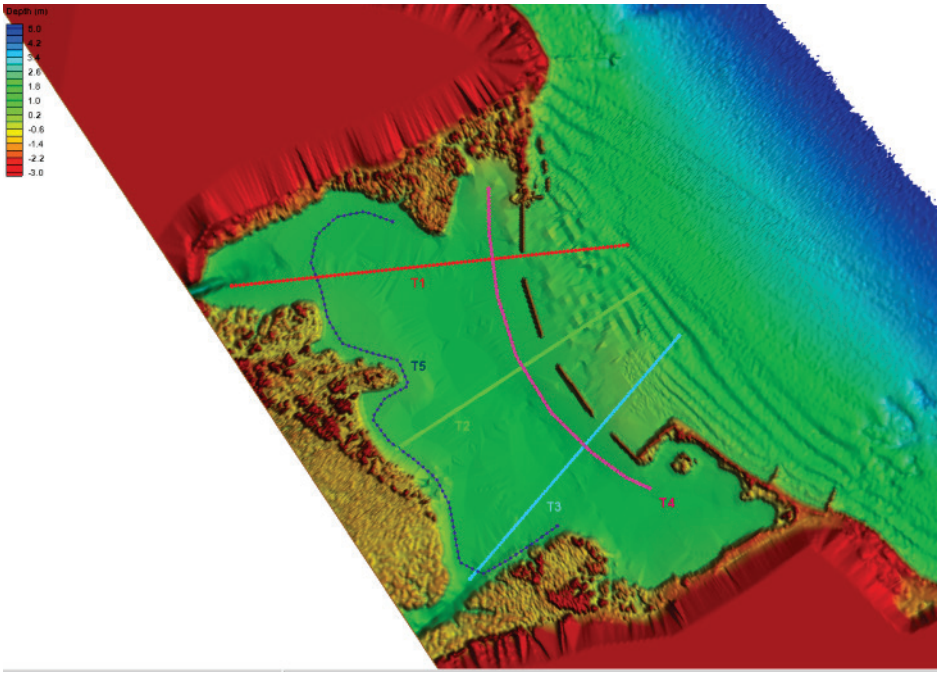

Figure 4-58. Depth variation extracted along transects T1 through T5 for S-2.

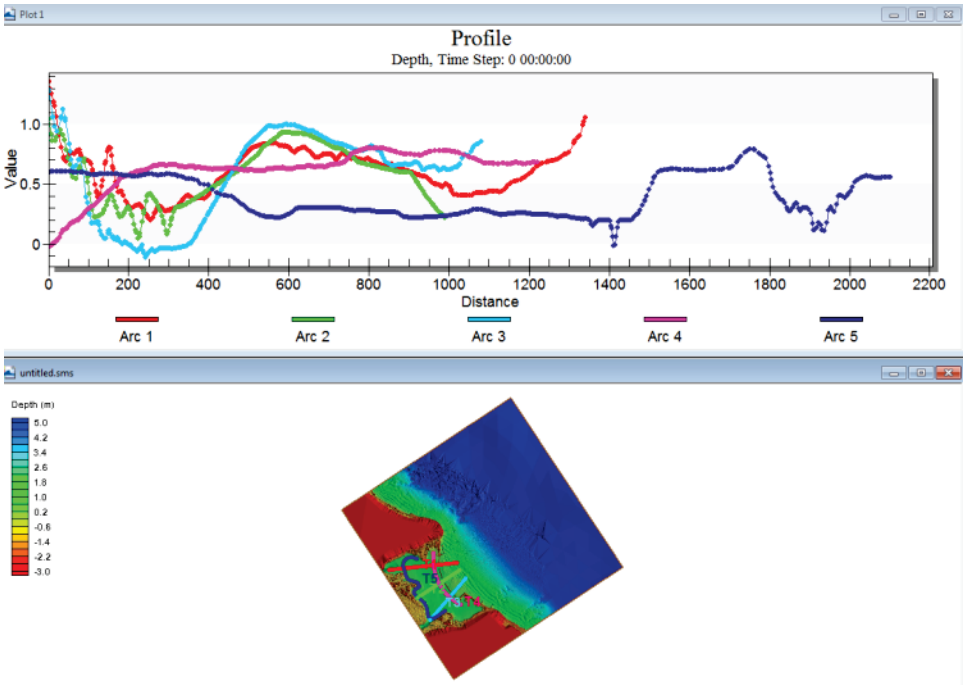

4.6 Quantitative measures

An efficiency or reduction factor may be used to compare the relative performance of alternatives, to determine the required breakwater crest elevation for design, or to determine the number of structural segments, gap width, or channel alignment and width, etc. This quantitative measure can be defined in different ways, and, in part, the definition depends on how the measure will ultimately be used. The selection of this measure also depends on the engineering design parameters and characteristics of modeling results used to construct such a measure.

For example, one could use the difference in the calculated output quantities (wave height, current, and morphology change) between the existing bay and three alternatives. The ratio of calculated output quantities from the existing bay and alternatives is another potential candidate to consider. One may also use the scaled ratio that has been referenced and normalized with respect to the existing bay baseline estimates. However, because the values of calculated output quantities can be very small or large, the first method is recommended for this study, which is the traditional difference metric, defined as follows:

Δ = ("with project" Output) - ("without project" Output)

where the with project output is from one of the alternatives and/or simulations conducted with different breakwater crest elevations, lengths, positions, number of structures, etc. A few observations about this metric are warranted. Using the above definition, we note that the Δ = diff metric will always be a negative number. A value of zero (0) signifies that the with project output matches the without project output. The larger the numerical value of diff, the greater the deviation between two compared outputs.

The diff metric is a direct measure of the reduction for the calculated wave heights, currents, and bed changes. The Δ metric will be used for Alternatives S-1 and S-2 to assess their effectiveness relative to the without project baseline. The method can be used for any part of solution varying in time, or it can be used for time of the peak event for any conditions simulated. Results of maximum wave heights are extracted along five transects (T1 to T5) for Hurricane Sandy, 9-month, and 20 yr design return period simulations.

Figures 4-59 and 4-60 show the calculated wave heights along transects T1, T2, T3, T4 and T5, respectively, representing the maximum wave height that occurred at 0300 GMT on 30 October 2012, during Hurricane Sandy for S-0, S-1, S-2, and S-3 with WL = 0 m. Similarly, Figures 4-61 and 4-62 show the maximum wave heights along T1 to T5 for the 9-month simulations. Figures 4-63 and 4-64 show the maximum wave heights along T1 to T5 for the Jan 1971, 20 yr design return period with low WL datum. Figures 4-65 and 4-66 show the maximum wave heights along T1 to T5 for the Mar 1993, 20 yr design return period with low WL.

For three meteorological and oceanographic forcing types shown in Figures 4-59 through 4-66, wave heights are generally large on the lake side along the three cross-shore transects (T1, T2, and T3), and continue to reduce after the transects pass through the structures, resulting in the smallest wave heights at the terminal ends (bayward) of the transects. The wave height variation along transects T4 and T5, respectively, in the lee of structures and along the central and southern shorelines, are comparatively smaller than the wave heights along the three cross-shore transects.

Figure 4-59. Calculated maximum wave height for S-0, S-1, and S-2 along T1, T2, and T3 during Hurricane Sandy.

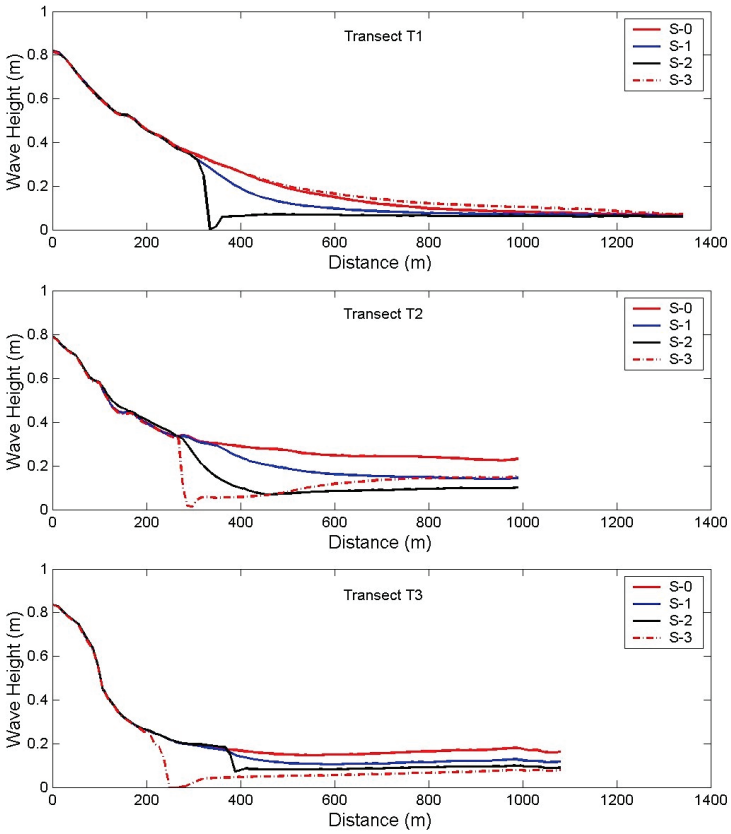

Figure 4-60. Calculated maximum wave height for S-0, S-1, and S-2 along T4 and T5 during Hurricane Sandy.

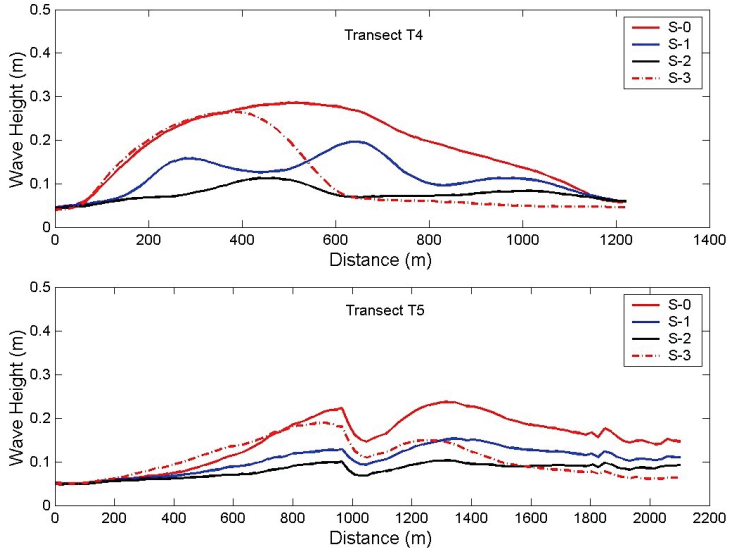

Figure 4-61. Calculated maximum wave height for S-0, S-1, and S-2 along T1, T2, and T3 during 9-month simulation.

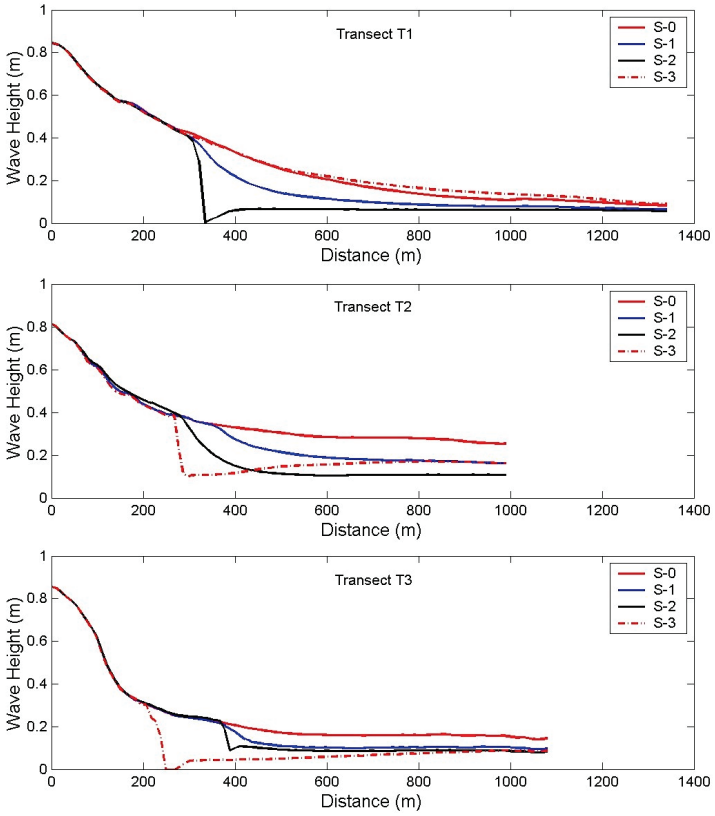

Figure 4-62. Calculated maximum wave height for S-0, S-1, and S-2 along T4 and T5 during 9-month simulation.

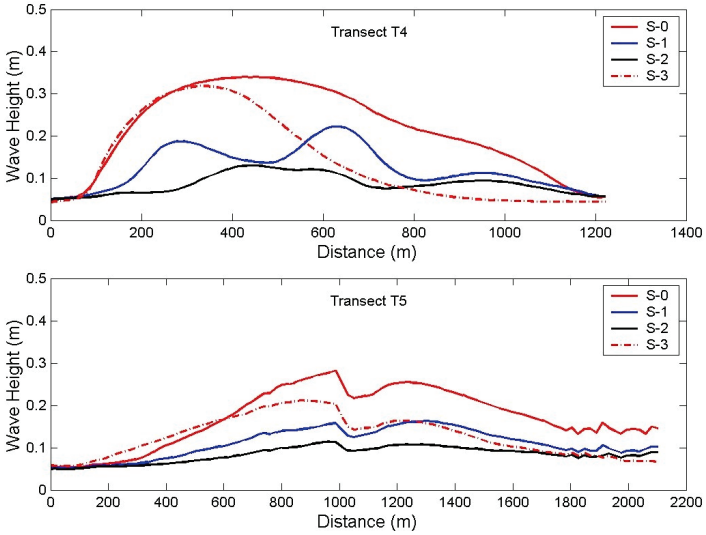

Figure 4-63. Calculated maximum wave height for S-0, S-1, S-2, and S-3 along T1, T2, and T3 during Jan 1971, 20 yr design return period storm.

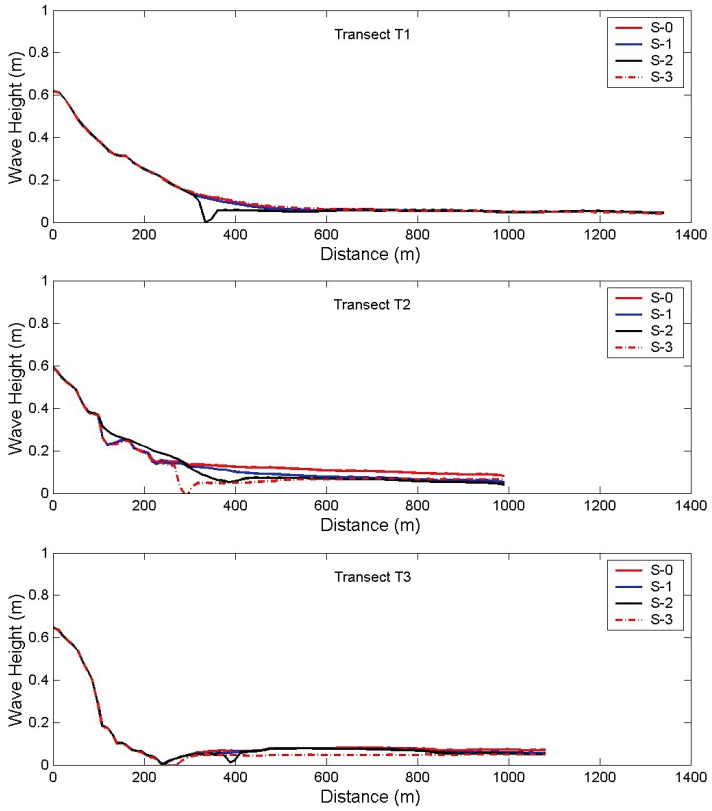

Figure 4-64. Calculated maximum wave height for S-0, S-1, S-2, and S-3 along T4 and T5 during Jan 1971, 20 yr design return period storm.

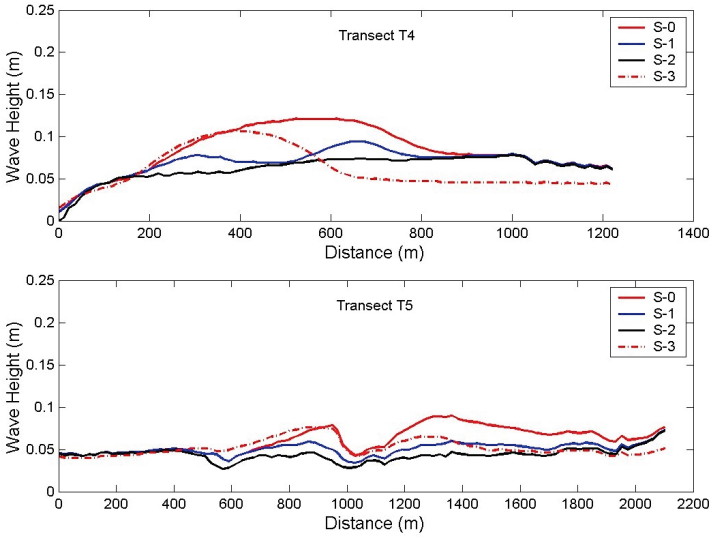

Figure 4-65. Calculated maximum wave height for S-0, S-1, S-2, and S-3 along T1, T2, and T3 during Mar 1993, 20 yr design return period storm.

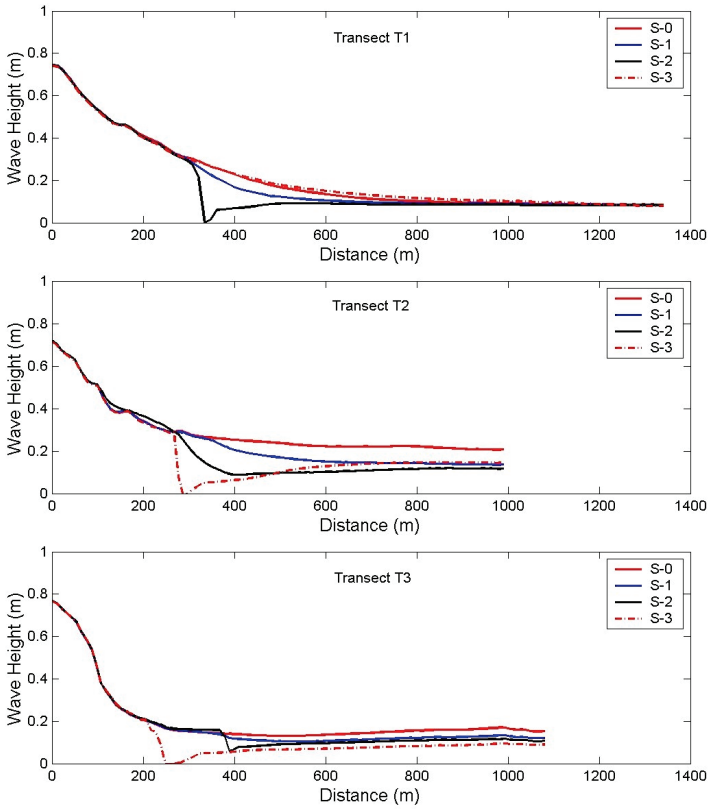

Figure 4-66. Calculated maximum wave height for S-0, S-1, S-2, and S-3 along T4 and T5 during Mar 1993, 20 yr design return period storm.

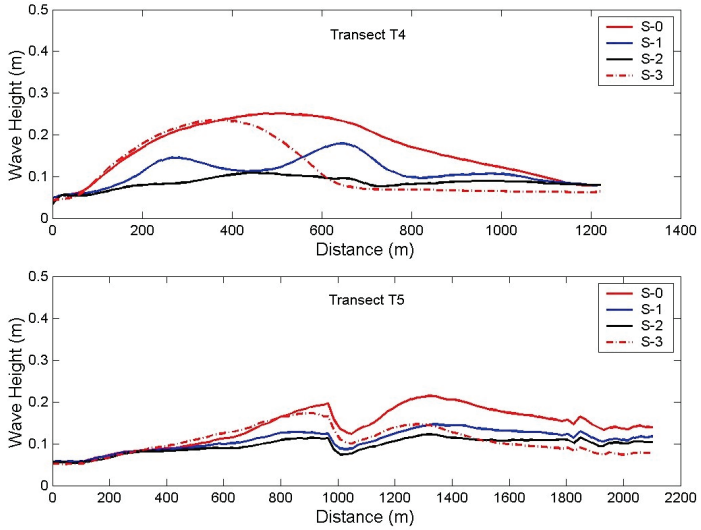

For all wind, wave directions, and water levels investigated in this study, the analysis of reduction from three alternatives was based on the wave-height reduction factor calculated as the difference of outputs with and without project scenarios. Among the three alternatives investigated, Alternative S-2 generally produced the largest wave-height reduction along transect T5. Under the extreme water level condition, the wave-height reduction may not be an appropriate proxy to use for ranking the alternatives or to determine the optimal breakwaters crest elevation. For this reason, the low water level (WL = 0 m) should be used in the ranking of alternatives based on their performance (e.g., calculated wave-height difference or reduction factor).

In the case of 20 yr design storms, the worst case scenario was assumed, and a similar analysis was performed for the two extreme waves that had occurred in 1971 and 1993, which approached the bay at a certain angle. These simulations were made with low, medium, and high water levels. Such waves were assumed to occur again in the future. However, if the approach angle of these storms were different, the impacts on the bay would also be different. Depending on direction of winds associated with such extreme and significant over-land drag of wind speeds, higher or lower water level pile-ups than these two past occurrences may develop inside the bay. If lower water levels occur in the future during such extreme storm events, less waves and currents may occur in the bay.

Based on results described so far, Alternative S-2 has performed better than S-1 and S-3 for all conditions evaluated, providing the maximum reduction of waves and currents for protection of wetlands. However, because S-2 achieves this by essentially blocking the entrance from north to south barrier beaches, it leaves a narrow structured inlet in the middle for access to/from the bay and Lake Ontario. Consequently, other factors should be taken into consideration to determine the preferred alternative for Braddock Bay. These may include 1) affordability relative to initial design cost for S-1, S-2, and S-3 systems; 2) anticipated long-term maintenance requirements for each system; and 3) long-term consequences (decades to century) of bay closure by each alternative on the biological and ecological well-being of the bay ecosystem.

Potential impacts of the three proposed alternatives (S-1, S-2, and S-3) on the wetlands and ecosystem of Braddock Bay are important factors for selecting an alternative that can best serve the bay's short- and long-term

needs. LRB has a contractor, LimnoTech, Inc., investigating the water-quality issues in the bay. ERDC provided the hydrodynamic model results described in this report to the contractor, and assisted in the usage of modeling results. The results of that study should help to determine the alternative that can meet the bay's ecosystem requirements. This may require performing a local analysis of ecosystem modeling results in the area of interest corresponding to Hurricane Sandy, 9-month and 20 yr design conditions.

4.7 Inlet maintenance in S-2

Further investigation is warranted for two reasons concerning potential maintenance required for the jettied inlet in Alternative S-2. First, in the present modeling results, the magnitude of currents increased both on the lake and bays sides of this naturally generated inlet (e.g., it was not dredged). Such increases in currents, even small, are of concern because of scouring by currents that can undermine the breakwater structures forming the inlet. Increasing currents speeds on the lake side can mobilize more sediment to form bars on the wind-ward face of breakwaters. These piled-up sediments can increase wave runup and overtopping of breakwaters, facilitating more wave energy to move into the bay side. Although the magnitude of maximum current from two-dimensional CMS simulations conducted in this study remained below the threshold necessary to initiate severe sedimentation, over longer time frames with sustained forcings, this could change. Consequently, a three-dimensional investigation of sediment transport is recommended prior to construction of breakwaters to address local scouring potential in the inlet and lake side of structures. After a comprehensive understanding of future behavior of sediment transport in the inlet and along the breakwaters, a periodic long-term maintenance plan for protective structures and navigation can be developed.

4.8 Maintenance of headland breakwaters in S-3

For two reasons, further investigation is warranted based on sediment transport results for Alternative S-3, which suggests potential maintenance might be required for the headland breakwaters used in Alternative S-3. Figure 4-67 to Figure 4-69 show calculated sediment transport (and ensuing morphology change) in the vicinity of Alternative S-3 system for three water levels. At low water level, the yellow-and-blue pattern displayed in Figure 4-67 represent erosional and depositional areas, respec-

tively, lakeward of the S-3 structures (headland breakwaters and groin). There is practically no sign of movement of sediments deposited near and on and around the structures. Sediment size used in these simulations was 0.7 mm, as specified by LRB study team. These coarse sediments were mobilized by waves and currents lakeward of structures when waves shoaled and broke over this zone. After waves broke, the reduction in wave energy allowed sediments near the structures to remain in place. However, as shown in Figure 4-68 and Figure 4-69, the increasing water levels produce larger waves and currents to reach the S-3 structures, which set the sediments near structures into motion. Erosional and depositional areas can be seen in both figures. At the highest water level, Figure 4-69 shows significant impoundment of sediments onto the S-3 structures and the connecting land pieces southward. Light and dark blue zones are indicative of potentially strong erosion at the trunks of the headland breakwater and groins. Although a large sediment size (D50=0.7 mm) was used in these simulations, it is unlikely that sediments placed on the lake-facing side of Alternative S-3 would remain in place over longer periods of time (years), and most likely an annual replenishment of lost sediments would be necessary. Any consideration of using the Alternative S-3 and its potential benefits should be weighed against this costly long-term expected maintenance of the system.

Figure 4-67. Calculated morphology changes at headland breakwater systems during Hurricane Sandy (WL= 0 m).

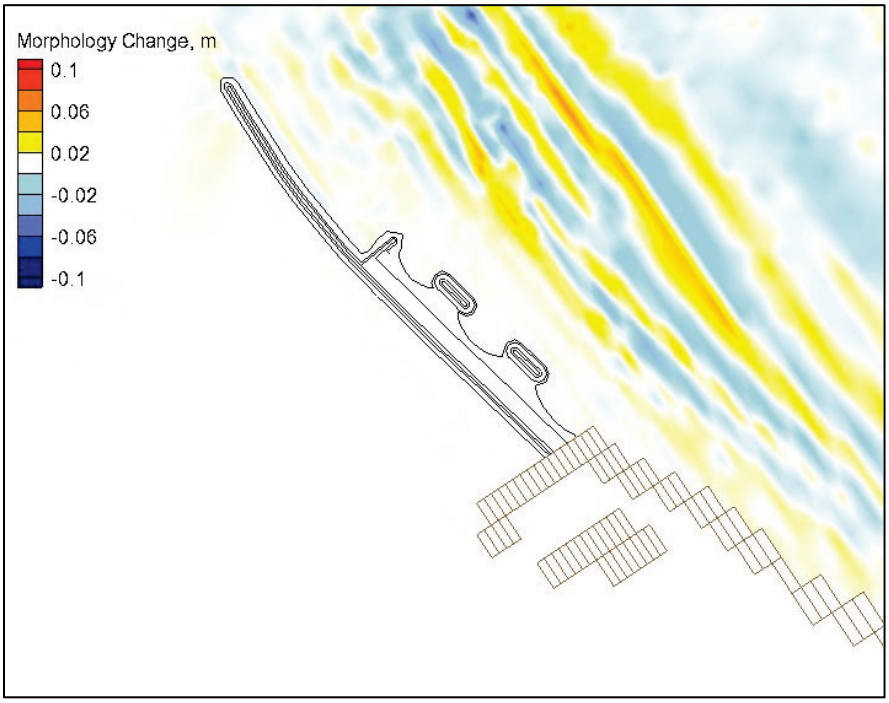

Figure 4-68. Calculated morphology changes at headland breakwater systems during Hurricane Sandy (WL= 0.61 m).

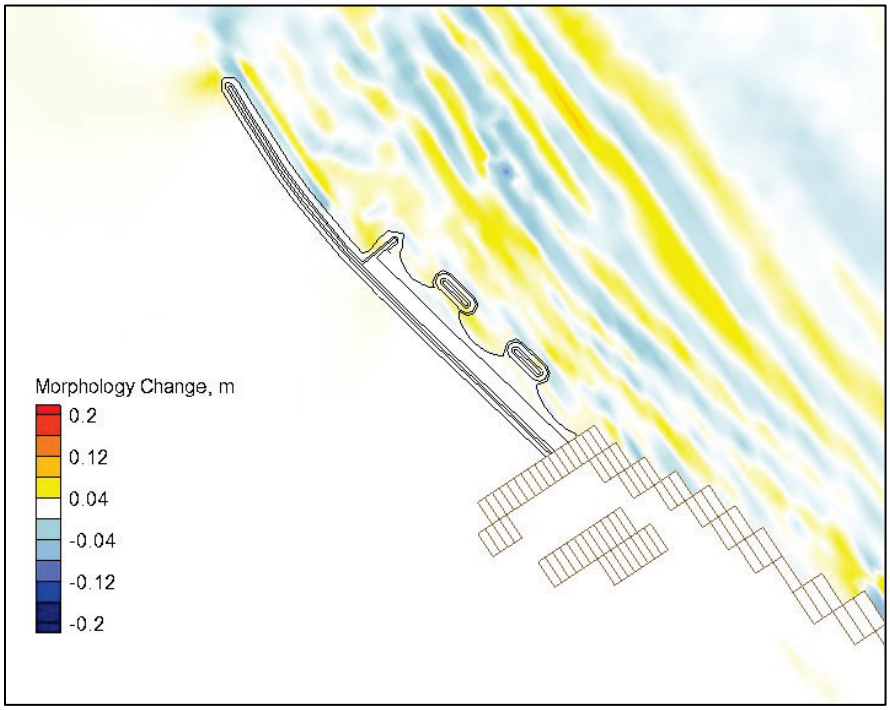

Figure 4-69. Calculated morphology changes at headland breakwater systems during Hurricane Sandy (WL= 1.43 m).

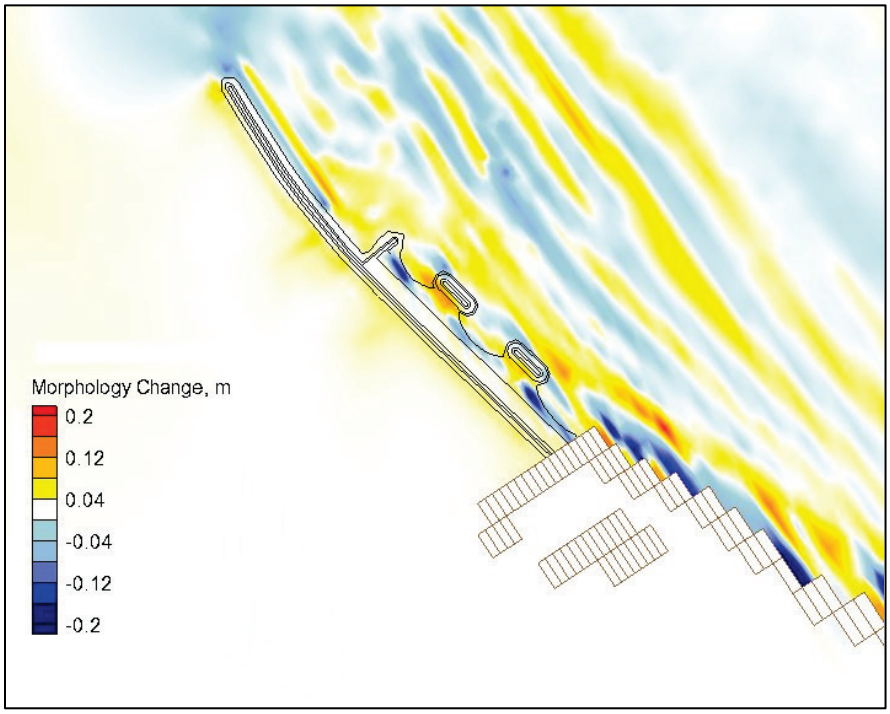

5 Conclusions

Braddock Bay is exposed to winds and waves approaching from the west to east half-plane sector. In the numerical simulations, Lake Ontario side forcings from W, NW, N, NE, and E directions were considered. For Hurricane Sandy, the numerical simulations without project (S-0) and with project (S-1, S-2, and S-3) were conducted for a storm surge of 1.3 ft (0.4 m) at three water levels: low (0 ft =0 m), medium (2 ft = 0.61 m) and high (4.7 ft = 1.43 m). The 9-month long-term simulations (Mar-Nov 2011) were conducted using the measured winds, waves, and water levels data described in Chapters 2 and 3. The simulations for the 20 yr design storm condition employed three water levels and two extreme incident-wave events occurring in Jan 1971 and Mar 1993. These large wave events were simulated for four days in each storm (26-30 Jan 1971, maximum wave height is 10 ft or 3.05 m at noon GMT on 27 Jan 1971; 13-16 Mar 1993, maximum wave height is 12.6 ft or 3.85 m at 06:00 GMT on 14 Mar 1993).

CMS-Wave and CMS-Flow explicit models were used in this study to develop estimates of wave, current, and sediment transport in the bay. Several improvements to CMS were necessary to address the project's needs and enhance the model's predictive capabilities, which were funded by the CIRP. The advances included a) an approach for developing 20-year design conditions (winds, waves, and water levels); b) a strategy for short- and long-term simulations of Superstorm Sandy, two northeasters, and non-storm waves using the full- and half-plane metocean forcings and variable grid capability of CMS-Wave; c) a procedure for validating models with the lake buoys and tide gauges near the project site; d) development of the pre- and post-processing analysis codes for improving model setup; e) development of the Fortran and Matlab utilities for analyses of wind, wave, and river discharge data; and f) development of the codes for extracting boundary conditions for sediment transport and water-quality models.

Based on the numerical modeling results, Alternative S-2 outperformed both Alternatives S-1 and S-3 for all conditions evaluated, and is recommended as the preferred design structure. Alternative S-2 consists of two breakwater structures attached to the northern and southern shorelines, and a jettied inlet formed in the center of the entrance where the two

breakwaters are separated. This narrow inlet is a 100 ft (30.5 m) wide passage allowing for the linkage between the bay and lake. The inlet is expected to be self-scouring, and not initially dredged. To determine future maintenance dredging requirements, a sediment-modeling study would be necessary; this will require a three-dimensional hydrodynamic and mixed sediment transport model coupled to a wave model. Alternative S-3 covers the south part of the Braddock Bay entrance, and it consists of headland breakwaters and groins connecting to the south shorelines and beach. With this finite extent of the system, Alternative S-3 cannot be expected to perform as well as Alternatives S-1 and S-2.

Both Alternatives S-1 and S-2 reduced waves and currents significantly in the central backbay peninsula region preceding the wetlands. The maximum wave height calculated for the Hurricane Sandy in this area for without project (S-0) was 0.86 m at high water level (1.43 m), and the associated bed change was -0.75 m (erosion). With Alternative S-1, the maximum wave height and bed change during Sandy reduced respectively to 0.63 m and -0.59 m. For Alternative S-2, the maximum wave height and bed change further reduced down to 0.5 m and -0.42 m, respectively. The maximum reduction factors obtained for S-1 were 27 and 21 percent, respectively. For S-2, the maximum reduction factors for wave height and bed change were 42 and 44 percent, respectively. In contrast, S-3 shelters only the south part of the bay, and therefore provides relatively limited protection to the bay as compared to S-1 and S-2.

For the 9-month (Mar-Nov 2011) long-term simulation, the maximum wave height and bed change values at the backbay were as follows: 0.26 m and -1.83 m for S-0; 0.17 m and -1.24m for S-1, and 0.11 m and -1.07 m for S-2. These corresponding reduction factors for wave height and bed change were 35 and 32 percent for S-1, and 58 and 42 percent for S-2. In comparison to the 5-day Hurricane Sandy simulation, more reduction was achieved for a 9-month long-term simulation.

For the 20 yr design storm simulations (with the 1993 storm, a 4-day simulation), the maximum wave height and bed change values at the backbay were as follows: 0.57 m and -0.67 m for S-0; 0.31 m and -0.51 m for S-1, and 0.27 m and -0.34 m for S-2. These correspond to the wave height and bed change reduction factors of 46 and 24 percent for S-1, and 53 and 49 percent for S-2. In comparison to the 5-day Hurricane Sandy simulations which had lower wave heights and water levels, a higher reduction factor

was obtained for wave heights for the extreme event, while reduction factor for the bed change was similar for both events. This suggests that no matter which alternative is selected for the final design, either S-1 or S-2 could effectively shelter the bay from severe environmental forcings.

Alternative S-3 provided the least wave reduction at three water levels as compared to S-1 and S-2, and its morphology change was about half those of S-1 and S-2. For S-3, the current magnitude inside the bay was much smaller than S-0 configuration. As was the case for S-0 and Alternatives S-1 and S-2, with increasing water level, the magnitude of current in Alternative S-3 decreases inside the bay. At the highest water level, modeling results indicated a higher propensity for more wave runup/overtopping of the breakwaters and groins than at the two lower water levels. Based on calculated sediment transport results for Alternative S-3, potential maintenance would be required to periodically replenish sediments placed on the lakeward face of S-3 due to erosion/scouring observed at the trunks of headland breakwaters and groins used in Alternative S-3. There was no movement of sediments deposited near and on and around the structures at low water, mainly because D_{50}= 0.7 mm, an unusually high sediment size was used in these simulations at the request of LRB study team. At low lake level, waves, and currents mobilized these extremely coarse sediments where waves shoaled and broke. However, with increasing water level, sediments impounded on the S-3 structures and also on the connecting land pieces southward. This trend in sediment transport would suggest that sediments placed on the lake side of Alternative S-3 cannot be expected to remain in place over long timeframes. Lost sediments have to be replenished periodically (e.g., annually). Potential benefits of Alternative S-3 should be judged against this potential long-term maintenance requirement, which could be costly.

Wave runup/overtopping, wave transmission, and foundation subsidence were considered in this study. It is noted that CMS-Wave uses CEM type empirical equations to calculate the runup, overtopping, and transmitted waves. A refined treatment of these wave/structure interactions for structure design optimization is possible by employing a more advanced model such as BOUSS-2D(Nwogu and Demirbilek 2001; Demirbilek and Nwogu 2007; Demirbilek et al. 2008; Demirbilek et al. 2009; Nwogu and Demirbilek 2010). By using the present modeling results (waves, current, and water levels) as inputs, these effects can be investigated with a Boussinesq wave model. In addition, due to three-dimensional nature of

circulation and sediment transport processes expected in close proximity of structures, a 3-D study should be conducted to determine foundation stability, scouring, and loading estimates necessary for design of structures. LTFATE is recommended for the 3-D integrated wave-hydro-sedtrans modeling (Hayter et al. 2012a; Hayter et al. 2012b; Demirbilek et al 2010).

It should also be noted that structures with low crest elevation generally are known to be susceptible to leeside damage by overtopping and transmitted waves (Hudson 1959; van Gent and Pouzueta 2004). If applicable, e.g., the rate of subsidence at the entrance of Braddock Bay (e.g., local settling caused by the weight of the structure on the *in situ* material), should be taken into consideration in the design. In the final structural design, the armor stone sizes for the lakeside and bayside of Alternatives S-1, S-2, and S-3 should be calculated separately.

Lastly, the design of the breakwaters for Alternatives S-1, S-2, and S-3 should be based on design storms. The design storm criteria used by LRB is the 20-year return period deepwater wave and 10-year all season water level or vice versa. As was noted in Chapter 3, the CMS development of fine-grain and mixed sediments is continuing. Consequently, the modeling estimates for the final design phase of this project should be validated either with field data or compared to the estimates obtained from other two- or three-dimensional hydrodynamic models. Because of the absence of field data at Braddock Bay, preliminary qualitative modeling results presented in this report have been used for a relative comparison of alternatives investigated.

References

Demirbilek, Z., L. Lin, S.J. Smith,. E. Hayter, E. Smith, J. Gailani, G. Norwood, and D, Michalsen, 2010. Waves, Hydrodynamics, and Sediment Transport Modeling at Grays Harbor, WA, ERDC/CHL Technical Report 10-13, U.S. Army Corps of Engineers Research and Development Center, Vicksburg, MS.

Demirbilek, Z., O.G., Nwogu, D.L. Ward, and A. Sanchez, 2009. Wave transformation over reefs: Evaluation of one-dimensional numerical models. ERDC/CHL Technical Report 09-1, U.S. Army Corps of Engineers Research and Development Center, Vicksburg, MS.

Demirbilek, Z, L. Lin, and O.G. Nwogu, 2008. Wave modeling for jetty rehabilitation at the mouth of the Columbia River, Washington/Oregon, USA. Technical Report ERDC/CHL 08-3, U.S. Army Corps of Engineers Research and Development Center, Vicksburg, MS

Demirbilek, Z., L. Lin, and A. Zundel. 2007. WABED model in the SMS: Part 2. Graphical interface. Tech. Note ERDC/CHL CHETN-I-74, U.S. Army Engineer R&D Center, Vicksburg, MS.

Demirbilek, Z. and Nwogu, O.G. 2007. Boussinesq modeling of wave propagation and runup over fringing coral reefs, Model evaluation report. ERDC/CHL Technical Report 07-12, U.S. Army Corps of Engineers Research and Development Center, Vicksburg, MS

Demirbilek, Z., L. Lin, and G.P. Bass. 2005. Prediction of Storm-induced High Water in Chesapeake Bay. Proc. of Solutions to Coastal Disasters 2005, ASCE, Charleston, SC, 187-201.

Demirbilek, Z. and J. Rosati. 2011. Verification and validation of the Coastal Modeling System, Report 1: Summary Report, ERDC/CHL Technical Report 11-10, U.S. Army Corps of Engineers Research and Development Center, Vicksburg, MS.

Hayter, E.J., S.J. Smith, D.R. Michalsen, Z. Demirbilek, and L. Lin. 2012a. “Dredged Material Placement Site Capacity Analysis for Navigation Improvement Project at disposed dredged material from placement sites in Grays Harbor, WA,” Technical Report ERDC/CHL TR-12-18, U.S. Army ERDC, Vicksburg, MS.

Hayter, E.J., S.J. Smith, D.R. Michalsen, Z. Demirbilek, L. Lin, and E.R. Smith. 2012b. “Modeling Transport of Disposed Dredged Material from Placement Sites in Grays Harbor, WA.” Proceedings 12th International Conference on Estuarine and Coastal Modeling, St. Augustine, FL. 560-582.

Hudson, R.Y. 1959. Laboratory investigation of rubble-mound breakwaters, J. Wtrwy. and Harb. Div., ASCE, 85(WW3), 93-121.

Lambert, S.S., S.S. Willey, T. Campbell, R.C. Thomas, H. Li, L. Lin, T.L. Welp, 2013 "Regional sediment management studies of Matagorda Ship Channel and Matagorda Bay System, Texas" ERDC/CHL TR-13-10. August 2013. US Army Engineer Research and Development Center, Vicksburg, MS.

Lin, L., Z. Demirbilek, R. Thomas, and J. Rosati. 2011. Verification and validation of the Coastal Modeling System, Report 2: CMS-Wave, ERDC/CHL Technical Report 11-10, U.S. Army Corps of Engineers Research and Development Center, Vicksburg, MS.

Lin, L., Z. Demirbilek, and H. Mase. 2011. Recent capabilities of CMS-Wave: A coastal wave model for inlets and navigation projects. Proceedings, Symposium to honor Dr. Nicholas Kraus. Journal of Coastal Research, Special Issue 59,7-14.

Lin, L., Z. Demirbilek, H. Mase, and F. Yamada. 2008. CMS-Wave: A nearshore spectral wave processes model for coastal inlets and navigation projects. Coastal and Hydraulics Laboratory Technical Report ERDC/CHL TR-08-13. Vicksburg, MS: U.S. Army Engineer Research and Development Center.

Lin, L., and Z. Demirbilek. 2005. Evaluation of two numerical wave models with inlet physical model. Journal of Waterway, Port, Coastal, and Ocean Engineering 131(4):149-161, ASCE

Nwogu, O. and Demirbilek, Z. 2010. Infragravity wave motions and runup over shallow fringing reefs, ASCE Journal of Waterway, Port, Coastal, and Ocean Engineering (http://dx.doi.org/10.1061/(ASCE)WW.1943-5460.0000050)

Nwogu, O., and Z. Demirbilek. 2001. "BOUSS-2D: A Boussinesq wave model for coastal regions and harbors." Technical Report ERDC/CHL 01-25, U.S. Army Corps of Engineers Research and Development Center, Vicksburg, MS.

Sanchez, A., W. Wu, T. Beck, H. Li, J. Rosati, R. Thomas, J. D. Rosati, Z. Demirbilek, M. Brown, and C. Reed. .2011a. Verification and Validation of the Coastal Modeling System, Report 3: CMS-Flow Hydrodynamics, ERDC/CHL Technical Report 11-10, U.S. Army Corps of Engineers Research and Development Center, Vicksburg, MS.

Sanchez, A., W. Wu, T. Beck, H. Li, J. Rosati, R. Thomas, J. D. Rosati, Z. Demirbilek, M. Brown, and C. Reed. .2011b. Verification and Validation of the Coastal Modeling System, Report 4: CMS-Flow Sediment Transport and Morphology Change, ERDC/CHL Technical Report 11-10, U.S. Army Corps of Engineers Research and Development Center, Vicksburg, MS.

Van Gent, M.R.A., and Pozueta, B. 2004. "Rear-side stability of rubble mound structures," Proc. ICCE 2004, ASCE, V4, Reston, VA, 3481-3493.

Zundel, A. K. 2006. Surface-water modeling system reference manual – Version 9.2. Provo, UT: Brigham Young University Environmental Modeling Research Laboratory.

Appendix A: Description of CMS

The Coastal Modeling System (CMS) was used for the numerical modeling estimates of waves, currents, and sediment transport at Braddock Bay. A brief description of the CMS is provided here for completeness.

As shown in Figure A-1, the CMS is an integrated suite of numerical models for waves, flows, sediment transport, and morphology change in coastal areas. This modeling system includes representation of relevant nearshore processes for practical applications of navigation channel performance, and sediment management at coastal inlets and adjacent beaches. The development and enhancement of CMS capabilities continues to evolve as a research and engineering tool for desk-top computers. CMS uses the Surface-water Modeling System (SMS; Zundel 2006) interface for grid generation and model setup, as well as plotting and post-processing. The Verification and Validation (V&V) Report 1 (Demirbilek and Rosati 2011) and Report 2 (Lin et al. 2011) have detailed information about the CMS-Wave features, and evaluation of model's performance skills in a variety of applications. Reports 3 and 4 in the V&V series describe coupling of wave-flow models, and hydrodynamic and sediment transport and morphology change aspects of CMS-Flow. The performance of CMS for a number of applications is summarized in Report 1 and details are described in the three companion V&V Reports 2, 3, and 4.

Figure A- 1. The CMS framework and its components.

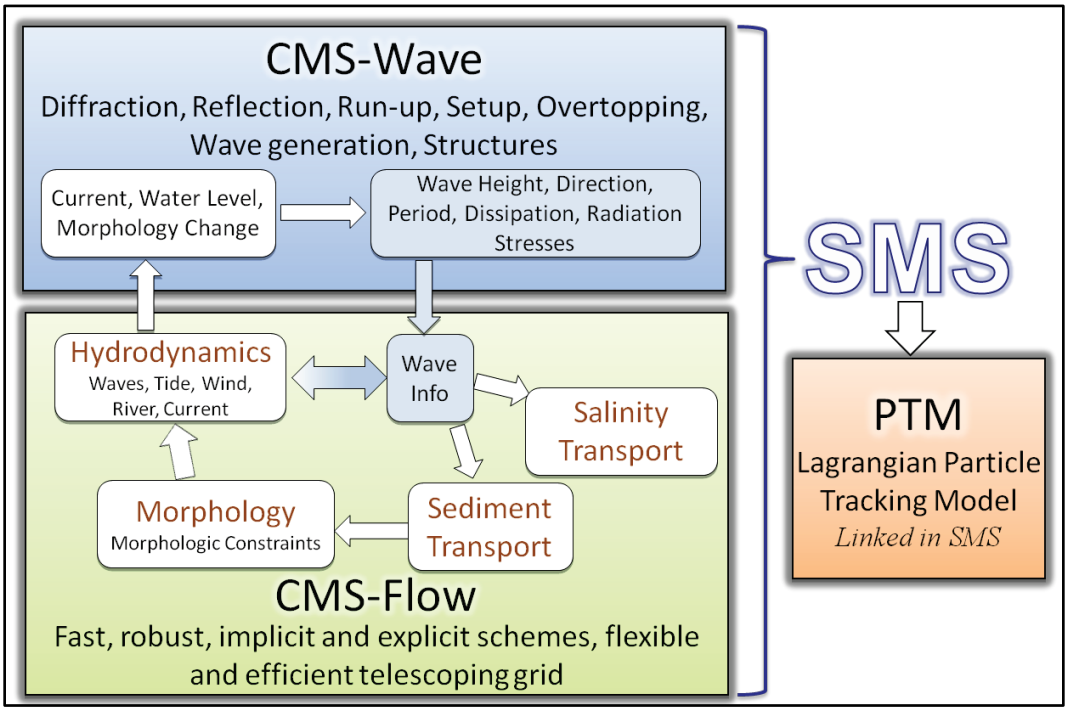

The CMS-Wave, a spectral wave model, is used in this study given the large extent of modeling domain over which wave estimates were required. Wind, wave generation and growth, diffraction, reflection, dissipation due to bottom friction, white-capping and breaking, wave-current interaction, wave run-up, wave setup, and wave transmission through structures are the main wave processes included in the CMS-Wave.

CMS-Wave model solves the steady-state, wave-action balance equation on a non-uniform Cartesian grid to simulate steady-state spectral transformation of directional random waves. CMS-Wave is designed to simulate wave processes with ambient currents at coastal inlets and in navigation channels. The model can be used either in half-plane or full-plane mode for spectral wave transformation (Lin et al. 2008; Demirbilek and Nwogu 2007). The half-plane mode is default because in this mode CMS-Wave can run more efficiently as waves are transformed primarily from the seaward boundary toward shore. See Lin et al. (2011 and 2008) for features of the model and step-by-step instructions with examples for application of CMS-Wave to a variety of coastal inlets, ports, structures, and other navigation problems. Publications listed in the V&V reports and this report provide additional information about the CMS-Wave and its engineering applications. Additional information about CMS-Wave is available from the CIRP website: http://cirp.usace.army.mil/wiki/CMS-Wave

The CMS-Flow, a two-dimensional shallow-water wave model, was used for hydrodynamic modeling (calculation of water level and current) in this study. The implicit solver of the flow model was used in this study. This circulation model provides estimates of water level and current given the tides, winds, and river flows as boundary conditions. CMS-Flow calculates hydrodynamic (depth-averaged circulation), sediment transport, morphology change, and salinity due to tides, winds, and waves.

The hydrodynamic model solves the conservative form of the shallow-water equations that includes terms for the Coriolis force, wind stress, wave stress, bottom stress, vegetation flow drag, bottom friction, wave roller, and turbulent diffusion. Governing equations are solved using the finite volume method on a non-uniform Cartesian grid. Finite-volume methods are a class of discretization schemes, and this formulation is implemented in finite-difference for solving the governing equations of coastal wave, flow, and sediment transport models. See the V&V Reports 3 & 4 by Sanchez et al. (2011a and 2011b) for the preparation of model at coastal inlet applications. Additional information about CMS-Flow is available from the CIRP website: http://cirp.usace.army.mil/wiki/CMS-Flow

CMS-Flow modeling task included specification of winds and water levels to the model. The effects of waves on the circulation were input to the CMS-Flow and have been included in the simulations performed for this study.

There are three sediment transport models available in CMS-Flow: a sediment mass balance model, an equilibrium advection-diffusion model, and a non-equilibrium advection-diffusion model. Depth-averaged salinity transport is simulated with the standard advection-diffusion model and includes evaporation and precipitation. The V&V Reports 1, 3, and 4 describe the integrated wave-flow-sediment transport and morphology change aspects of CMS-Flow. The performance of CMS-Flow is described for a number of applications in the V&V reports.

Appendix B: Sediment Sampling and Laboratory Test Report

Sediment data in Braddock Bay and vicinity were based on sediment sampling and laboratory testing performed by USACE Buffalo District. Sampling activities were performed during August 2012. Figure B-1 presents the sampling locations. Sediment grab samples with an "S" prefix were collected using a ponar sampler. Grab samples with a "B" prefix were collected using a shovel and/or a drive tube sampler. Most of the material sampled consisted of fine sand and peat layers. The shoreline to the north and south of the bay opening consists of cobbles and/or boulders.

Figure B-1. Sampling locations.

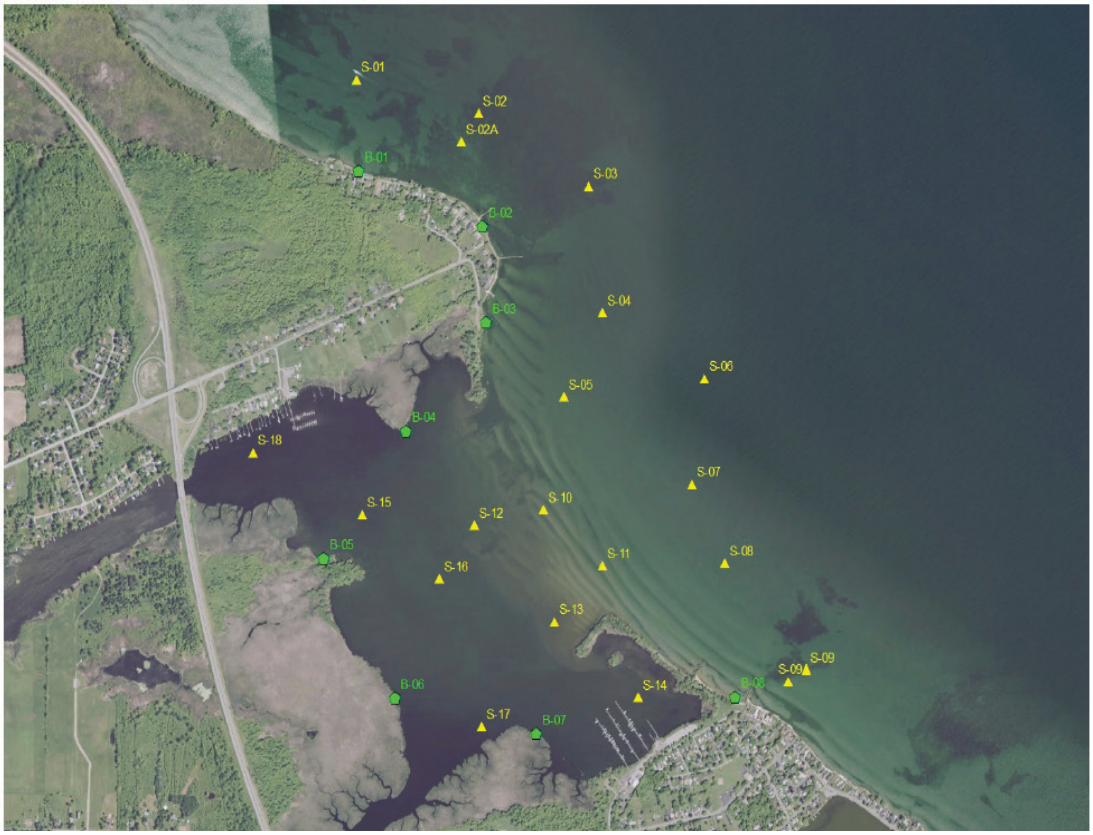

REPORT DOCUMENTATION PAGE

Form Approved
OMB No. 0704-0188

1. REPORT DATE (DD-MM-YYYY)	2. REPORT TYPE	3. DATES COVERED (From - To)
March 2015	Final	

4. TITLE AND SUBTITLE
Modeling of Waves, Hydrodynamics and Sediment Transport for Protection of Wetlands at Braddock Bay, New York

5a. CONTRACT NUMBER

5b. GRANT NUMBER

5c. PROGRAM ELEMENT NUMBER

6. AUTHOR(S)
Zeki Demirbilek, Lihwa Lin, Earl Hayter, Colleen O'Connell, Michael Mohr, Shanon Chader, and Craig Forgette

5d. PROJECT NUMBER

5e. TASK NUMBER

5f. WORK UNIT NUMBER

7. PERFORMING ORGANIZATION NAME(S) AND ADDRESS(ES)
US Army Engineer Research and Development Center
3909 Halls Ferry Road
Vicksburg, MS

8. PERFORMING ORGANIZATION REPORT NUMBER
ERDC TR-14-8

9. SPONSORING / MONITORING AGENCY NAME(S) AND ADDRESS(ES)
U.S. Army Corps of Engineers, Buffalo District
1776 Niagara Street,
Buffalo, NY 14207

Headquarters, U.S. Army Corps of Engineers
441 G Street NW
Washington, DC 20314-1000

10. SPONSOR/MONITOR'S ACRONYM(S)
HQUSACE

11. SPONSOR/MONITOR'S REPORT NUMBER(S)

12. DISTRIBUTION / AVAILABILITY STATEMENT
Approved for public release; distribution is unlimited.

13. SUPPLEMENTARY NOTES

14. ABSTRACT

This report describes a numerical modeling study of waves, currents, and sediment transport at Braddock Bay, New York, which are affecting the wetlands in this estuary. The wetlands have had damage by waves that penetrate deep into the bay from the Lake Ontario side. The purpose of this study was to investigate three proposed alternatives using different structural systems at the entrance of Braddock Bay to minimize the impacts of environmental forces on wetlands. Braddock Bay has had steady erosion and retreat of the shorelines outside and within the bay system in the last century. The bay complex in the present state has become fully exposed directly to the winds and waves from the lake side.

The proposed structural alternatives at the bay entrance were evaluated on their ability to reduce potential impacts of waves and currents on wetlands. Study results indicated all three proposed alternatives were able to reduce waves, currents, and sediment transport substantially in the bay. The primary goal of the study was to develop a quantitative estimate of waves and flow in the bay for a relative comparison of the alternatives investigated.

15. SUBJECT TERMS
Numerical modeling, evaluation, hydrodynamics, wave reduction, Braddock Bay, NY

16. SECURITY CLASSIFICATION OF:			17. LIMITATION OF ABSTRACT	18. NUMBER OF PAGES	19a. NAME OF RESPONSIBLE PERSON
a. REPORT	b. ABSTRACT	c. THIS PAGE			19b. TELEPHONE NUMBER (include area code)
Unclassified	Unclassified	Unclassified		122	